Contribution to algorithmic strategies for solving coupled thermo-mechanical problems by an energy-consistent variational approach

Charbel Bouery

École Centrale Nantes
École Doctorale

Science Pour l'Ingénieur, Géosciences, Architecture

Année 2012 N°B.U. : ...

Thèse de Doctorat

Spécialité : Mécanique des solides, des matériaux, des structures et des surfaces

Présentée et soutenue par:

Charbel BOUERY

Le 12 Décembre 2012
à l'École Centrale Nantes

Contribution to algorithmic strategies for solving coupled thermo-mechanical problems by an energy-consistent variational approach

Jury

Président	Pierre VILLON	Professeur, Université de Technologie de Compiègne
Rapporteurs	David DUREISSEIX	Professeur, INSA Lyon
	Jörn MOSLER	Professeur, TU Dortmund
Examinateurs	Jean-Philippe PONTHOT	Professeur, Université de Liège
	Francisco CHINESTA	Professeur, Ecole Centrale de Nantes
	Laurent STAINIER	Professeur, Ecole centrale de Nantes
Directeur de thèse	Laurent STAINIER	
Laboratoire	Institut de Recherche en Génie Civil et Mécanique, École Centrale de Nantes	

N°E.D. : ...

Résumé

Les sources de couplage thermomécanique dans les matériaux viscoélastiques sont multiples : thermo-élasticité, dissipation visqueuse, évolution des caractéristiques mécaniques avec la température. La simulation numérique de ces couplages en calcul des structures présente encore un certain nombre de défis, spécialement lorsque les effets de couplage sont très marqués (couplage fort). De nombreuses approches algorithmiques ont été proposées dans la littérature pour ce type de problème. Ces méthodes vont des approches monolithiques, traitant simultanément l'équilibre mécanique et l'équilibre thermique, aux approches étagées, traitant alternativement chacun des sous-problèmes mécanique et thermique. La difficulté est d'obtenir un bon compromis entre les aspects de précision, stabilité numérique et coût de calcul. Récemment, une approche variationnelle des problèmes couplés a été proposée par Yang et al. (2006), qui permet d'écrire les équations d'équilibre mécanique et thermique sous la forme d'un problème d'optimisation d'une fonctionnelle scalaire. Cette approche variationnelle présente notamment les avantages de conduire à une formulation numérique à structure symétrique, et de permettre l'utilisation d'algorithmes d'optimisation. Dans ce travail on utilise l'approche variationnelle pour résoudre le problème thermo-visco-elastique fortement couplé, puis on compare plusieurs schémas algorithmiques afin de trouver celui qui présente des meilleures performances

Mots-clés: Formulation variationnelle, couplage thermo-mécanique, problèmes couplés, thermo-visco-élasticité, approche monolithique.

Abstract

Sources of thermo-mechanical coupling in visco-elastic materials are various: viscous dissipation, dependence of material characteristics on temperature, ...
Numerical simulation of these kinds of coupling can be challenging especially when strong coupling effects are present. Various algorithmic approaches have been proposed in the literature for this type of problem, and fall within two alternative strategies:

- Monolithic (or simultaneous) approaches that consists of resolving simultaneously mechanical and thermal balance equations, where time stepping algorithm is applied to the full problem of evolution.
- Staggered approaches in which the coupled system is partitioned and each partition is treated by a different time stepping algorithm.

The goal is to obtain a good compromise between the following aspects: precision, stability and computational cost. Monolithic schemes have the reputation of being unconditionally stable, but they may lead to impossibly large systems, and do not take advantage of the different time scales involved in the problem, and often lead to non-symmetric formulations. Staggered schemes were designed to overcome these drawbacks, but unfortunately, they are conditionally stable (limited in time step size).
Recently, a new variational formulation of coupled thermo-mechanical boundary value problems has been proposed (Yang et al., 2006), allowing to write mechanical and thermal balance equations under the form of an optimisation problem of a scalar energy-like functional. This functional is analysed in the framework of a thermo-visco-elastic strongly coupled problem, considering at first a simplified problem, and then a more general 2D and 3D case. The variational approach has many advantages, in particular the fact that it leads to a symmetric numerical formulation has been exploited in deriving alternative optimization strategies. These various algorithmic schemes were tested and analysed aiming to find the one that exhibits the best computational costs.

Keywords: Variational formulation, thermo-mechanics, coupled problems, monolithic approaches, thermo-visco-elasticity

École Centrale Nantes
École Doctorale

Science Pour l'Ingénieur, Géosciences, Architecture

Année 2012 N°B.U. : ...

Thèse de Doctorat

Spécialité : Mécanique des solides, des matériaux, des structures et des surfaces

Présentée et soutenue par:

Charbel BOUERY

Le 12 Décembre 2012
à l'École Centrale Nantes

Contribution to algorithmic strategies for solving coupled thermo-mechanical problems by an energy-consistent variational approach

Jury

Président	Pierre VILLON	Professeur, Université de Technologie de Compiègne
Rapporteurs	David DUREISSEIX	Professeur, INSA Lyon
	Jörn MOSLER	Professeur, TU Dortmund
Examinateurs	Jean-Philippe PONTHOT	Professeur, Université de Liège
	Francisco CHINESTA	Professeur, Ecole Centrale de Nantes
	Laurent STAINIER	Professeur, Ecole centrale de Nantes
Directeur de thèse	Laurent STAINIER	
Laboratoire	Institut de Recherche en Génie Civil et Mécanique, École Centrale de Nantes	

N°E.D. : ...

Acknowledgments

I would like to offer my sincerest gratitude to my supervisor Professor Laurent Stainier for his guidance, support and encouragement throughout my Ph.D. study at the Ecole Centrale de Nantes. His outstanding expertise, advice and his human qualities made me enjoy working with him and learn a lot. I guess that without his good supervision, my thesis would not have finished.
A special thanks to Prashant Rai, Kamran Ali Syed and Hodei Etxezarreta Olano for having lengthly discussions about teaching philosophies and life in general. Additionally I would like to thank Augusto Emmel-Selke, Shaopu Su, Laurent Gornet, Elias Safatly and Chady Ghnatios for their time spent to answer my questions when I was stucked.
I am grateful to my collegues in the Simulation & structure team for their help and friendship. Additionally I want to thank many of the great friends that I have met in my time at Nantes, Hodei Etxezarreta Olano, Willington Samedi, Josu Imaz Aranguren, Oscar Fornier, Tony Khalil, Modesto Mateos, Prashant Ray, Alexandre Langlais, Rocio Aguirre Garcia, Isabelle Farinotte, Farah Mourtada, Jane Becker, Vanessa Menut among others who made me feel at home, and given me an outlet outside the school.
All these years, I owe a lot to the SWAPS-Nantes that provided me dancing and sports activities, thus allowed me to get away from the lab and keep my sanity in some of those very difficult days. A special thanks also to "café polyglotte" (language exchange events) organized by the association "Autour du Monde". Without these hobbies and many good friends it would have been very hard to finish my Ph.D.
A special thanks to Dr. Patrick Rozycki, Pascal Cosson and Jean-Yves monteau for the opportunity they offered me as a teacher associate in solid mechanics, vibration and automatics. These teaching reaffiremed my motivation to finish this degree and look for an academic position.
The author would like to acknowledge the direct support of the Pays de la Loire region during the last three years.
Last but not the least, I am grateful to the support of my family and my very close friend Roger A-smith that i missed his company and these deep conversations we used to share in those old days

Contents

General Introduction

With the development of science and research, the design of engineering products demands a more accurate description of different physics involved, since many important engineering problems require an integrated treatment of coupled fields. In recent years there has been an increasing interest in the computational modelling of coupled systems [89, 87, 112, 94, 95, 97, 100, 19, 21, 104]. Note that non-linearities and the interaction between its different components often results in complex systems.
Coupled systems are systems whose behavior is driven by the interaction of functionally distinct components. Multi-physics treats simulations that involve multiple physical models or multiple simultaneous physical phenomena [103, 37].
This field of study is so crucial, since chosen models, algorithms and implementation grow systematically in the number of components, and often models that work correctly with isolated components break down when coupled. Therefore it is useful to proceed in particular solution algorithms.

Sources of thermo-mechanical coupling are various in nature: thermo-elasticity, viscous dissipation, dependence of material characteristics on temperature and so on ...
Numerical simulation of these kinds of coupling can be challenging, especially when a strong coupling effect is present.
Various solution algorithms are found in the engineering literature of coupled problems. In the framework of this thesis we will consider concurrent approaches that can be classified into two broad categories: monolithic and staggered approaches

- Monolithic (or simultaneous) approaches that consist of resolving simultaneously mechanical and thermal balance equations, where time stepping algorithm is applied to the full problem of evolution. In this case, using implicit schemes always lead to unconditional stability, which mean that the difference between two initially close solution always remains bounded independently by the time step size [32, 43, 60, 108] etc...

- Staggered approaches where coupled system is partitioned, then each of the mechanical and thermal problem is solved alternatively, and each partition is treated by a different time stepping algorithm [31, 24, 108, 42, 37] etc...

Monolithic schemes have the advantage of being unconditionally stable, but their disadvantage is that it might lead to impossibly large systems, same time scale involved in the problem and this scheme is in general non-symmetric.
The goal of the partitioned (or staggered) schemes is to overcome these inconveniences, but unfortunately, often at the expense of unconditional stability.
In the framework of this thesis, we treat the thermo-mechanical coupled problem, via an energy-consistent variational formulation for coupled thermo-mechanical problems proposed by in 2006 by Yang *et al* [115].
This variational approach has many advantages: it leads to a symmetric numerical formulation, possibility to derive staggered or simultaneous schemes, it is useful for adaptive approach (adaptive time, mesh), and allows the use of optimization algorithms in particular for strongly coupled problems.

We start the first part by introducing notions about continuum thermo-mechanics, where we introduce basic notions of general continuum mechanics and thermodynamics and we can write the general heat equation.
Secondly, we introduce classical solving of the coupled thermo-mechanical problem, and different algorithmic schemes used in the literature.
Eventually, we expose the variational formulation of coupled thermo-mechanical boundary-value problem, where our work reclines.

The main objective of this framework is the validation, analysis and improvement of monolithic algorithmic schemes via an energy-consistent variational formulation of coupled thermo-mechanical problems.
Since the variational formulation allows to write mechanical and thermal balance equation under the form of an optimization problem of a scalar energy-like functional, different optimization algorithmic schemes will be used, the classical Newton-Raphson scheme, the alternated algorithm, and Uzawa-like algorithms.

To show the validation of the energetic formulation, and compare the efficiency of different algorithms, various applications of coupled thermo-mechanical problems have been exposed in details, such as thermo-visco-elastic strong coupled problem from a simplified problem consisting of an infinitesimal control volume to a more general $2D$ and $3D$ coupled thermo-elastic boundary-value problem, and then another application of a necking in a bar with an thermo-elasto-plastic coupling.
In each case the effects of heat capacity, intrinsic dissipation and the heat exchange with the environment are included in the model.

Introduction générale

Les sources de couplage thermo-mécanique dans les matériaux visco-élastiques sont multiples : thermo-élasticité, dissipation visqueuse, évolution des caractéristiques mécaniques avec la température. La simulation numérique de ces couplages en calcul des structures présente encore un certain nombre de défis, spécialement lorsque les effets de couplage sont très marqués (couplage fort).
De nombreuses approches algorithmiques ont été proposées dans la littérature pour ce type de problème et se résument en deux stratégies alternatives:

- *Approches monolithiques (ou simultanées)* qui consistent de résoudre simultanément les équations d'équilibre mécanique et thermique. Dans ce cas, l'utilisation des schémas implicites conduisent toujours à une stabilité inconditionelle .

- *Approaches étagées* où le problème thermo-mécanique est décomposé en deux sous-problèmes thermique et mécanique, et chaque partition est traité par un algorithme différent.

La difficulté est d'obtenir un bon compromis entre les aspects de précision, stabilité numérique et coût de calcul.

Récemment, une approche variationnelle des problèmes couplés a été proposée par Yang *et al.* (2006), qui permet d'écrire les équations d'équilibre mécanique et thermique sous la forme d'un problème d'optimisation d'une fonctionnelle scalaire. Cette approche variationnelle, présente notamment les avantages de conduire à une formulation numérique à structure symétrique, et de permettre l'utilisation d'algorithmes d'optimisation.

Dans le cadre de ce travail, on s'intéresse à la validation de la formulation énergétique variationnelle du problème thermo-visco-mécanique couplé, ainsi que l'analyse des schémas algorithmiques monolithiques, traitant un problème allant d'un cas simplifié consistant en un élément de volume jusqu'au cas plus général $2D$ et 3D consistant en une plaque trouée en son centre et soumise à un chargement en contrainte, avec un comportement thermo-visco-élastique de type kelvin voigt, en incluant les effects de capacité thermique, dissipation intrinsèque et d'échange de chaleur avec l'environnement. Le couplage thermo-mécanique est complété en incluant une dépendance forte des coefficients

mécaniques par rapport à la température.
Le problème thermo-visco-élastique à été testé considérant différents schémas algorithmiques dont une approche intéressante de type Uzawa qui semble réduire le temps global de calcul. Cependant, ces résultats ont été obtenus sur un cas particulier, ce qui nous a amené à considerer un autre problème (striction d'une barre) avec un comportement elasto-plastique, où le schéma de Newton semble donner des meilleures performances.
On peut conclure, d'après ce travail, que l'algorithme le plus robuste dépend du type du couplage considéré. Cependant il reste intéressant de tester les différents schémas sur d'autre type de problème (visco-plasticité etc...)

Chapter 1

Introduction to coupled systems

Résumé

Le premier chapitre introduit des concepts généraux liés à la multi-physique et les problèmes couplés.
Avec l'avancement de la technologie, la simulation des systèmes mécanique demandent plus de précision. La multi-physique sera indispensable lorsqu'on a besoin de concevoir un produit qui ne peut être décrit qu'en couplant des différentes physiques. Prenant par exemple l'action du vent sur un panneau solaire, la partie de dynamique des fluides agit comme une entrée de la partie mécanique, mais il en est de même dans le sens inverse, la partie mécanique provoque un changement de l'écoulement du fluide. Pour faire face à ce problème, on a besoin de combiner les modèles physiques. La multi-physique reflète plus exactement ce qui se passe dans le monde réel, qui est le but de tous les scientifiques et les ingénieurs.

1.1 Introduction

Pace of scientific investigation and research is faster today then ever before, this accelerated development is directly due to advancements made in understanding the laws of nature, and in using that understanding to make better products, therefore computer simulation has emerged as an indispensable tool. In fact it is plausible to say that the future of technology and simulation are vitally linked. Simulation of physical systems was one of the first applications of digital computers, with today advances and simulation technology and computational power one can solve just about any physics based engineering problem on a standard PC, such as heat transfer, structural mechanics, fluid dynamics, electromagnetism, chemical reactions, acoustics and so on.
The multi-physics come when we need to design a product where it can only be described accurately by coupling different physics, lets take for instance the wind mode on a solar panel, the fluid dynamics part of the simulation act as input to the mechanical part, but the same is true in reverse, the mechanics causes the change in the flow pattern. To deal with this issue, engineers using simulation software knew to combine physical models

and algorithms, simulating all these physics together is required to achieve reliable simulation results. Multi-physics ultimately reflects what happens in the real world more accurately, which is the goal for all scientists and engineers.

1.2 Coupled systems

The dictionary states eight meanings for the word "*system*". In multi-physics, a *system* is used in the sense of a functionally related group of components forming or regarded as a collective entity [109], in other words a system is a set of interacting entities, such as fields of continuum mechanics, evolving in time.

A coupled system is one in which physically or computationally heterogeneous mechanical components interact dynamically. In other words a coupled system is a set of interacting sub-systems, where each sub-system is different by :

- The type of differential equation
- The type of discretization technique
- The type of physics
- The geometric domain

Sub-systems interact through interfaces, the interaction is called "*one way*" if there is not feedback between subsystems for two subsystems as X and Y. The interaction is called "*two-way*" or "*multiway*" if there is feedback between sub-systems
We are interested in this case, where the response has to be obtained by solving simultaneously the coupled equations which model the system.

1.3 Strong vs weak coupling

In computational multi-physics, two types of coupling exist, strong and weak coupling. Each of those two coupling is linked directly to computational cost and performance.
Consider for instance a system, where u_1 and u_2 are the two fields.
We can write the coupled system $u_1(t)$ and $u_2(t)$ as:

$$\frac{du_1}{dt} = \mathcal{L}_1(u_1, u_2) \tag{1.1}$$

$$\frac{du_2}{dt} = \mathcal{L}_2(u_1, u_2) \tag{1.2}$$

1.3.1 Weak coupling

A system is weakly coupled[1] if sub-system 1 has significant influence on sub-system 2, while subsystem 2 has moderate (or small) influence on subsystem 1.
In this case we can apply a sequential solution scheme where we can solve sub-system 1 first (subsystem 1 as an input), then we solve sub-system 2.

$$\mathcal{L}_1(u_1, u_2) \simeq \hat{\mathcal{L}}_1(u_1) \tag{1.3}$$

$$\frac{du_1}{dt} \simeq \hat{\mathcal{L}}_1(u_1) \Rightarrow u_1(t) \tag{1.4}$$

$$\frac{du_2}{dt} = \mathcal{L}_2(u_2, u_1(t)) \tag{1.5}$$

1.3.2 Strong coupling

A system is called strongly coupled[2], if both sub-system 1 and sub-system 2 have influences on each others.
In this case we can apply different kind of schemes to solve the problem :

- Concurrent solution scheme such monolithic schemes where we solve simultaneously all equations in one algorithm.
- Staggered schemes where the coupled problem is split and each physic is treated by different strategy.

1.4 Monolithic and staggered schemes

1.4.1 Monolithic scheme:

Consider the interaction between two scalar fields u_1 and u_2, where each field has only one state variable $u_1(t)$ and $u_2(t)$.
The monolithic scheme consists of resolving simultaneously the fields equations $u(t)$ (in $u1$ and $u2$) with one algorithm (whether implicit or explicit), where $u(t)$ is defined as:

[1]Examples of weakly coupled systems : aero-accoustics

[2]examples of strongly coupled systems : thermo-mechanics, thermo-visco-elasticity, aero-elasticity and so on

$$\{u(t)\} = \{u_1(t), u_2(t)\}^T \tag{1.6}$$
$$\{u(0)\} = \{u_0\} \tag{1.7}$$
$$\frac{d\{u\}}{dt} = \mathcal{L}(\{u\}) \tag{1.8}$$

Therefore we obtain a complex system with a very large size, but have the benefit to be unconditional stable for implicit algorithms, meaning that we can go for larger time steps without affecting the stability of the system.
On the other hand, explicit algorithms lead to conditional stability, which means that the stability of the system is influenced by the size of time step, the time step shall be less than a critical time step $\Delta t < \Delta t_{crit}$.
If we denote Δt_{crit_1} the critical time step for the stability of the sub-system 1, and Δt_{crit_2} the critical time step for the stability of the sub-system 2, $\min(\Delta t_{crit_1}, \Delta t_{crit_2})$ *may be* $\ll$ $\max(\Delta t_{crit_1}, \Delta t_{crit_2})$
The system obtained is very large, and the tangent matrix has the following form:

$$\begin{bmatrix} \frac{\delta \mathcal{L}_1}{\delta u_1} & \frac{\delta \mathcal{L}_1}{\delta u_2} \\ \frac{\delta \mathcal{L}_2}{\delta u_1} & \frac{\delta \mathcal{L}_2}{\delta u_2} \end{bmatrix} \tag{1.9}$$

The system obtained is generally non-symmetric due to the coupled terms of $\frac{\delta \mathcal{L}_1}{\delta u_2}$ and $\frac{\delta \mathcal{L}_2}{\delta u_1}$, and this lead to big computational cost generated by the inversion of the tangent matrix, especially when the coupling is strong, where the sub-diagonal matrices should be taken into account. In fact, when coupling is weak, these matrices can be neglected. Strong coupling may influence convergence, but not inversion time with direct solvers.

1.4.2 Staggered scheme

The goal of a staggered scheme is to split the coupled problem into a set of sub-problems, therefore the staggered scheme (also called partitioned (without a fixed point)) solves different physic separately $\mathcal{L}(\{u\}) = \mathcal{L}_2 \circ \mathcal{L}_1(\{u\})$. The system becomes simpler due to the reduction of degrees of freedom of each sub-system. Some of the advantages is that we can use the best algorithm of resolution for each sub-system, the best discretization for each sub-system and may use the best time increments for each sub-system (which is not so obvious in practice). One of the disadvantages is that a staggered scheme is not always stable [101, 102].

1.5 Application

Consider strong coupling between two scalar fields X and Y. Each field has one state variable identified as x(t) and y(t), respectively, which are assumed to be governed by

the first-order differential equation:

$$\begin{aligned} \dot{x} + ax + cy &= f(t) && (1.10)\\ \dot{y} + by + dx &= g(t) && (1.11) \end{aligned}$$

where $f(t)$ and $g(t)$ are the applied forces.
Equation 1.10 can be written in the following form:

$$\begin{aligned} \mathcal{L}_1(x,y) &= f(t) - ax - cy && (1.12)\\ \mathcal{L}_2(x,y) &= g(t) - dx - by && (1.13) \end{aligned}$$

or more generally $\mathcal{L}_i(x,y) = A_i(x,y) + f_i(t)$.
The initial conditions are given by:

$$\begin{aligned} x(0) &= x_0 \qquad & \dot{x}(0) &= \dot{x}_0 && (1.14)\\ y(0) &= y_0 \qquad & \dot{y}(0) &= \dot{y}_0 && (1.15) \end{aligned}$$

1.5.1 Monolitic approach

Let's treat the system by Backward Euler integration in each component:

$$\begin{aligned} x_{n+1} &= x_n + \Delta t \dot{x}_{n+1} && (1.16)\\ y_{n+1} &= y_n + \Delta t \dot{y}_{n+1} && (1.17) \end{aligned}$$

$$\begin{aligned} x_{n+1} &= x_n + \Delta t \left(f(t_{n+1}) - a x_{n+1} - c y_{n+1} \right) && (1.18)\\ y_{n+1} &= y_n + \Delta t \left(g(t_{n+1}) - b y_{n+1} - d x_{n+1} \right) && (1.19) \end{aligned}$$

where $x_n = x(t_n)$, etc. At each time step $n = 0, 1, 2, ...$ we get:

$$\begin{bmatrix} x_{n+1} \\ y_{n+1} \end{bmatrix} = \begin{bmatrix} 1 + a\Delta t & c\Delta t \\ d\Delta t & 1 + b\Delta t \end{bmatrix}^{-1} \begin{bmatrix} x_n + \Delta t f_{n+1} \\ y_n + \Delta t g_{n+1} \end{bmatrix} \qquad (1.20)$$

in which $[x_0, y_0]$ are provided by the initial conditions. In the monolithic or simultaneous solution approach, the system (1.20) is solved at each time step till the final time t_f.

1.5.2 Staggered scheme

The system treated above can be written as:

$$\begin{bmatrix} 1 + a\Delta t & c\Delta t \\ d\Delta t & 1 + b\Delta t \end{bmatrix} \begin{bmatrix} x_{n+1} \\ y_{n+1} \end{bmatrix} = \begin{bmatrix} x_n + \Delta t f_{n+1} \\ y_n + \Delta t g_{n+1} \end{bmatrix} \qquad (1.21)$$

A simple partitioned solution procedure is obtained by treating the system (1.21) with the following staggered partition with prediction on y:

$$\begin{bmatrix} 1+a\Delta t & 0 \\ d\Delta t & 1+b\Delta t \end{bmatrix} \begin{bmatrix} x_{n+1} \\ y_{n+1} \end{bmatrix} = \begin{bmatrix} x_n + \Delta t f_{n+1} - c\Delta t y^p_{n+1} \\ y_n + \Delta t g_{n+1} \end{bmatrix} \tag{1.22}$$

1. Predictor : $y^p_{n+1} = y_n + \Delta t \dot{y}_n$
2. Solve x (or Advance x) : $x_{n+1} = \frac{1}{1+a\Delta t}\left(x_n + \Delta t f_{n+1} - c y^p_{n+1}\right)$
3. Transfer (or Substitute) : $x_{n+1} = x_{n+1}$
4. Solve y (or Advance y) : $y_{n+1} = \frac{1}{1+b\Delta t}\left(y_n + \Delta t g_{n+1} - d\Delta t x_{n+1}\right)$

where y^p_{n+1} is the predictor. Two common choices for the predictor are $y^p_{n+1} = y_n$ (called the last solution predictor) and $y^p_{n+1} = y_n + \Delta t \dot{y}_n$

1.5.3 Comments on respective advantages and merits

Since Backward Euler integration conserves the stability of the system, the features of each schemes will be commented as follows:

A scheme is called stable if the eigenvalues of the amplification matrix is < 1.

For the monolithic scheme the amplification matrix is given by

$$\begin{bmatrix} 1+a\Delta t & c\Delta t \\ d\Delta t & 1+b\Delta t \end{bmatrix}^{-1} \tag{1.23}$$

For the staggered scheme, we can write system (1.22) in a alternative manner, by considering the predictor $y^p_{n+1} = y_n$:

$$\begin{bmatrix} 1+a\Delta t & 0 \\ d\Delta t & 1+b\Delta t \end{bmatrix} \begin{bmatrix} x_{n+1} \\ y_{n+1} \end{bmatrix} = \begin{bmatrix} 1 & -c\Delta t \\ 0 & 1 \end{bmatrix} \begin{bmatrix} x_n \\ y_n \end{bmatrix} + \begin{bmatrix} \Delta t f_{n+1} \\ \Delta t g_{n+1} \end{bmatrix} \tag{1.24}$$

In this case the amplification matrix is given by:

$$\begin{bmatrix} 1+a\Delta t & 0 \\ d\Delta t & 1+b\Delta t \end{bmatrix}^{-1} \begin{bmatrix} 1 & -c\Delta t \\ 0 & 1 \end{bmatrix} \tag{1.25}$$

If we select certain values for a, b, c *and* d where $a > 0,\ b > 0$ and $a \times b - c \times d > 0$, we can see clearly that the eigenvalues of the amplification matrix (eq. 1.23) are < 1, while the eigenvalues of the amplification matrix (eq. 1.25) may be > 1, then we can deduce that the monolithic schemes are unconditionally stable, whereas the staggered schemes are conditionally stable.

Chapter 2

Basics of coupled thermo-mechanical problem

Résumé

Dans ce chapitre on rappelle les concepts de base, et la formulation des équations réagissant le comportement d'un milieu continu, ainsi que les principes fondamentaux de la thermodynamique et du transfert de chaleur. Le formalisme développé peut prendre en compte la production de grandes déformations ainsi que les couplages pouvant apparaître entre les champs mécanique et thermique.

L'approche adoptée est basé sur l'hypothèse d'état local thermodynamique à l'équilibre, d'où les fonctions thermodynamique sont déterminées à partir des variables d'état, qui ne dépendent que de ces derniers (indépendant de leur gradient et leur dérivées temporelles). Les variables d'état sont de trois types, décrivant l'état de déformation du corps, sa température et sa structure interne représentée par des variables d'état interne. Le choix de ces variables d'état , qui doit être bien adéquat, est une des difficultés d'utilisation de la formulation thermodynamique

Afin de développer l'équation de chaleur, qui met en evidence les termes de couplage thermo-mécanique, il convient de rappeler les fonctions thermodynamiques (comme l'énergie libre) qui sont des fonctions des variables d'état, ou bien de leur grandeur thermodynamiquement conjuguée.

A la fin de ce chapitre, l'équation de chaleur la plus générale est développée, afin de mettre en évidence l'évolution de la variable température, qui se traduit par le principe de conservation de l'énergie. L'équation de la chaleur est une réécriture du premier principe en utilisant les lois d'état et les lois complémentaire exposées dans le chapitre. Elle permet de mettre en évidence les couplages entre les effets mécaniques et thermique et de préciser les grandeurs énergétiques qui se transforment en chaleur lors d'un processus thermo-mécanique.

2.1 Introduction

In this chapter we recall the basic concepts in continuum mechanics and the fundamental principles of thermodynamics and heat transfer. The theories that we examine here are all based on the assumption of local thermodynamic state in equilibrium, this means that the thermodynamic functions are determined through a finite set of variables, called state variables. These functions depending only on these variables will be independent of their gradients (local state) and their time derivatives (system in equilibrium). In these theories, the state variables are almost always describing three types: the state of deformation of the body, its temperature and internal structure [47, 83, 67, 48, 56, 98].

2.2 Basics of continuum mechanics

Continuum mechanics is a branch of mechanics that deals with the analysis of the kinematics and the mechanical behavior of materials modelled as a continuous mass rather than as discrete particles. The French mathematician Augustin Louis Cauchy was the first to formulate such models in the 19th century, but research in the area continues today.
On a macroscopic scale, materials have cracks and discontinuities. However, certain physical phenomena can be modelled assuming the materials exist as a continuum, meaning the matter in the body is continuously distributed and fills the entire region of space it occupies. A continuum is a body that can be continually sub-divided into infinitesimal elements with properties being those of the bulk material.
To develop an appropriate formalism, we will need to refer to two different configurations of a continuous body. Let $\mathcal{B}_0$ denotes the reference configuration that represents the configuration at time $t = t_0$, occupying a volume V_0 defined by a boundary A_0, and by $\mathcal{B}_t$ the current configuration at time t, occupying a volume V_t and a boundary A_t. The positions of material particles belonging to the reference configuration $\mathcal{B}_0$ are denoted by $\mathbf{X}$, and those belonging to the current configuration $\mathcal{B}_t$, are denoted by $\mathbf{x}$. Each material point will move and have its own trajectory path. Hence, the trajectory is defined by the evolution of the material point $\mathbf{x}$ as follow:

$$\mathbf{x} = \phi(\mathbf{X}, t) \tag{2.1}$$

The gradient of the deformation relative to the motion between the reference and the current configuration is defined as follow:

$$\mathbf{F} = \frac{\partial \phi(\mathbf{X}, t)}{\partial \mathbf{X}} = \frac{\partial \mathbf{x}(\mathbf{X}, t)}{\partial \mathbf{X}} \tag{2.2}$$

where $\mathbf{F}$ is a second order tensor.
In general $\mathbf{F}$ is a non symmetric tensor. The measurement of deformation is dependent on the configuration (the actual configuration $\mathcal{B}_0$ or the current configuration $\mathcal{B}_t$. In our work, the chosen configuration is the reference configuration ($\mathcal{B}_0$). In this case, the

deformation is measured through the Green-Lagrange deformation tensor , defined by:

$$\mathbf{E} = \frac{1}{2}\left(\mathbf{C} - \mathbf{I}\right) = \frac{1}{2}\left(\mathbf{F}^T\mathbf{F} - \mathbf{I}\right) \tag{2.3}$$

where the index T is the transpose of the tensor $\mathbf{F}$, $\mathbf{C} = \mathbf{F}^T\mathbf{F}$ is called right Cauchy-Green stretch tensor, it is symmetric, and $\mathbf{I}$ is the identity tensor.

The gradient of the transformation can be written in function of the gradient of displacement:

$$\mathbf{F} = \frac{\partial \mathbf{x}}{\partial \mathbf{X}} = \frac{\partial(\mathbf{X} + \mathbf{u})}{\partial \mathbf{X}} = \bar{\bar{\mathbf{I}}} + \frac{\partial \mathbf{u}}{\partial \mathbf{X}} \tag{2.4}$$

Where $\mathbf{u}$ is the displacement vector.
We can write then the Green-Lagrange tensor as follow:

$$\begin{aligned} \mathbf{E} &= \frac{1}{2}(\mathbf{C} - \mathbf{I}) && (2.5)\\ &= \frac{1}{2}(\mathbf{F}^T\mathbf{F} - \mathbf{I}) && (2.6)\\ &= = \frac{1}{2}\left((\frac{\partial \mathbf{u}}{\partial \mathbf{X}}) + (\frac{\partial \mathbf{u}}{\partial \mathbf{X}})^T + (\frac{\partial \mathbf{u}}{\partial \mathbf{X}})^T \cdot (\frac{\partial \mathbf{u}}{\partial \mathbf{X}})\right) && (2.7) \end{aligned}$$

2.2.1 Small perturbations assumption

Small perturbations assumption states that displacements (and rotations) between the reference and actual configuration are very small, as well as the gradient of the displacement.

Under these conditions (small perturbations), the current and the reference configurations are very close to each others, then we can substitute the variable $\mathbf{x}$ by $\mathbf{X}$, $\forall$ $\mathbf{x} \in \Omega$, therefore we can neglect the quadratic term in equation (2.7):

$$\mathbf{E} \approx \frac{1}{2}\left(\frac{\partial \mathbf{u}}{\partial \mathbf{X}} + (\frac{\partial \mathbf{u}}{\partial \mathbf{X}})^T\right) = \boldsymbol{\epsilon} \tag{2.8}$$

In this case, the deformation tensor of the current configuration, called Euler-Almansi tensor, gives the same expression as (2.8).

2.2.2 Balance laws

Let $f(\mathbf{x}, t)$ be a physical quantity that is defined through a field. Let $g(\mathbf{x}, t)$ be sources on the surface of the body and let $h(\mathbf{x}, t)$ be sources inside the body. Let $\mathbf{n}(\mathbf{x}, t)$ be the outward unit normal to the surface A . Let $\mathbf{u}(\mathbf{x}, t)$ and $\mathbf{v}(\mathbf{x}, t)$ be the displacement and the velocity field of the physical particles that carry the physical quantity that is flowing respectively. Also, let the speed at which the bounding surface A is moving be u_n (in

the direction $\mathbf{n}$).
Then, balance laws can be expressed in the general form:

$$\frac{d}{dt}\left[\int_V f(\mathbf{x},t)\ \mathrm{dV}\right] = \int_A f(\mathbf{x},t)[u_n(\mathbf{x},t) - \mathbf{v}(\mathbf{x},t)\cdot\mathbf{n}(\mathbf{x},t)]\ \mathrm{dA} + \int_A g(\mathbf{x},t)\ \mathrm{dA} + \int_V h(\mathbf{x},t)\ \mathrm{dV} \tag{2.9}$$

Note that the functions $f(\mathbf{x},t)$, $g(\mathbf{x},t)$, and $h(\mathbf{x},t)$ can be scalar valued, vector valued, or tensor valued depending on the physical quantity that the balance equation deals with. If there are internal boundaries in the body, jump discontinuities also need to be specified in the balance laws.
In the followings, we write the balance laws of a solid (balance laws of mass, momentum, and energy) under the Lagrangian point of view.

Law of Conservation of Mass

The mass M is defined as:

$$M = \int_{V_0} \rho_0 dV_0 = \int_V \rho_0 dV \tag{2.10}$$

The law of conservation of mass is written as :

$$\frac{dM}{dt} = \int_V (\dot{\rho_0} + \rho_0\ \boldsymbol{\nabla}\cdot\mathbf{v}) = 0 \tag{2.11}$$

Where ρ_0 initial density (kg/m^3), ρ_0 current density ,$\mathbf{v}$ the velocity of the body (m/s), and $\boldsymbol{\nabla}$ is the divergence operator.
Local form of equation 2.11 is written as :

$$\dot{\rho_0} + \rho_0\ \boldsymbol{\nabla}\cdot\mathbf{v} = 0 \tag{2.12}$$

Law of conservation of Linear momentum

The linear momentum Q is defined as:

$$\mathbf{Q} = \int_V \rho_0\ \mathbf{v} dV \tag{2.13}$$

Where $\mathbf{Q}$ is the linear momentum $(kg.m/s)$.
Let $\bar{\mathbf{t}}$ be denoted as the applied traction forces on the boundary (N/m^2), $\mathbf{b}$ body forces vector (N/kg), then the resultant mechanical force of the body $\mathbf{R}$ (N) can be written as:

$$\mathbf{R} = \int_A \bar{\mathbf{t}} dA + \int_V \rho_0 \mathbf{b} dV \tag{2.14}$$

The law of conservation of linear momentum is written under the following form:

$$\frac{d\mathbf{Q}}{dt} = \mathbf{R} \tag{2.15}$$

Using the relation linking the traction vector force on the boundary $\bar{\mathbf{t}}_{\mathbf{0}}$ to Cauchy stress tensor $\bar{\mathbf{t}}_{\mathbf{0}} = \boldsymbol{\sigma} \cdot \mathbf{n}$, where $\boldsymbol{\sigma}$ is the cauchy stress tensor (N/m^2) and $\mathbf{n}$ is the normal to the surface. The local equation of the linear momentum is written under the following form :

$$\rho_0 \dot{\mathbf{v}} = \rho_0 \mathbf{b} + \boldsymbol{\nabla} \cdot \boldsymbol{\sigma} \tag{2.16}$$

Law of conservation of angular momentum

The angular momentum M_Q is defined as :

$$\mathbf{M_Q} = \int_V \rho_0 (\mathbf{x} \wedge \mathbf{v}) dV \tag{2.17}$$

The resultant moment of mechanical forces is:

$$\mathbf{M_R} = \int_A (\mathbf{x} \wedge \bar{\mathbf{t}}) dA + \int_V \rho_0 (\mathbf{x} \wedge \mathbf{b}) dV \tag{2.18}$$

the conservation of angular momentum is written as:

$$\frac{d\mathbf{M_Q}}{dt} = \mathbf{M_R} \tag{2.19}$$

The local equation of the conservation of angular momentum shows that Cauchy stress tensor is symmetric.

$$\bar{\bar{\boldsymbol{\sigma}}} = \boldsymbol{\sigma}^T \tag{2.20}$$

Note that the law of conservation of energy will be presented in a subsequent section, since we need to expose general concepts of heat transfer and thermodynamics.

2.3 Basics of heat transfer

Heat transfer is a discipline of thermal engineering that concerns the generation, use, conversion, and exchange of thermal energy and heat between physical systems. Heat transfer is classified into various mechanisms, such as heat conduction, convection, thermal radiation, and transfer of energy by phase changes. Engineers also consider the transfer of mass of differing chemical species, either cold or hot, to achieve heat transfer. While these mechanisms have distinct characteristics, they often occur simultaneously in the same system [2, 75].
Heat is defined in physics as the transfer of thermal energy across a well defined boundary around a thermodynamic system. Fundamental methods of heat transfer in engineering include conduction, convection, and radiation. Physical laws describe the behavior and characteristics of each of these methods. Real systems often exhibit a complicated combination of them. Heat transfer methods are used in numerous disciplines, such as automotive engineering, thermal management of electronic devices and systems, climate control, insulation, materials processing, and power plant engineering.

Various mathematical methods have been developed to solve or approximate the results of heat transfer in systems. The amount of heat transferred in a thermodynamic process that changes the state of a system depends on how that process occurs, not only the net difference between the initial and final states of the process. Heat flux is a quantitative, vectorial representation of the heat flow through a surface [76].
Heat conduction, also called diffusion, is the direct microscopic exchange of kinetic energy of particles through the boundary between two systems. When an object is at a different temperature from another body or its surroundings, heat flows so that the body and the surroundings reach the same temperature, at which point they are in thermal equilibrium. Such spontaneous heat transfer always occurs from a region of high temperature to another region of lower temperature, as required by the second law of thermodynamics [96, 63].
Heat convection occurs when bulk flow of a fluid (gas or liquid) carries heat along with the flow of matter in the fluid. The flow of fluid may be forced by external processes, or sometimes (in gravitational fields) by buoyancy forces caused when thermal energy expands the fluid (for example in a fire plume), thus influencing its own transfer. The latter process is sometimes called "natural convection". All convective processes also move heat partly by diffusion, as well. Another form of convection is forced convection. In this case the fluid is forced to flow by use of a pump, fan or other mechanical means.
The final major form of heat transfer is by radiation, which occurs in any transparent medium (solid or fluid) but may also even occur across vacuum (as when the Sun heats the Earth). Radiation is the transfer of energy through space by means of electromagnetic waves in much the same way as electromagnetic light waves transfer light. The same laws that govern the transfer of light govern the radiant transfer of heat.

2.3.1 Fundamental modes of heat transfer

Conduction

On a microscopic scale, heat conduction occurs as hot, rapidly moving or vibrating atoms and molecules interact with neighboring atoms and molecules, transferring some of their energy (heat) to these neighboring particles. In other words, heat is transferred by conduction when adjacent atoms vibrate against one another, or as electrons move from one atom to another. Conduction is the most significant means of heat transfer within a solid or between solid objects in thermal contact. Fluids, especially gases are less conductive.
The law of heat conduction, also known as Fourier's law, states that the time rate of heat transfer through a material is proportional to the negative gradient in the temperature and to the area, at right angles to that gradient, through which the heat is flowing [45]. The differential form of fourier's law for isotropic materials is written as follow:

$$\mathbf{H} = -k\boldsymbol{\nabla}T \tag{2.21}$$

Where $\mathbf{H}$ is the local heat flux (Wm^{-2}), k is the material's conductivity ($Wm^{-1}K^{-1}$), and $\boldsymbol{\nabla}T$ is the temperature gradient (Km^{-1}).

The thermal conductivity, k, is often treated as a constant, though this is not always true. While the thermal conductivity of a material generally varies with temperature, the variation can be small over a significant range of temperatures for some common materials. In anisotropic materials, the thermal conductivity typically varies with orientation; in this case **K** is represented by a second-order tensor. In heterogeneous materials, **K** varies with spatial location.

Convection

Convection is the transfer of thermal energy from one place to another by the movement of fluids. Convection is usually the dominant form of heat transfer in liquids and gases. Although often discussed as a distinct method of heat transfer, convection describes the combined effects of conduction and fluid flow or mass exchange [10].
Two types of convective heat transfer may be distinguished:

1. *Free or natural convection* : when fluid motion is caused by buoyancy forces that result from the density variations due to variations of temperature in the fluid. In the absence of an external source, when the fluid is in contact with a hot surface, its molecules separate and disperse, causing the fluid to be less dense. As a consequence, the fluid is displaced while the cooler fluid gets denser and the fluid sinks. Thus, the hotter volume transfers heat towards the cooler volume of that fluid.

2. *Forced convection* : when a fluid is forced to flow over the surface by an external source such as fans, by stirring, and pumps, creating an artificially induced convection current.

Internal and external flow can also classify convection. Internal flow occurs when a fluid is enclosed by a solid boundary such when flowing through a pipe. An external flow occurs when a fluid extends indefinitely without encountering a solid surface. Both of these types of convection, either natural or forced, can be internal or external because they are independent of each other.
Convection-cooling can sometimes be described by Newton's law of cooling in cases where convection coefficient is independent or relatively independent of the temperature difference between object and environment.
Newton's law states that the rate of heat loss of a body is proportional to the difference in temperatures between the body and its surroundings. Mathematically, this can be written as:

$$\frac{dQ}{dt} = \dot{Q} = hA(T_{\text{env}} - T(t)) = -hA\Delta T(t) \tag{2.22}$$

where, Q is the thermal energy (J) and h is the heat transfer coefficient ($Wm^{-2}K^{-1}$).

Radiation

Thermal radiation is the emission of electromagnetic waves from all matter that has a temperature greater than absolute zero (theoretical temperature at which entropy reaches its minimum value) [81], it represents a conversion of thermal energy into electromagnetic energy.
The Stefan-Boltzmann law states that the total energy radiated of a black body[1] is directly proportional to the fourth power of the black body's thermodynamic temperature T:

$$e(T) = \sigma T^4. \tag{2.23}$$

where σ is the Stefan-Boltzmann constant ($5.67 \times 10^{-8}\ Wm - 2K - 4$) and e is the total energy (J/m^2).
A more general case is of a grey body, the one that doesn't absorb or emit the full amount of radiative flux. Instead, it radiates a portion of it, characterized by its emissivity, ϵ:

$$e(T) = \varepsilon \sigma T^4 \tag{2.24}$$

where ε is the emissivity of the grey body ($\varepsilon \leq 1$); if it is a perfect blackbody, $\epsilon = 1$. Still in more general (and realistic) case, the emissivity depends on the wavelength, $\epsilon = \epsilon(\lambda)$.
In space engineering, thermal radiation is considered one of the fundamental methods of heat transfer such as in satellites and outer space, but is counted less in industrial problem where only convection and conduction heat transfer are only considered.

2.4 Basics of thermodynamics

Thermodynamics is a physical science that studies the effects on material bodies, of transfer of heat and of work done on or by the bodies. It interrelates macroscopic variables, such as temperature, volume and pressure, which describe physical properties of material bodies, which in this science are called thermodynamic systems.
A thermodynamic system is a system that performs heat exchange under the form of heat/work with the environment.

2.4.1 Thermodynamic state

A thermodynamic state is a set of values of properties of a thermodynamic system that must be specified to reproduce the system. The individual parameters are known as state variables, state parameters or thermodynamic variables. Once a sufficient set of thermodynamic variables have been specified, values of all other properties of the system are uniquely determined. The number of values required to specify the state depends on the system, and is not always known.

[1] A black body is an idealized physical body that absorbs all incident electromagnetic radiation, regardless of frequency or angle of incidence

2.4.2 Thermodynamic state variable

A state variable is a characteristic quantity of a thermodynamic system or sub-system, that can be scalar (temperature ...), a vector, or a tensor (strain ...).
When a system is at thermodynamic equilibrium under a given set of conditions, it is said to be in a definite thermodynamic state, which is fully described by its state variables.
Thermodynamic state variables are of two kinds, extensive (mass, volume ...) and intensive (temperature, pressure ...).
The choice of state variables is guided by the desired fineness of the description and the observation of phenomena to be modeled

2.4.3 Entropy

Entropy is a thermodynamic property that can be used to determine the energy not available for work in a thermodynamic process, such as in energy conversion devices, engines, or machines. Such devices can only be driven by convertible energy, and have a theoretical maximum efficiency when converting energy to work. During this work, entropy accumulates in the system, which then dissipates in the form of waste heat [90].
The concept of entropy is defined by the second law of thermodynamics, which states that the entropy of an isolated system always increases or remains constant.
Entropy is a tendance of a process to reduce the state of order of the initial systems (spontaneous flow of thermal energy), and therefore entropy is an expression of disorder or randomness.

2.4.4 Specific internal energy

In thermodynamics, the internal energy is the total energy contained by a thermodynamic system. The internal energy is a state function of a system, because its value depends only on the current state of the system and not on the path taken or process undergone to arrive at this state. It is an extensive quantity. A corresponding intensive thermodynamic property called specific internal energy is defined as internal energy per a unit of mass [13].
The expression that relates the specific internal energy to specific entropy is given by:

$$T = \frac{du(\eta)}{d\eta} \tag{2.25}$$

where T is the temperature (K), u is the specific internal energy (J/kg), and η is the specific entropy (entropy per unit mass) $(J.kg/K)$, and $u(\eta)$ is a convex state function in order to ensure material stability.

2.4.5 First law of thermodynamics

The first law of thermodynamics states that energy can be transformed, but cannot be created nor destroyed. It is usually formulated by stating that the change in the internal energy of a system is equal to the amount of heat supplied to the system, minus the amount of work performed by the system on its surroundings, in other words it is a transformation from heat energy to mechanical energy and vice versa. It can be written as:

$$\frac{dU}{dt} + \frac{dK_e}{dt} = P_{ext} + P_{th} \tag{2.26}$$

Where

$$U = \int_V \rho_0 u dV \tag{2.27}$$

$$K_e = \int_V \frac{1}{2}\rho_0 \mathbf{v}\cdot\mathbf{v} dV \tag{2.28}$$

$$P_{ext} = \int_V \mathbf{b}\cdot\mathbf{v} dV - \int_A \mathbf{t}\cdot\mathbf{v} dA \tag{2.29}$$

$$P_{th} = \int_V \rho_0 r dV - \int_A \mathbf{H}\cdot\mathbf{n} dA \tag{2.30}$$

Where

- U : Internal energy of the system
- K_e : Kinetic energy of the system
- P_{ext} : Power done by external forces
- P_{th} : Power done by heat supplies
- r : Heat supply field
- $\mathbf{H}$: Heat flux
- u : Specific internal energy

Using the principle of virtual power, with physical velocity field chosen as virtual field, we can write :

$$P_i + P_{ext} = P_a = \frac{dK_e}{dt} \tag{2.31}$$

Where P_i, P_{ext} and P_a are the virtual power of internal, external and acceleration forces respectively.
The internal power is given by the following expression [99]

$$P_i = -\boldsymbol{\sigma} : \boldsymbol{D} \tag{2.32}$$

where $\boldsymbol{\sigma}$ is the Cauchy stress tensor and $\boldsymbol{D}$ is the rate of deformation tensor.

Equations (2.26) and (2.31) lead to:

$$\frac{dU}{dt} = -P_i + P_{th} \tag{2.33}$$

and

$$\frac{d}{dt}\int_V \rho_0 u dV = \int_V \boldsymbol{\sigma} : \boldsymbol{D} dV + \int_V \rho_0 r dV - \int_A \mathbf{H} \cdot \mathbf{n} dA \tag{2.34}$$

The local form is given as follow:

$$\rho_0 \frac{du}{dt} = \boldsymbol{\sigma} : \boldsymbol{D} + \rho_0 r - \boldsymbol{\nabla} \cdot \mathbf{H} \tag{2.35}$$

where $\boldsymbol{\nabla} \cdot \mathbf{H}$ is the divergence operator.

2.4.6 Free energy

The internal free energy (or Helmholtz free energy) is a thermodynamic potential that measures the useful work obtainable from a closed thermodynamic system at a constant temperature and volume. The internal free energy W is a state function, concave function of T, Legendre-Fenchel transform of the specific internal energy with respect to the specific entropy η. Mathematically it is written as follows:

$$W(T) = \inf_{\eta} \left(u(\eta) - \eta T\right) \tag{2.36}$$

Where η linked with T through equation (2.25)
We can write the heat equation (2.35) in entropy form:

$$\dot{u} = \frac{du}{d\eta}\dot{\eta} = T\dot{\eta} \tag{2.37}$$

$$\rho_0 \dot{\eta} = \frac{1}{T}\left(\boldsymbol{\sigma} : \boldsymbol{D} + \rho_0 r - \boldsymbol{\nabla} \cdot \mathbf{H}\right) \tag{2.38}$$

Lets denote η^* by the solution of (2.36), therefore:

$$W(T) = u(\eta^*) - \eta^* T \tag{2.39}$$

$$\frac{dW}{dT} = \frac{du}{d\eta}\frac{d\eta^*}{dT} - \frac{d\eta^*}{dT}T - \eta^* \tag{2.40}$$

$$\frac{dW}{dT} = \left(\frac{du}{d\eta} - T\right)\frac{d\eta^*}{dT} - \eta^* \tag{2.41}$$

Comparing equations (2.41) and (2.25), we can write

$$\eta = -\frac{dW(T)}{dT} \tag{2.42}$$

If we consider a pure thermal problem, the heat equation in entropy form is written as :

$$\rho_0 \dot{\eta} = \frac{1}{T}\left(\rho_0 r - \boldsymbol{\nabla}\cdot\mathbf{H}\right) \tag{2.43}$$

$$\rho_0 \frac{d\eta}{dT}\dot{T} = \frac{1}{T}\left(\rho_0 r - \boldsymbol{\nabla}\cdot\mathbf{H}\right) \tag{2.44}$$

$$-\rho_0 \frac{d^2W}{dT^2}\dot{T} = \frac{1}{T}\left(\rho_0 r - \boldsymbol{\nabla}\cdot\mathbf{H}\right) \tag{2.45}$$

We define the specific heat capacity as:

$$C(T) = -T\frac{d^2W(T)}{dT^2} \tag{2.46}$$

Therefore the heat equation is written in its classical form as:

$$\rho_0 C\dot{T} = \rho_0 r - \boldsymbol{\nabla}\cdot\mathbf{H} \tag{2.47}$$

2.4.7 Second law of thermodynamics

The second law of thermodynamics is an expression of the tendency that over time, differences in temperature, pressure, and chemical potential equilibrate in an isolated physical system. From the state of thermodynamic equilibrium, the law deduced the principle of the increase of entropy and explains the phenomenon of irreversibility in nature [55].
The first law of thermodynamics provides the basic definition of thermodynamic energy (or internal energy), associated with all thermodynamic systems, and states the rule of conservation of energy in nature. However, the concept of energy in the first law does not account for the observation that natural processes have a preferred direction of progress. For example, spontaneously, heat always flows to regions of lower temperature, never to regions of higher temperature without external work being performed on the system. The first law is completely symmetrical with respect to the initial and final states of an evolving system. The key concept for the explanation of this phenomenon through the second law of thermodynamics is the definition of a new physical property, the entropy S, defined as :

$$\mathcal{S} = \int_V \rho_0 \eta dV \tag{2.48}$$

and verifying

$$\frac{d\mathcal{S}}{dt} \geq \int_V \frac{Q}{T} dV = \int_V \frac{\rho_0 r}{T} dV - \int_A \frac{\mathbf{H}\cdot\mathbf{n}}{T} dA \tag{2.49}$$

where Q, r, $\mathbf{H}$, η are the total heat transfer, body heat supply, heat flux arriving on the surface and specific entropy, respectively.
Using the divergence theorem, equation (2.48) can be written under the local form :

$$\rho_0 \dot{\eta} - \frac{Q}{T} \geq 0 \tag{2.50}$$

or

$$\rho_0 \dot{\eta} + \boldsymbol{\nabla} \cdot \frac{\mathbf{H}}{T} - \frac{\rho_0 r}{T} \geq 0 \tag{2.51}$$

To note that in the particular case of a closed system driving a reversible process, the entropy equation will be written under the following

$$\frac{dS}{dt} = \int_V \frac{Q}{T} dV \tag{2.52}$$

By developing equation (2.51), we write:

$$\underbrace{\rho_0 \dot{\eta} - \frac{1}{T}\rho_0 r + \frac{1}{T}\boldsymbol{\nabla} \cdot \mathbf{H}}_{=0 \text{ (eq. (2.43))}} - \frac{1}{T^2}\mathbf{H} \cdot \boldsymbol{\nabla} T \geq 0 \tag{2.53}$$

Considering a purely thermal problem, by comparing equations (2.43) and (2.53) we deduce:

$$-\frac{1}{T^2}\mathbf{H} \cdot \boldsymbol{\nabla} T \geq 0 \tag{2.54}$$

often written under an alternative manner

$$\frac{1}{T} D^*_{ther} \geq 0 \tag{2.55}$$

where

$$D^*_{ther} \equiv -\mathbf{H} \cdot \frac{\boldsymbol{\nabla} T}{T} \qquad \text{is the thermal dissipation} \tag{2.56}$$

The thermal dissipation D^*_{ther} is always positive, physically it means that energy cannot be created, while the system can lose it. More interestingly, it shows why conduction k in Fourier law must be positive.

2.4.8 Clausius-Duhem inequality

Coming back to the general case, combining equations (2.35) and (2.53), and applying the divergence theorem:

$$\boldsymbol{\nabla} \cdot \left(\frac{\mathbf{H}}{T}\right) = (\frac{1}{T})\boldsymbol{\nabla} \cdot \mathbf{H} - \frac{1}{T^2}\mathbf{H} \cdot \boldsymbol{\nabla} T \tag{2.57}$$

we obtain the fundamental inequality of Clausius-Duhem:

$$\rho_0 \left(T\dot{\eta} - \dot{u}\right) - \boldsymbol{\sigma} : \mathbf{D} - \frac{\mathbf{H} \cdot \boldsymbol{\nabla} T}{T} \geq 0 \tag{2.58}$$

Equation (2.39) gives

$$\dot{W} = \dot{u} - \dot{T}\eta - T\dot{\eta} \tag{2.59}$$

Combining equations (2.58) and (2.59) leads to Clausius-Duhem inequality:

$$\boldsymbol{\sigma} : \mathbf{D} - \rho_0 \left(\dot{W} + \eta \dot{T} \right) - \frac{\mathbf{H} \cdot \boldsymbol{\nabla} T}{T} \geq 0 \tag{2.60}$$

The left hand side is the total dissipation that can be decomposed into mechanical and thermal dissipation denoted by D^*_{mech} and D^*_{therm}, respectively.
We have already showed that the thermal dissipation is always positive (2.55). It is usually assumed that the mechanical dissipation is also positive on its own, therefore we can write:

$$D^*_{mech} = \boldsymbol{\sigma} : \mathbf{D} - \rho_0 \left(\dot{W} + \eta \dot{T} \right) \geq 0 \tag{2.61}$$

$$D^*_{ther} = -\frac{\mathbf{H} \cdot \boldsymbol{\nabla} T}{T} \geq 0 \tag{2.62}$$

The two local equations of the first and the second principle, as well as the Clausius-Duhem inequality, constitute the fundamental concepts of thermodynamics.

2.4.9 Developping the general thermo-mechanical heat equation

To define the thermodynamic state of the system, we will need to refer to state variables . The hypothesis of local state postulate that the continuum thermodynamic state is defined through state variables that can be external or internal. Internal variables are linked to dissipative processes and describe the internal structure of the material on the microscopical level.
In thermo-mechanical context, states variables are the strain ϵ, the temperature T and internal variables $\boldsymbol{\xi}$ that can be scalar valued, vector valued, or tensor valued.
The free energy W is dependent on the strain tensor, temperature and internal variables

$$W = W\left(\boldsymbol{\epsilon}, T, \boldsymbol{\xi}\right) \tag{2.63}$$

Therefore

$$\dot{W} = \frac{\partial W}{\partial \boldsymbol{\epsilon}} \dot{\boldsymbol{\epsilon}} + \frac{\partial W}{\partial T} \dot{T} + \frac{\partial W}{\partial \boldsymbol{\xi}} \dot{\boldsymbol{\xi}} \tag{2.64}$$

Combining equations (2.60) and (2.64), and splitting the stress into a reversible and irreversible part

$$\boldsymbol{\sigma} = \boldsymbol{\sigma}^{rev} + \boldsymbol{\sigma}^{irr} \tag{2.65}$$

leads to

$$\left(\boldsymbol{\sigma}^{rev} - \rho_0 \frac{\partial W}{\partial \boldsymbol{\epsilon}} \right) : \dot{\boldsymbol{\epsilon}} - \rho_0 \left(\eta + \frac{\partial W}{\partial T} \right) \dot{T} + \boldsymbol{\sigma}^{irr} : \mathbf{D} - \rho_0 \frac{\partial W}{\partial \boldsymbol{\xi}} \dot{\boldsymbol{\xi}} - \frac{\mathbf{H} \cdot \boldsymbol{\nabla} T}{T} \geq 0 \tag{2.66}$$

where $\mathbf{D}$ is identified as the strain rate $\dot{\boldsymbol{\epsilon}}$[114], $\boldsymbol{\sigma}^{rev}$ and $\boldsymbol{\sigma}^{irr}$ are the reversible and irreversible stress, respectively.
To obtain a simpler equation, we consider the case of thermo-elastic process with a uniform temperature, therefore we can write equation (2.66) as

$$\left(\boldsymbol{\sigma}^{rev} - \rho_0 \frac{\partial W}{\partial \boldsymbol{\epsilon}}\right) : \dot{\boldsymbol{\epsilon}} - \rho_0 \left(\eta + \frac{\partial W}{\partial T}\right) \dot{T} \geq 0 \tag{2.67}$$

where the terms between brackets are independent of time derivative terms, therefore

$$\boldsymbol{\sigma}^{rev} = \frac{\partial \rho_0 W}{\partial \boldsymbol{\epsilon}} = \rho_0 \frac{\partial W}{\partial \boldsymbol{\epsilon}} \tag{2.68}$$

and

$$\eta = -\frac{\partial W}{\partial T} \tag{2.69}$$

Note that ρ_0 is considered constant in small strain hypothesis.
We admit that equations (2.68) and (2.69) are verified for all different admissible processes. Growth of entropy implies that the specific free energy is concave with respect to temperature.
We deduce the reduced form of the Clausius-Duhem inequality

$$\boldsymbol{\sigma}^{irr} : \mathbf{D} - \rho_0 \frac{\partial W}{\boldsymbol{\partial \xi}} \dot{\boldsymbol{\xi}} - \frac{\mathbf{H} \cdot \boldsymbol{\nabla} T}{T} \geq 0 \tag{2.70}$$

or

$$\boldsymbol{\sigma}^{irr} : \mathbf{D} + \mathbf{X} \cdot \dot{\boldsymbol{\xi}} - \frac{\mathbf{H} \cdot \boldsymbol{\nabla} T}{T} \geq 0 \tag{2.71}$$

where

$$\mathbf{X} = -\frac{\partial \rho_0 W}{\partial \boldsymbol{\xi}} \tag{2.72}$$

$\mathbf{X}$ are called the thermodynamic forces associated to the internal variables $\boldsymbol{\xi}$, or simply, $\mathbf{X}$ is conjugate to $\boldsymbol{\xi}$. From equations (2.68) and (2.69) we can say that the specific entropy η is conjugate to temperature T, and the reversible stress $\boldsymbol{\sigma}^{rev}$ is conjugate to strain $\boldsymbol{\epsilon}$.

From equation (2.71) we can write the mechanical dissipation as

$$D^*_{mech} = \boldsymbol{\sigma}^{irr} : \dot{\boldsymbol{\epsilon}} + \mathbf{X} \cdot \dot{\boldsymbol{\xi}} \tag{2.73}$$

where $\boldsymbol{D}$ is identified to the strain rate $\dot{\boldsymbol{\epsilon}}$.
We notice that the mechanical dissipation is composed into a sum of products "force-flux" involving the state variable's rate. The notion of force-flux is very common and consists of assuming a linear dependency. However this assumption is not always satisfied when the material behavior presents some aspect of plasticity or nonlinear visco-elasticity. The generalized standard material framework assumes that forces, or the dual force-flux is derived from a dissipation pseudo-potential function.

Table 2.1: Number of unkowns

Variable(s)	number of unknown(s)
Displacement $\mathbf{u}$	3
Deformation $\boldsymbol{\epsilon}$	6
reversible stress $\boldsymbol{\sigma}^{rev}$	6
stress tensor $\boldsymbol{\sigma}$	6
Temperature T	1
Heat flux $\mathbf{H}$	3
Entropy η	1
Internal variables $\boldsymbol{\xi}$	n
Conjugate to internal variables $\mathbf{X}$	n
Total number of unknowns	$2n + 26$

Generalized standard materials

When we count the number of equations and the number of unknowns in a thermo-mechanical problem, we find that the number of unknowns is $2n+26$ and the number of equations is $n + 20$, where n is the number of internal state variables (table 2.1 & 2.2), therefore we are interested in introducing the generalized standard material formalism allowing to write dissipative processes and obtain the missing $n + 6$ equations [28].

For this, we consider that there exists a pseudo-potential function denoted by $D(\dot{\boldsymbol{\epsilon}}, \dot{\boldsymbol{\xi}})$ that depends on the rate $\dot{\boldsymbol{\epsilon}}$ and $\dot{\boldsymbol{\xi}}$, positive, minimum and $D(0, 0) = 0$, where

$$\sigma^{irr} = \frac{\partial D(\dot{\boldsymbol{\epsilon}}, \dot{\boldsymbol{\xi}})}{\partial \dot{\boldsymbol{\epsilon}}} \tag{2.74}$$

and

$$\mathbf{X} = \frac{\partial D(\dot{\boldsymbol{\epsilon}}, \dot{\boldsymbol{\xi}})}{\partial \dot{\boldsymbol{\xi}}} \tag{2.75}$$

2.5 General thermo-mechanical heat equation

The heat equation is deduced from the first principle using state and complementary laws. It reveals the coupling between mechanical and thermal effects and specifies the variables that transform energy into heat during thermo-mechanical processes. The heat sources are diverse in nature and can be directly related to microstructural transformations undergone by the material [57].

To develop the heat equation, we have to rewrite equation (2.35) by substituting the

Table 2.2: Number of equations

Variable(s)	Number of equation(s)
Equations of motion	3
Constitutive law of the material	6
State law $\boldsymbol{\sigma}^{rev} = \rho_0 \frac{\partial W}{\partial \boldsymbol{\epsilon}}$	6
Heat equation	1
Fourier's law	3
State law $\eta = -\frac{\partial W}{\partial T}$	1
Conjugate to internal variables $\mathbf{X} = -\frac{\partial \rho_0 W}{\partial \boldsymbol{\xi}}$	n
Total number of equations	$n + 20$

specific internal energy $\dot{u}$ by the internal free energy $\dot{W}$, for this, we write:

$$\rho_0 \dot{u} = \rho_0 r - \boldsymbol{\nabla} \cdot \mathbf{H} + \boldsymbol{\sigma} : \dot{\boldsymbol{\epsilon}} \tag{2.76}$$

knowing that

$$u\left(\eta, \boldsymbol{\epsilon}, \boldsymbol{\xi}\right) = \sup_{T} \left[W\left(T, \boldsymbol{\epsilon}, \boldsymbol{\xi}\right) + \eta T\right] \tag{2.77}$$

leads to

$$\rho_0 \dot{u} = \rho_0 \frac{\partial u}{\partial \eta} \dot{\eta} + \frac{\partial \rho_0 u}{\partial \boldsymbol{\epsilon}} \dot{\boldsymbol{\epsilon}} + \frac{\partial \rho_0 u}{\partial \boldsymbol{\xi}} \dot{\boldsymbol{\xi}} \tag{2.78}$$

$$\rho_0 \dot{u} = \rho_0 T \dot{\eta} + \frac{\partial \rho_0 W}{\partial \boldsymbol{\epsilon}} \dot{\boldsymbol{\epsilon}} + \frac{\partial \rho_0 W}{\partial \boldsymbol{\xi}} \dot{\boldsymbol{\xi}} \tag{2.79}$$

$$\rho_0 \dot{u} = T \rho_0 \dot{\eta} + \boldsymbol{\sigma}^{\boldsymbol{rev}} : \dot{\boldsymbol{\epsilon}} - \mathbf{X} \cdot \dot{\boldsymbol{\xi}} \tag{2.80}$$

Combining equations 2.76 & 2.80, and splitting $\boldsymbol{\sigma}$ to $\boldsymbol{\sigma}^{rev} + \boldsymbol{\sigma}^{irr}$ lead to:

$$\rho_0 T \dot{\eta} = \mathbf{X} \cdot \dot{\boldsymbol{\xi}} + \mathbf{P}^{irr} + \rho_0 r - \boldsymbol{\nabla} \cdot \mathbf{H} \tag{2.81}$$

where

$$\mathbf{P}^{irr} = \boldsymbol{\sigma}^{irr} : \dot{\boldsymbol{\epsilon}} \tag{2.82}$$

Equation (2.81) is the heat equation in entropy form. Note that the internal dissipation (the term $\mathbf{X}\dot{\boldsymbol{\xi}}$) can be more than one variable.
Knowing that

$$\eta = -\frac{\partial W}{\partial T}\left(T, \boldsymbol{\epsilon}, \boldsymbol{\xi}\right) \tag{2.83}$$

leads to

$$\rho_0 \dot{\eta} = -\frac{\partial^2 \rho_0 W}{\partial T^2} \dot{T} - \frac{\partial^2 \rho_0 W}{\partial T \partial \boldsymbol{\epsilon}} \dot{\boldsymbol{\epsilon}} - \frac{\partial^2 \rho_0 W}{\partial T \partial \boldsymbol{\xi}} \dot{\boldsymbol{\xi}} \tag{2.84}$$

By defining the specific heat capacity C as:

$$C = -T\frac{\partial^2 \rho_0 W}{\partial T^2}(T, \boldsymbol{\epsilon}, \boldsymbol{\xi}) \tag{2.85}$$

we obtain the general thermo-mechanical heat equation:

$$\rho_0 C\dot{T} = T\frac{\partial^2 \rho_0 W}{\partial T \partial \boldsymbol{\epsilon}} : \dot{\boldsymbol{\epsilon}} + T\frac{\partial^2 \rho_0 W}{\partial T \partial \dot{\boldsymbol{\xi}}}\dot{\boldsymbol{\xi}} + \mathbf{X}\cdot\dot{\boldsymbol{\xi}} + \mathbf{P}^{irr} + \rho_0 r - \boldsymbol{\nabla}\cdot\mathbf{H} \tag{2.86}$$

The term $\mathbf{X}\dot{\boldsymbol{\xi}} + \mathbf{P}^{irr} = \mathbf{X}\dot{\boldsymbol{\xi}} + \boldsymbol{\sigma}^{irr} : \dot{\boldsymbol{\epsilon}}$ is the mechanical dissipation D^*_{mech} (equation 2.73). We can rewrite the equation under the following:

$$\rho_0 C\dot{T} + \boldsymbol{\nabla}\cdot\mathbf{H} = T\frac{\partial^2 \rho_0 W}{\partial T \partial \boldsymbol{\epsilon}} : \dot{\boldsymbol{\epsilon}} + T\frac{\partial^2 \rho_0 W}{\partial T \partial \dot{\boldsymbol{\xi}}}\dot{\boldsymbol{\xi}} + D^*_{mech} + \rho_0 r \tag{2.87}$$

This latter equation, shows that the variation of temperature created by the coupled terms, as well as by the stress and heat supply, will modify the temperature of the system (term $\rho_0 C\dot{T}$), or will be evacuated through conduction, outside the system (term $\boldsymbol{\nabla}\cdot\mathbf{H}$).
In our applications, we will model the heat flux by Fourier's law (eq.2.21).

2.5.1 Interpretation of coupled terms

In this section we will interpret the coupled terms in the heat equation (eq. 2.86). The coupled terms reveal the interactions between the temperature and other state variables that define the material. For a defined material in a thermo-mechanical problem, the state variables are the temperature, and a set of other state variables ($\boldsymbol{\epsilon}, \xi_i$ ...).
The general form of the coupled terms in heat equation has the following form:

$$T\frac{\partial^2 \rho_0 W}{\partial T \partial \alpha}\dot{\alpha}$$

Where α is any state variable ($T,\ \boldsymbol{\epsilon},\ \boldsymbol{\xi}$).

As an example, a material that has a thermo-elastic behaviour, the state variables are T and $\boldsymbol{\epsilon}$, and in this case the corresponding coupled term deformation-temperature (also called isentropic term), will be written as:

$$T\frac{\partial^2 \rho_0 W}{\partial T \partial \epsilon_{ij}}\dot{\epsilon_{ij}} \tag{2.88}$$

The coupled terms are interpreted as follows:

Term 1: $\mathbf{P}^{tot} = \boldsymbol{\sigma}^{irr} : \dot{\boldsymbol{\epsilon}} + \mathbf{X} \cdot \dot{\boldsymbol{\xi}}$ These classical terms are called: irreversible total power, and they describe the total irreversible power produced in the material. The first term $\boldsymbol{\sigma}^{irr} : \dot{\boldsymbol{\epsilon}}$ is the viscous dissipation, and the second term $\mathbf{X}\dot{\boldsymbol{\xi}}$ is the dissipation due to plasticity.

Term 2 : $\mathbf{P}^{s} = T\frac{\partial^2 \rho_0 W}{\partial T \partial \boldsymbol{\xi}}\dot{\boldsymbol{\xi}}$ This term models the irreversible power that is stored in the material, that is due to the disorder and creation of defects during an irreversible process and which is not dissipated as heat.

Term 3 : $\mathbf{P}^{ThElas} = T\frac{\partial^2 \rho_0 W}{\partial T \partial \boldsymbol{\epsilon}}\dot{\boldsymbol{\epsilon}}$ This term models the thermo-elastic power developed in the material. It is connected to Gough-Joule effect that predicts a decrease of temperature when the body is extended, and vice versa, an increase of temperature when elastic deformation is created by compression.

Note that the evaluation of the increase of temperature is done by neglecting the term $\mathbf{P}^s$ [4]. Various work where exposed in the engineering literature concerning this area [50, 117, 38, 12, 82] including the pioneering work of Taylor & Quinney [35]. After many experiments, they have concluded that the term $\mathbf{X} \cdot \dot{\boldsymbol{\xi}}$ represent between $[5 - 15\%]$ of the term $\boldsymbol{\sigma}^{rev} : \dot{\boldsymbol{\epsilon}}^p$, therefore we can write

$$\mathbf{P}^{tot} = \boldsymbol{\sigma}^{irr} : \dot{\boldsymbol{\epsilon}} + \beta \boldsymbol{\sigma}^{rev} : \dot{\boldsymbol{\epsilon}}^p \tag{2.89}$$

where β is called Taylor-Quinney factor $\beta \leq 1$, often fixed to 0.9.

2.6 Applications

2.6.1 Linear thermo-elasticity

State variables The state variables of a linear thermo-elastic problem are:

- T: the temperature
- $\boldsymbol{\epsilon}$: the strain tensor

Free energy There's no internal variable in linear thermo-elasticity, therefore the free energy is only function of the temperature and the stress tensor:

$$\rho_0 W\left(T, \boldsymbol{\epsilon}\right) = \frac{1}{2}\boldsymbol{\epsilon} : \overline{\overline{\overline{\mathbf{C}}}} : \boldsymbol{\epsilon} - \boldsymbol{\epsilon} : \overline{\overline{\overline{\mathbf{C}}}} : \boldsymbol{\alpha}\left(T - T_0\right) - \rho_0 C \frac{\left(T - T_0\right)^2}{2T_0} \tag{2.90}$$

where $\overline{\overline{\overline{\mathbf{C}}}}$ is the elasticity tensor (tensor of order 4), $\boldsymbol{\alpha}$ is the thermal dilatation tensor (tensor of order 2), and T_0 is the initial temperature of the body, usually taken equal to the environmental temperature (or the outside temperature).

Mechanical dissipation

$$D^*_{mech} = \boldsymbol{\sigma}^{irr} : \dot{\boldsymbol{\epsilon}} = 0$$

No mechanical dissipation in thermo-elasticity $\boldsymbol{\sigma}^{irr} = \frac{\partial D}{\partial \dot{\boldsymbol{\epsilon}}} = 0$.

Constitutive law of the material

$$\boldsymbol{\sigma} = \boldsymbol{\sigma}^{rev} + \boldsymbol{\sigma}^{irr} \tag{2.91}$$

$$\begin{aligned} \boldsymbol{\sigma} &= \boldsymbol{\sigma}^{rev} + \boldsymbol{\sigma}^{irr} \\ &= \frac{\partial \rho_0 W}{\partial \boldsymbol{\epsilon}} \\ &= \overline{\overline{\overline{\mathbf{C}}}} : (\boldsymbol{\epsilon} - \boldsymbol{\alpha}\,(T - T_0)) \end{aligned}$$

Hypothesis of small temperature fluctuations We consider that temperature fluctuations are small, therefore we can write:

$$T - T_{ref} = \theta < \varepsilon \tag{2.92}$$

or

$$|\frac{T}{T_{ref}} - 1| < \varepsilon \tag{2.93}$$

where T_{ref} is the reference temperature, usually taken equal to T_0, the initial temperature, and ε is an infinitesimal value close to zero.

Specific heat capacity In this section we will consider that the mechanical coefficients and dilatation coefficient are independent of temperature therefore we can write the heat capacity as

$$C = -T\frac{\partial^2 W}{\partial T^2} = C\frac{T}{T_0} \simeq C$$

Thermo-elastic heat equation

$$\rho_0 C\dot{T} = T\frac{\partial^2 \rho_0 W}{\partial T \partial \boldsymbol{\epsilon}} : \dot{\boldsymbol{\epsilon}} + \rho_0 r - \boldsymbol{\nabla} \cdot \mathbf{H} \tag{2.94}$$

$$\rho_0 C\dot{T} = -T\boldsymbol{\alpha} : \overline{\overline{\overline{\boldsymbol{C}}}} : \dot{\boldsymbol{\epsilon}} + \rho_0 r - \boldsymbol{\nabla} \cdot \mathbf{H} \tag{2.95}$$

Isotropic case In an isotropic case, the thermo-elastic equation can be rewritten as follows:

$$\rho_0 C\dot{T} = -T\alpha_0 \bar{\bar{\mathbf{I}}} : \bar{\bar{\bar{\bar{\boldsymbol{C}}}}} : \dot{\boldsymbol{\epsilon}} + \rho_0 r - \boldsymbol{\nabla} \cdot \mathbf{H} \tag{2.96}$$

where $\bar{\bar{\mathbf{I}}}$ is the identity matrix and

$$\bar{\bar{\mathbf{I}}} : \bar{\bar{\bar{\bar{\boldsymbol{C}}}}} : \dot{\boldsymbol{\epsilon}} = \kappa \; tr(\dot{\boldsymbol{\epsilon}})$$

where κ is the bulk modulus and $tr(\dot{\boldsymbol{\epsilon}}) = \dot{\epsilon_{11}} + \dot{\epsilon_{22}} + \dot{\epsilon_{33}}$ is the trace of $\dot{\boldsymbol{\epsilon}}$.
We can also write, in this case, the $2D$ elastic tensor as (Voigt notation):

$$\bar{\bar{\bar{\bar{\boldsymbol{C}}}}} = \begin{pmatrix} \lambda + 2\mu & \lambda & 0 \\ \lambda & \lambda + 2\mu & 0 \\ 0 & 0 & 2\mu \end{pmatrix} \tag{2.97}$$

where λ and μ are Lamé's coefficients defined as:

$$\lambda = \frac{\nu E}{(1+\nu)(1-2\nu)}$$

and

$$\mu = \frac{E}{2(1+\nu)} \tag{2.98}$$

where E and ν are Young and Poisson moduli, respectively.
The stress tensor is written as

$$\boldsymbol{\sigma} = \boldsymbol{\sigma}^{rev} = \frac{\partial \rho_0 W}{\partial \boldsymbol{\epsilon}} = \frac{T}{T_0} \bar{\bar{\bar{\bar{\mathbf{C}}}}} : (\boldsymbol{\epsilon} - \boldsymbol{\alpha}(T - T_0))$$

For $1D$ case we can write

$$\sigma = E\,(\epsilon - \alpha_0 (T - T_0))$$

If σ is constant and $\neq 0$, we can see clearly that an increase of temperature will lead to a decrease of strain.

2.6.2 Thermo-visco-elasticity

In our work, we will consider Kelvin-Voight's behaviour for visco-elastic problems. This model consists of a Newtonian damper and Hookean elastic spring connected in parallel, (see picture 2.1). It is used to explain the creep behaviour of polymers [105].

State variables The state variables are the same as introduced in the linear elastic model (temperature T and the strain $\boldsymbol{\epsilon}$)

Free energy It has the same expression as in thermo-elasticity, as a consequence, the heat capacity and the reversible stress as well.

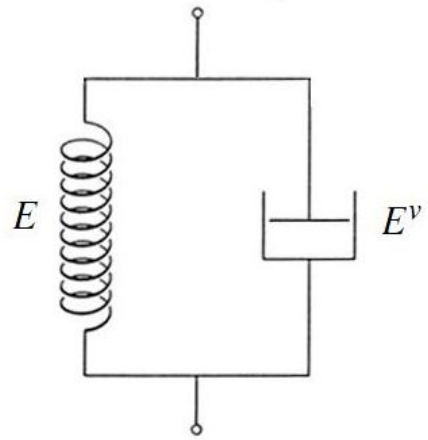

Figure 2.1: Kelvin Voigt model

Dissipation potential The dissipation potential has a quadratic form with respect to the strain rate, and is written as:

$$\mathcal{D} = \phi(\dot{\boldsymbol{\epsilon}}) = \frac{1}{2}\dot{\boldsymbol{\epsilon}} : \overline{\overline{\overline{\overline{\mathbf{C^v}}}}} : \dot{\boldsymbol{\epsilon}} \tag{2.99}$$

Where $\overline{\overline{\overline{\overline{\mathbf{C^v}}}}}$ is the viscosity tensor of order 4.

Mechanical dissipation

$$\boldsymbol{\sigma}^{irr} = \frac{\partial \phi}{\partial \dot{\boldsymbol{\epsilon}}} = \overline{\overline{\overline{\overline{\mathbf{C}^v}}}} : \dot{\boldsymbol{\epsilon}} \tag{2.100}$$

The mechanical dissipation will be written as

$$D^*_{mech} = \dot{\boldsymbol{\epsilon}} : \overline{\overline{\overline{\overline{\mathbf{C}^v}}}} : \dot{\boldsymbol{\epsilon}} \tag{2.101}$$

Constitutive law of the material The reversible part of the stress has the same expression as in linear elasticity

$$\boldsymbol{\sigma}^{rev} = \frac{\partial \rho_0 W}{\partial \boldsymbol{\epsilon}} = \overline{\overline{\overline{\overline{\mathbf{C}}}}} : (\boldsymbol{\epsilon} - \boldsymbol{\alpha}(T - T_0))$$

while the irreversible stress is written as

$$\boldsymbol{\sigma}^{irr} = \frac{\partial \phi}{\partial \dot{\boldsymbol{\epsilon}}} \tag{2.102}$$

$$= \overline{\overline{\overline{\overline{\mathbf{C^v}}}}} : \dot{\boldsymbol{\epsilon}} \tag{2.103}$$

Therefore the total stress is

$$\boldsymbol{\sigma} = \boldsymbol{\sigma}^{rev} + \boldsymbol{\sigma}^{irr} = \overline{\overline{\overline{\overline{\mathbf{C}}}}} : (\boldsymbol{\epsilon} - \boldsymbol{\alpha}(T - T_0)) + \overline{\overline{\overline{\overline{\mathbf{C}^v}}}} : \dot{\boldsymbol{\epsilon}} \tag{2.104}$$

Heat equation of a thermo-visco-elastic problem

$$\rho_0 C\dot{T} = T\frac{\partial^2 \rho_0 W}{\partial T \partial \boldsymbol{\epsilon}} : \dot{\boldsymbol{\epsilon}} + D^*_{mech} + \rho_0 r - \boldsymbol{\nabla}\cdot\mathbf{H} \tag{2.105}$$

$$\rho_0 C\dot{T} = -T\boldsymbol{\alpha} : \overline{\overline{\boldsymbol{C}}} : \dot{\boldsymbol{\epsilon}} + \dot{\boldsymbol{\epsilon}} : \overline{\overline{\mathbf{C}^v}} : \dot{\boldsymbol{\epsilon}} + \rho_0 r - \boldsymbol{\nabla}\cdot\mathbf{H} \tag{2.106}$$

In the case of an isotropic material, the viscous rigidity matrix (in $2D$) is written as:

$$\overline{\overline{\boldsymbol{C^v}}} = \begin{pmatrix} \lambda^v + 2\mu^v & \lambda^v & 0 \\ \lambda^v & \lambda^v + 2\mu^v & 0 \\ 0 & 0 & 2\mu^v \end{pmatrix} \tag{2.107}$$

where λ^v and μ^v are viscous Lamé's coefficients defined as:

$$\lambda^v = \frac{\nu^v E^v}{(1+\nu^v)(1-2\nu^v)}$$

and

$$\mu^v = \frac{E^v}{2(1+\nu^v)} \tag{2.108}$$

where E^v and ν^v are viscous Young modulus and Poisson ratio moduli, respectively.

2.6.3 Thermo-plasticity

State variables The state variables in thermoplasticity are

- The temperature T
- The strain $\boldsymbol{\epsilon}$
- The plastic part of strain $\boldsymbol{\epsilon}^p$

Free energy The free energy in thermo-plasticity is defined as

$$\rho_0 W(T, \boldsymbol{\epsilon}, \boldsymbol{\epsilon}^p) = \rho_0 W^e(T, \boldsymbol{\epsilon} - \boldsymbol{\epsilon}^p) + \rho_0 W^p(\boldsymbol{\epsilon}^p, T) + \rho_0 W^h(T) \tag{2.109}$$

Mechanical dissipation In thermo-plasticity, the mechanical dissipation can be written as

$$D^*_{mech} = \mathbf{X} : \dot{\boldsymbol{\epsilon}}^p \tag{2.110}$$

where the driving thermodynamic force of the plastic strain is written as

$$\boldsymbol{X} = -\frac{\partial \rho_0 W}{\partial \boldsymbol{\epsilon}^p} = -\left(-\frac{\partial \rho_0 W^e}{\partial \boldsymbol{\epsilon}^e} + \frac{\partial \rho_0 W^p}{\partial \boldsymbol{\epsilon}^p}\right) \tag{2.111}$$

where

$$\boldsymbol{\sigma}^{rev} = \frac{\rho_0 W^e}{\partial \epsilon^e} = \overline{\overline{\overline{\mathbf{C}}}} : ((\boldsymbol{\epsilon} - \boldsymbol{\epsilon}^p) - \boldsymbol{\alpha}(T - T_0)) \tag{2.112}$$

and

$$-\frac{\partial \rho_0 W^p}{\partial \boldsymbol{\epsilon}^p} \equiv \boldsymbol{\sigma}^c \tag{2.113}$$

where $\boldsymbol{\sigma}^c$ is called back-stress. Therefore equation (2.111) becomes

$$\mathbf{X} = \boldsymbol{\sigma} - \boldsymbol{\sigma}^c \tag{2.114}$$

Therefore we obtain the mechanical dissipation

$$D^*_{mech} = (\boldsymbol{\sigma} - \boldsymbol{\sigma}^c) : \dot{\boldsymbol{\epsilon}}^p \tag{2.115}$$

In simulation normally we replace the term $\boldsymbol{\sigma} - \boldsymbol{\sigma}^c$ by the term $\beta\boldsymbol{\sigma}$, with β a scalar ≤ 1. The mechanical dissipation becomes

$$D^*_{mech} = \beta\boldsymbol{\sigma} : \dot{\boldsymbol{\epsilon}}^p \tag{2.116}$$

Taylor, Quinney have measured $\beta \in [0.8, 1.0]$ for most material, but for some other material it can have different range, but never greater than one.

Constitutive law of the material

$$\boldsymbol{\sigma} = \boldsymbol{\sigma}^{rev} = \frac{\partial \rho_0 W^e}{\partial \epsilon^e} \tag{2.117}$$

$$\boldsymbol{\sigma} = \overline{\overline{\overline{\mathbf{C}}}} : ((\boldsymbol{\epsilon} - \boldsymbol{\epsilon}^p) - \boldsymbol{\alpha}(T - T_0)) \tag{2.118}$$

Heat equation of thermo-plasticity In a thermo-plastic problem, the heat equation is written as

$$\rho_0 C\dot{T} = T\frac{\partial^2 \rho_0 W}{\partial T \partial \boldsymbol{\epsilon}} : \dot{\boldsymbol{\epsilon}} + T\frac{\partial^2 \rho_0 W}{\partial T \partial \boldsymbol{\epsilon}^p} : \dot{\boldsymbol{\epsilon}}^p + D^*_{mech} + \rho_0 r - \boldsymbol{\nabla} \cdot \mathbf{H} \tag{2.119}$$

where

$$\frac{\partial^2 \rho_0 W}{\partial T \partial \boldsymbol{\epsilon}^p} = -\frac{\partial^2 \rho_0 W^e}{\partial T \partial \boldsymbol{\epsilon}^e} + \frac{\partial^2 \rho_0 W^p}{\partial T \partial \boldsymbol{\epsilon}^p} \tag{2.120}$$

The heat equation of a thermo-plastic problem becomes

$$\rho_0 C\dot{T} = T\frac{\partial^2 \rho_0 W^e}{\partial T \partial \boldsymbol{\epsilon}^e} : (\dot{\boldsymbol{\epsilon}} - \dot{\boldsymbol{\epsilon}}^p) + T\frac{\partial^2 \rho_0 W^p}{\partial T \partial \boldsymbol{\epsilon}^p} : \dot{\boldsymbol{\epsilon}}^p + \beta\boldsymbol{\sigma} : \dot{\boldsymbol{\epsilon}}^p + \rho_0 r - \boldsymbol{\nabla} \cdot \mathbf{H} \tag{2.121}$$

Where the term $T\frac{\partial^2 \rho_0 W^2}{\partial T \partial \boldsymbol{\epsilon}} : (\dot{\boldsymbol{\epsilon}} - \dot{\boldsymbol{\epsilon}}^p)$ is the thermo-elastic contribution, whereas $T\frac{\partial^2 \rho_0 W^p}{\partial T \partial \boldsymbol{\epsilon}^p} : \dot{\boldsymbol{\epsilon}}^p$ is the thermal effect on backstress. Note that the heat capacity does not change by hardening [44].
Dissipation and dilatation terms contribute much in thermo-elasticity and thermo-plasticity

(thermo-elastic contribution is typically smaller than plastic contribution, by at least one order of magnitude)
Thermal behaviour depend on the type of loading we apply (fast or slow loading).

In the section of applications in the next chapters, we will consider different thermo-mechanical problems, using the concepts defined in this chapter,many tests will be done considering different behaviours from weak to strong coupled problems.

Chapter 3

Numerical simulation of classical coupled thermo-mechanical problems

Résumé

Dans ce chapitre, on considère la formulation thermo-mécanique classique, telle que développée dans le chapitre précédent. On décrit l'implémentation de la formulation élément fini, ainsi que les différentes méthodes de résolution, avec une analyse numérique de chaque schéma algorithmique.

La simulation numérique des couplages thermo-mécaniques en calcul des structures présente encore un certain nombre de défis, spécialement lorsque les effets de couplage sont très marqués (couplage fort). De nombreuses approches algorithmiques ont été proposées dans la littérature pour ce type de problème. Les méthodes les plus utilisées sont:

- *les approches monolithiques, qui traitent simultanément l'équilibre mécanique et l'équilibre thermique, où l'algorithme de résolution est appliqué au problème non partitionné. Dans ce cas, l'utilisation des schémas implicites conduisent toujours à une stabilité inconditionelle.*
- *les approches étagées, qui traitent alternativement chacun des sous-problèmes mécanique et thermique, où chaque partition est traitée avec un algorithme different.*

La difficulté est d'obtenir un bon compromis entre les aspects de précision, stabilité numérique et coût de calcul.

Les schémas monolithiques on l'avantage d'être inconditionnellement stable, mais ils présentent des désavantages tel que les coûts de calculs énormes qu'ils peuvent engendrer (liés à l'inversion de la matrice tangente totale qui est en générale non-symmétrique),

ainsi que leur incapacité à tirer avantage des différents temps caractéristiques des problèmes mécanique et thermique.

Les schémas étagés on été conçus dans le but de surmonter les difficultés liées aux schémas monolithiques. Ils consistent à décomposer le problème thermo-mecanique afin de réduire la taille des système algébriques. Dans ce cas la matrice tangente est plus facilement évaluée, comme les sous-matrices de couplage n'existent plus ou quasi-plus.

3.1 Introduction

In this chapter, we will consider the thermo-mechanical formulation developed in the previous chapter, implementation of the finite element method, exposing different algorithmic procedures, and numerical analysis for each scheme.

Various time stepping algorithmic approaches have been proposed in the literature for thermo-mechanical problems [106, 108, 80, 32], such as :

- Monolithic (or simultaneous) approaches that consist of resolving simultaneously mechanical and thermal balance equations, where time stepping algorithm is applied to the full problem of evolution. In this case, using implicit schemes always lead to unconditional stability, which mean that the difference between two initially close solution always remains bounded independently by the time step size [9] (precision is always affected by time step size, but numerical error are not amplified (stability)).

- Staggered approaches where coupled system is partitioned (without a fixed point), then each of the mechanical and thermal problem is solved alternatively, and each partition can be treated by a different time stepping algorithm [110, 41, 111, 112].

Monolithic schemes have the advantage of being unconditionally stable, but their disadvantages is that they might lead to impossibly large systems, do not take advantage of the different time scales involved in the problem and often lead to non-symmetric structure (non-symmetric tangent matrix).
The goal of the partitioned (or staggered) schemes is to overcome these inconveniences, but unfortunately, they often lead to conditional stability [31, 39, 42, 108].
Two types of staggered algorithm will be presented is this chapter: "isothermal split staggered algorithm" and "adiabatic split staggered algorithm".
Stability analysis is exposed in the appendix, and summarized in this chapter when exposing monolithic and staggered schemes that are generalized to all non-linear coupled problems.

3.2 Finite element discretization of the classical non-symmetric thermo-mechanical problem

In this section we will apply the finite element method to the general thermo-mechanical problem. In subsequent sections FEM will be applied to particular cases such as thermo-elastic and thermo-visco-elastic problems.

Let $\nu \subset \mathbb{R}^{n_{dim}}$ denote the admissible thermo-mechanical configurational space of a continuum body $\mathcal{B}_0$, where $\partial\mathcal{B}_0$ is its smooth boundary, with $n_{dim} = 1, 2$ or 3. Let $\mathbf{u}$ and T denote the displacement field and the temperature field, respectively.
The evolution of thermal and mechanical equations treated in the previous chapter (eq. 2.16 & eq. 2.86 respectively) are supplemented by the following boundary conditions:

$$\nu^{mech} = \left\{ \mathbf{u} : \mathcal{B}_0 \to \mathbb{R}^3 | \mathbf{u} = \overline{\mathbf{u}} \text{ on } \partial_{\mathbf{u}}\mathbf{B}_0 \times [0,t]; \boldsymbol{\sigma} : \mathcal{B}_0 \to \mathbb{R}^6 | \boldsymbol{\sigma} \cdot \mathbf{n} = \overline{\mathbf{t}}_0 \text{ on } \partial_\sigma \mathbf{B}_0 \times [0,t] \right\} \tag{3.1}$$

and

$$\nu^{th} = \left\{ T : \mathcal{B}_0 \to \mathbb{R}_+ | T = \overline{T} \text{ on } \partial_T \mathbf{B}_0 \times [0,t]; \mathbf{H} : \mathcal{B}_0 \to \mathbf{R}^3 | \mathbf{H} \cdot \mathbf{n} = \overline{\mathbf{H}}\mathbf{n} \text{ on } \partial_H \mathbf{B}_0 \times [0,t] \right\} \tag{3.2}$$

where

$$\nu = \nu^{mech} \cup \nu^{th} \tag{3.3}$$

The boundary $\partial\Omega$ is decomposed as:

$$\partial\Omega = \partial_u\mathcal{B}_0 \cup \partial_\sigma\mathcal{B}_0 = \partial_T\mathcal{B}_0 \cup \partial_H\mathcal{B}_0 \tag{3.4}$$

with

$$\partial_u\mathcal{B}_0 \cap \partial_\sigma\mathcal{B}_0 = \partial_T\mathcal{B}_0 \cap \partial_H\mathcal{B}_0 = \varnothing \tag{3.5}$$

The initial conditions are given by

$$\begin{cases} \mathbf{u} = \mathbf{u}_0 \\ \dot{\mathbf{u}}_0 = \mathbf{v}_0 \\ T = T_0 \end{cases} \qquad \text{in } \mathcal{B}_0 \times \{0\} \tag{3.6}$$

From local mechanical and thermal equations (eq. 2.16 & eq. 2.86 respectively), we apply weighted residual method in order to obtain the weak form linked to thermo-mechanical operator, that will be discretized using the finite element method.

$$\int_{\mathcal{B}_0} \boldsymbol{\zeta} \cdot (\rho_0 \dot{\mathbf{v}} - \rho_0 \mathbf{b} - \boldsymbol{\nabla} \cdot \boldsymbol{\sigma})\, dV = 0 \tag{3.7}$$

where $\boldsymbol{\zeta}$ is the weighted function, and is set to zero on the boundary $\partial_u\mathcal{B}_0$.
By integrating by part we obtain:

$$\int_{\mathcal{B}_0} (\boldsymbol{\zeta} \cdot \rho_0 \dot{\mathbf{v}} - \boldsymbol{\zeta} \cdot \rho_0 \mathbf{b} - \boldsymbol{\nabla} \cdot (\boldsymbol{\zeta} \cdot \boldsymbol{\sigma}) + \boldsymbol{\nabla}\boldsymbol{\zeta} : \boldsymbol{\sigma})\, dV = 0 \tag{3.8}$$

Using equation 2.20 leads to

$$\boldsymbol{\sigma} : \boldsymbol{\nabla}_s \mathbf{u} = (\boldsymbol{\nabla} \cdot \mathbf{u}) \cdot \boldsymbol{\sigma} - \mathbf{u} \cdot (\boldsymbol{\nabla} \cdot \boldsymbol{\sigma}) \tag{3.9}$$

where

$$\boldsymbol{\nabla}_s \mathbf{u} = \frac{1}{2} \left(\boldsymbol{\nabla} \mathbf{u} + \boldsymbol{\nabla}^{\mathcal{T}} \mathbf{u} \right) \tag{3.10}$$

where the $\mathcal{T}$ index denotes the transpose.
Using the divergence theorem, we can rewrite equation 3.9 under

$$\int_{\mathcal{B}_0} \left(\boldsymbol{\zeta} \cdot \rho_0 \dot{\mathbf{v}} - \boldsymbol{\zeta} \cdot \rho_0 \mathbf{b} + \boldsymbol{\nabla} \boldsymbol{\zeta} : \boldsymbol{\sigma} \right) dV - \int_{\partial_\sigma \mathbf{B}_0} \boldsymbol{\zeta} \cdot \bar{\mathbf{t}}_0 dA = 0 \tag{3.11}$$

Following the same manner, we obtain the weak form for the thermal problem:

$$\int_{\mathcal{B}_0} \zeta \left(\rho_0 C \dot{T} - T \frac{\partial^2 \rho_0 W}{\partial T \partial \boldsymbol{\epsilon}} : \dot{\boldsymbol{\epsilon}} - T \frac{\partial^2 \rho_0 W}{\partial T \partial \dot{\boldsymbol{\xi}}} \dot{\boldsymbol{\xi}} - \mathbf{X} \cdot \boldsymbol{\xi} - \sigma^{irr} : \dot{\boldsymbol{\epsilon}} - \rho_0 r + \boldsymbol{\nabla} \cdot (\mathbf{H}) \right) dV = 0 \tag{3.12}$$

By integrating by part we can write

$$\zeta \boldsymbol{\nabla} \cdot (\mathbf{H}) = \boldsymbol{\nabla} \cdot (\mathbf{H} \zeta) - \mathbf{H} \cdot \boldsymbol{\nabla} \zeta$$

Using divergence theorem leads to

$$\begin{aligned} &\int_{\mathcal{B}_0} \left[\zeta \left(\rho_0 C \dot{T} - T \frac{\partial^2 \rho_0 W}{\partial T \partial \boldsymbol{\epsilon}} : \dot{\boldsymbol{\epsilon}} - T \frac{\partial^2 \rho_0 W}{\partial T \partial \dot{\boldsymbol{\xi}}} \dot{\boldsymbol{\xi}} - \mathbf{X} \boldsymbol{\xi} - \sigma^{irr} : \dot{\boldsymbol{\epsilon}} - \rho_0 r \right) - \mathbf{H} \cdot \boldsymbol{\nabla} \zeta \right] dV \\ &- \int_{\partial_{\overline{H}} \mathcal{B}_0} \zeta \overline{\mathbf{H}} \cdot \mathbf{n} dA - \int_{\partial_h \mathcal{B}_0} \zeta h (T - T_{env}) dA = 0 \end{aligned} \tag{3.13}$$

where the term $\int_{\partial_h \mathcal{B}_0} \zeta h (T - T_{env}) dA$ is the heat exchange with the environment by convection, where T_{env} is the outside temperature and h is the convection coefficient. We recall that $\mathbf{H}$ usually follows Fourier's law ($\mathbf{H} = -\mathbf{K} \cdot \boldsymbol{\nabla} T$), where $\mathbf{K}$ is the thermal conduction matrix.

The discretization of the thermal and mechanical weak form equation (eq. 3.11 & eq. 3.13) will lead to a set of non-linear algebraic equations, that are function of the generalized displacements $\mathbf{u}_i$ and T_i evaluated at node i of the discretized space, where $\mathbf{u}_i$ and T_i are the displacement and the temperature connected to node i.
Inside each element the unknown generalized displacements are obtained through interpolation of nodal values using the shape function ϕ_i of the element. We have chosen here, for simplicity, the same shape function for the thermal and mechanical problem.
Using iso-parametric elements (fig. 3.1), the geometry of each element is deduced through shape functions and the position of nodes.

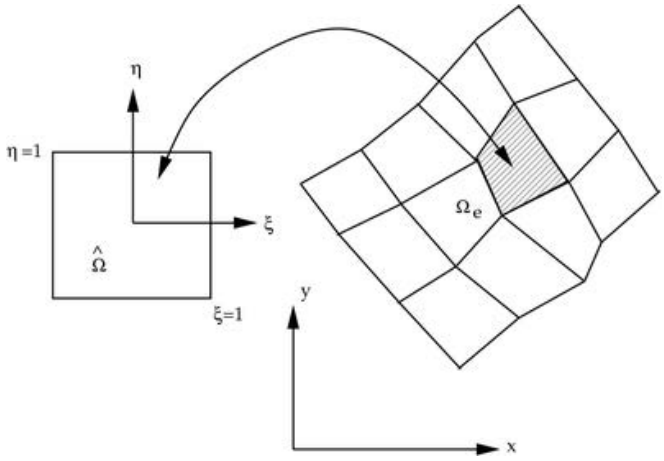

Figure 3.1: Connection between isoparametric coordinates and real coordinates

If we denote by $\mathbf{z} = [\varphi_i, T_i]^{\mathcal{T}} = [u_i, T_i]^{\mathcal{T}}$ the generalized displacement in the real space, then we can write

$$\mathbf{z}\,(\xi, \eta) = \sum_{i=0}^{N_{nodes}} \phi_{\mathrm{i}}(\xi, \eta)\mathbf{z}_i(t)$$

where $\mathbf{z}_i = [u_i, T_i]^{\mathcal{T}}$, N_{nodes} the total number of nodes that make up the finite elements, and $\phi_{\mathrm{i}}(\xi, \eta)$ is the shape function that is independent of time.

FEM implementation Applying the finite element method as described previously, we can rewrite equations 3.11 and 3.13 as follow:

$$\left(\int_{\hat{\Omega}} \rho_0 \boldsymbol{\phi}\boldsymbol{\phi}^{\mathcal{T}} \hat{J} d\hat{V}\right) \dot{\mathbf{v}} - \int_{\hat{\Omega}} \rho_0 \boldsymbol{\phi}\mathbf{b}\hat{J} d\hat{V} + \int_{\hat{\Omega}} \mathbf{B}\boldsymbol{\sigma}\hat{J} d\hat{V} - \int_{\partial_t \hat{\Omega}} \boldsymbol{\phi}\bar{\mathbf{t}}\hat{J} d\hat{A} = 0 \tag{3.14}$$

and

$$\begin{aligned}&\left(\int_{\hat{\Omega}} \rho_0 C \boldsymbol{\phi}\boldsymbol{\phi}^{\mathcal{T}} \hat{J} d\hat{V}\right) \dot{T} - \int_{\hat{\Omega}} \dot{W}\boldsymbol{\phi}\hat{J} d\hat{V} - \int_{\hat{\Omega}} \mathbf{K}\mathbf{B}\mathbf{B}^{\mathcal{T}} \hat{J} d\hat{V}\; T - \int_{\partial_H \hat{\Omega}} \bar{\mathbf{H}}\boldsymbol{\phi}\hat{J} d\hat{V} \\ &- \left(\int_{\partial_h \hat{\Omega}} h\boldsymbol{\phi}\boldsymbol{\phi}^{\mathcal{T}} \hat{J} d\hat{A}\right) T + \int_{\partial_h \hat{\Omega}} h T_{env}\boldsymbol{\phi}\hat{J} d\hat{A} = 0\end{aligned} \tag{3.15}$$

where

- $\hat{\Omega}$: Domain in the iso-parametric space
- $\hat{V}$: Elementary volume in the iso-parametric space
- $\hat{A}$: Elementary surface in the isoparametric space
- $\mathbf{B}$: Gradient Matrix of shape functions
- $\boldsymbol{\phi}$: Assembly matrix of shape functions ϕ_i

Note that the matrix $\boldsymbol{\phi}$ has a different form for the mechanical or the thermal field. For the mechanical field $\boldsymbol{\phi}$ a matrix of dimension $(N_{node} \times n_{dim})$ where $n_{dim} = 1, 2$ *or* 3 is the space dimension, N_{node} is the total number of nodes. For the thermal field $\boldsymbol{\phi}$ is an array of dimension N_{nodes}.

3.3 Solving the coupled thermo-mechanical problem

The general thermo-mechanical problem with boundary and initial conditions, is reduced to a system of nonlinear algebraic equations, through space and temporal discritization. State variable being known at time $t = t^n$, the system of algebraic equations will solve the state variable at $t = t^{n+1}$.
Equations (3.14) and (3.15) can be written in an alternative way:

$$\mathbf{F}_i^{int} - \mathbf{F}_i^{ext} = 0 \quad where\ i = 1, ..., N^{nodes} \tag{3.16}$$

where $\mathbf{F}^{int}$ is the assembly of all mechanical and thermal volumic forces, and $\mathbf{F}^{ext}$ is the assembly of all mechanical and thermal surface forces.
For this case we can write

$$\begin{aligned}\mathbf{F}_{int}^{mechanical} = \bigcup_{e=1}^{N_{elements}} \left(\int_{\hat{\Omega}^e} \rho_0 \boldsymbol{\phi}\boldsymbol{\phi}^{\mathcal{T}} \hat{J} d\hat{V} \right) \dot{\mathbf{v}} - \bigcup_{e=1}^{N_{elements}} \int_{\hat{\Omega}^e} \rho_0 \boldsymbol{\phi}\mathbf{b}\hat{J} d\hat{V} \\ + \bigcup_{e=1}^{N_{elements}} \int_{\hat{\Omega}^e} \mathbf{B}\boldsymbol{\sigma}\hat{J} d\hat{V}\end{aligned} \tag{3.17}$$

$$\mathbf{F}_{ext}^{mechanical} = \bigcup_{e=1}^{N_{elements}} \int_{\partial_t \hat{\Omega}^e} \boldsymbol{\phi}\bar{\mathbf{t}}\hat{J} d\hat{A} \tag{3.18}$$

$$\begin{aligned}\mathbf{F}_{int}^{thermal} = \bigcup_{e=1}^{N_{elements}} \left(\int_{\hat{\Omega}^e} \rho_0 C \boldsymbol{\phi}\boldsymbol{\phi}^{\mathcal{T}} \hat{J} d\hat{V} \right) \dot{T} - \bigcup_{e=1}^{N_{elements}} \int_{\hat{\Omega}^e} \dot{W}\boldsymbol{\phi}\hat{J} d\hat{V} \\ - \bigcup_{e=1}^{N_{elements}} \int_{\hat{\Omega}^e} \mathbf{K}\mathbf{B}\mathbf{B}^{\mathcal{T}} \hat{J} d\hat{V} T\end{aligned} \tag{3.19}$$

$$\begin{aligned}\mathbf{F}_{ext}^{thermal} = \bigcup_{e=1}^{N_{elements}} \int_{\partial_H \hat{\Omega}^e} \bar{\mathbf{H}}\boldsymbol{\phi}\hat{J} d\hat{V} + \bigcup_{e=1}^{N_{elements}} \left(\int_{\partial_h \hat{\Omega}^e} h\phi\phi^{\mathcal{T}} \hat{J} d\hat{A} \right) T \\ - \bigcup_{e=1}^{N_{elements}} \int_{\partial_h \hat{\Omega}^e} hT_{env}\boldsymbol{\phi}\hat{J} d\hat{A} = 0\end{aligned} \tag{3.20}$$

where

$$\mathbf{F}_{int} = \mathbf{F}_{int}^{mechanical} \cup \mathbf{F}_{int}^{thermal} \tag{3.21}$$

and

$$\mathbf{F}_{ext} = \mathbf{F}_{ext}^{mechanical} \cup \mathbf{F}_{ext}^{thermal} \tag{3.22}$$

The solution of the thermo-mechanical problem is achieved when the generalized displacement $\mathbf{z}^* = [\mathbf{u}_i^*, T_i^*]$ satisfies equation 3.16. In next sections, we will skim the two alternative strategies for time stepping algorithms of the thermo-mechanical problem.

3.4 Monolithic solution scheme

In monolithic (also called simultaneous) strategies, the time stepping algorithm is applied to the full problem of evolution. The coupling between mechanical and thermal fields is done at each iteration where the internal and external mechanical forces are evaluated by taking into account the actual temperature, and for the thermal problem, the internal and external thermal force are evaluated by taking into account the actual displacement. It is until the last iteration that the actual temperature and displacement characterize the mechanical and thermal equilibrium state. Implicit schemes are most often used as a mean of achieving unconditional stability.

What we have exposed in the previous paragraph reveals the simultaneous solution of thermal and mechanical equilibrium. The goal is to find the generalized displacement that satisfies equation (3.16). For this we will solve the system of equations in an iterative manner, therefore we introduce the notion of residual force (or off-balance force) denoted by $\mathbf{F}_{o-b}$ and defined as:

$$\mathbf{F}_{o-b} = \mathbf{F}_{int} - \mathbf{F}_{ext} \tag{3.23}$$

By linearizing the system of equations (eq. 3.23), we can write

$$\mathbf{F}_{o-b}(\mathbf{z}^{k+1}) = \mathbf{F}_{o-b}(\mathbf{z}^{k}) + \left(\frac{\partial \mathbf{F}_{o-b}(\mathbf{z}^{k})}{\partial \mathbf{z}^{k}} \right) \Delta \mathbf{z} \tag{3.24}$$

where $\Delta \mathbf{z} = \mathbf{z}^{k+1} - \mathbf{z}^{k}$, and the index k stands for the iteration number.
We define the tangent stiffness matrix as

$$\mathbf{K} = \left(\frac{\partial \mathbf{F}_{o-b}(\mathbf{z}^{k})}{\partial \mathbf{z}^{k}} \right) \tag{3.25}$$

In our applications, the thermo-mechanical problem is solved using Newton schemes, that consist of iterating on the generalized displacement until the thermal and mechanical equilibrium is achieved (see table 4.1).

The decomposition of the generalized displacement $\mathbf{z} = [\boldsymbol{\varphi}_{n+1}, T_{n+1}]^T = [\mathbf{u}_{n+1}, T_{n+1}]^T$, and the residual forces $\mathbf{F}_{o-b} = [\mathbf{F}_{o-b}^{mechanical}, \mathbf{F}_{o-b}^{thermal}]$ allows us to rewrite the tangent matrix as follow:

$$\mathbf{K} = \begin{bmatrix} \mathbf{K}_{UU} & \mathbf{K}_{UT} \\ \mathbf{K}_{TU} & \mathbf{K}_{TT} \end{bmatrix} = \begin{bmatrix} \frac{\partial \mathbf{F}_{o-b}^{mechanical}}{\partial U} & \frac{\partial \mathbf{F}_{o-b}^{mechanical}}{\partial T} \\ \frac{\partial \mathbf{F}_{o-b}^{thermal}}{\partial U} & \frac{\partial \mathbf{F}_{o-b}^{thermal}}{\partial T} \end{bmatrix} \tag{3.26}$$

where

$$\mathbf{F}_{o-b}^{mechanical} = \mathbf{F}_{int}^{mechanical} - \mathbf{F}_{ext}^{mechanical} \tag{3.27}$$

and

$$\mathbf{F}_{o-b}^{thermal} = \mathbf{F}_{int}^{thermal} - \mathbf{F}_{ext}^{thermal} \tag{3.28}$$

The size of the tangent stiffness matrix $\mathbf{K}$ is $\left(ndof^{mechanical} + ndof^{thermal}\right) \times \left(ndof^{mechanical} + ndof^{thermal}\right)$, where $ndof^{mechanical}$ & $ndof^{thermal}$ denote numbers of mechanical and thermal degrees of freedom. The tangent stiffness matrix $\mathbf{K}$ is generally non-symmetric. We will expose in the next chapter the variational formulation of coupled thermo-mechanical problems that will lead to a symmetric formulation [79].

The goal is being to obtain a set of generalized displacement $\mathbf{z}^{k+1}$ until balance is attained, this is written as

$$\mathbf{F}_{o-b}(\mathbf{z}^{k+1}) \approx 0 \tag{3.29}$$

Therefore equation (3.24) is written as:

$$\begin{bmatrix} \mathbf{K}_{UU} & \mathbf{K}_{UT} \\ \mathbf{K}_{TU} & \mathbf{K}_{TT} \end{bmatrix} \begin{bmatrix} \delta\mathbf{U} \\ \delta\mathbf{T} \end{bmatrix} = - \begin{bmatrix} R_U \\ R_T \end{bmatrix} \tag{3.30}$$

where $\mathbf{R}_U = \mathbf{F}_{o-b}^{mechanical}(t = t^k)$ and $\mathbf{R}_T = \mathbf{F}_{o-b}^{thermal}(t = t^k)$ are the residuals of the mechanical and thermal problem respectively.

The inversion of the tangent stiffness matrix is the most crucial parameter determining the computational cost. In fact the evaluation of the coupled off-diagonal sub-matrices $\mathbf{K}_{UT}$ & $\mathbf{K}_{TU}$ that can be difficult to determine analytically, influences considerably the time cost. The accurate evaluation of the coupled sub-matrices is indispensable for the conservation of quadratic convergence rate of Newton scheme, otherwise convergence rate is deteriorated, as well as the limitation of the scheme stability, if coupled sub-matrices are neglected.
For this, alternative algorithms for the monolithic schemes are developed in this framework, aimed to circumventing this drawback, by neglecting, or at the limit taking into account a part of the coupled sub-matrices (for Uzawa-like scheme). Both algorithms will be exposed in the next chapter, and will be applied to thermo-mechanical problems in the application section.
Another disadvantage of the monolithic scheme is that it does not take advantage of the different time scales involved in the problem which means its inability to take into consideration the difference between thermal and mechanical characteristic time. For example, during a given time step, even though the initial temperature may be a good approximation of the solution problem, the tangent stiffness matrix still has the same dimension $\left(ndof^{mechanical} + ndof^{thermal}\right) \times \left(ndof^{mechanical} + ndof^{thermal}\right)$, and not $(ndof^{mechanical} \times ndof^{mechanical})$ as we expect to have.

Aside from these disadvantages, the monolithic (or simulataneous) scheme benefits from the unconditional stability property and has a better precision due to taking into account the coupled terms (see annex A for more details about stability).

3.5 Staggered schemes

Despite the unconditional stability property of monolithic schemes, they may lead to non-symmetric large systems that sometimes are hard to solve, and staggered schemes were designed to overcome the disadvantages linked to simultaneous schemes.
Staggered schemes (also called sequential schemes) were developed since two decades by Argyris & Doltsinis [110], Park & Felippa [41], Simo & Miehe [74, 30], Pelerin [80], etc... they were designed to decompose the coupled problem into a set of sub-problems, that will lead to a reduced size algebraic systems. In this case, the evaluation of the tangent stiffness matrix is easier given that coupled sub-matrices are no longer here (recall that difficulties in monolithic schemes were mainly from coupling stiffness matrices).

In this chapter, we will only deal with two types of staggered schemes:

- Isothermal staggered scheme
- Adiabatic staggered scheme

Despite they lead to a smaller system, and take advantage of the different time scales involved in the problem, staggered schemes methods are not all unconditional stable.

Staggered scheme reduces considerably the size of the system, in this case we obtain two systems of reduced size, $\left(ndof^{mechanical} \times ndof^{mechanical}\right)$ and $\left(ndof^{thermal} \times ndof^{thermal}\right)$ for the mechanical and thermal phase respectively.
In the classical approach the mechanical stiffness matrix can be symmetric if the stress in the material is small with respect to elastic material properties [113] and if pressure or contact boundary conditions are not present in the problem, the thermal stiffness matrix is symmetric if thermal conductivity is independent of time, and if thermo-mechanical contact boundary conditions are not present [114], whereas in variational approach these matrices are always symmetric [73, 79]

In the following sections, we will discuss the features of each staggered schemes.

3.5.1 Isothermal staggered scheme

The isothermal split, is a strategy in which first a mechanical phase is solved at constant temperature, followed by a purely thermal phase at fixed configuration (displacement). The split will be dealt at time step level in such a way that Newton-Raphson iterations

Table 3.1: Isothermal staggered scheme

1	*Predict the temperature field*	$\mathbf{z}^{thermal}(t = t^{k+1}) = \mathbf{z}^{thermal}(t = t^{k})$
2	*Solve for the mechanical field*	$\mathbf{F}_{h-e}^{mechanical}(\mathbf{z}) = 0$
3	*Which provides*	$\mathbf{z}^{mechanical}(t = t^{k+1})$
4	*Correct the temperature field*	$\mathbf{F}_{h-e}^{thermal}(\mathbf{z}) = 0$
5	*Which provides*	$\mathbf{z}^{thermal}(t = t^{k+1})$
6	*Compute velocity, acceleration and flux fields*	$\dot{\mathbf{u}}, \ddot{\mathbf{u}}$ *and* $\mathbf{H}$
7	*Move to next step*	$t = t + \Delta t$

are performed, until convergence, on the mechanical phase, and then Newton iterations are applied on the thermal phase.
To be more explicit, the mechanical phase is solved, where $T(t^{n+1}) = T(t^n)$ until mechanical equilibrium:

$$\mathbf{F}_{o-b}^{mechanical}\left(\mathbf{z}\left(t = t^{n+1}\right)\right) \approx 0 \tag{3.31}$$

then we solve the thermal phase at constant configuration until thermal equilibrium (see table 3.1).

Despite their time cost benefits, isothermal staggered schemes lead to conditional stability when the thermo-mechanical system exhibit a strong coupling, even if each of the phases is solved with an unconditionally stable implicit method (see annex A). For thermo-elastic problems, a convenient measure of the strength of the coupling is given by [108]:

$$\epsilon = \frac{(3\lambda + 2\mu)^2 \alpha^2 T^{ref}}{C(\lambda + 2\mu)} \tag{3.32}$$

where ϵ is a dimensionless parameter ($\epsilon < 1$ for weak coupling), λ *and* μ denote the Lamé constants, and α, T^{ref} *and* C denote the coefficient of thermal expansion, the reference temperature (usually taken equal to the environmental temperature) and the heat capac-

ity, respectively. Note that for most metals, ϵ has a value range between $[1.5-3.5\times10^{-2}]$.

Stabilization techniques have been proposed in the literature aiming to acquire the unconditional stability property of staggered schemes [91, 9, 92, 7, 24, 31, 5, 39] etc..., they are efficient to a certain extent and do not represent a general methodology that leads to the unconditionally stable staggered schemes (stabilization techniques are restricted to the linear semi-discrete problem).

3.5.2 Adiabatic staggered scheme

The adiabatic staggered scheme consists of partitioning the thermo-mechanical problem into an adiabatic elasto-dynamic phase, in which the entropy of the system is held constant, followed by a heat conduction phase at fixed configuration (eq. 3.33 & 3.34). This scheme allows to overcome the conditional stability property exposed by the isothermal staggered scheme.

Even though adiabatic staggered scheme solves a part of the heat equation (since the entropy and not the temperature is held constant), it is still interesting time costwise, in addition to, the heat equation can be solved analytically under certain hypotheses [114].

$$\left.\begin{aligned}\dot{\varphi} &= \mathbf{V}\\ \rho_0\dot{\eta} &= 0\\ \mathbf{F}^{mec}_{h-e}(\mathbf{z}) &= 0\end{aligned}\right\} \quad \text{Problem 1 : elasto-dynamic phase} \Longrightarrow \text{constant entropy} \tag{3.33}$$

$$\left.\begin{aligned}\dot{\varphi} &= 0\\ \rho_0\dot{\mathbf{V}} &= 0\\ \mathbf{F}^{the}_{h-e} &= 0\end{aligned}\right\} \quad \text{Problem 2 : heat conduction phase at fixed configuration} \tag{3.34}$$

From first principle, free energy, stress and entropy equations we have shown in the previous chapter (eq. 2.81) that:

$$\rho_0 T\dot{\eta} = \rho_0 r - \boldsymbol{\nabla}\cdot\mathbf{H} + \boldsymbol{\sigma}^{irr} : \dot{\boldsymbol{\epsilon}} + \mathbf{X}\cdot\dot{\boldsymbol{\xi}} \tag{3.35}$$

The first phase of the adiabatic scheme being at constant entropy, we can write

$$\rho_0 r - \boldsymbol{\nabla}\cdot\mathbf{H} + \boldsymbol{\sigma}^{irr} : \dot{\boldsymbol{\epsilon}} + \mathbf{X}\cdot\dot{\boldsymbol{\xi}} = 0 \tag{3.36}$$

Therefore the heat equation becomes

$$\rho_0 C\dot{T} = T\frac{\partial^2 \rho_0 W}{\partial T \partial \boldsymbol{\epsilon}} : \dot{\boldsymbol{\epsilon}} + T\frac{\partial^2 \rho_0 W}{\partial T \partial \dot{\boldsymbol{\xi}}} \cdot \dot{\boldsymbol{\xi}} \tag{3.37}$$

or we can write it in an alternative way

$$\rho_0 C\dot{T} = T\frac{\partial \boldsymbol{\sigma}^{rev}}{\partial T} : \dot{\boldsymbol{\epsilon}} + T\frac{\partial \mathbf{X}}{\partial T} \cdot \dot{\boldsymbol{\xi}} \tag{3.38}$$

The second member of the equation 3.38 can be neglected [4] (see chapter 2 section 2.5.1).
By assuming that elastic properties are independent of temperature, the heat equation becomes [114]

$$\rho_0 C\dot{T} = -3\kappa\alpha T\dot{\epsilon}_{ii} \tag{3.39}$$

where α and $\kappa = \lambda + \frac{2}{3}\mu$ denote the thermal dilatation and the bulk modulus, respectively. Under certain conditions (incompressibility of strain and if damage is not present ([114] chapter 4)), $\dot{\epsilon}_{ii}$ is given by

$$\dot{\epsilon}_{ii} = \frac{\dot{J}}{J} \tag{3.40}$$

where J is the Jacobian of the deformation. The analytical solution of the adiabatic temperature field T_a can be written as:

$$T_a(t = t^{n+1}) = T(t = t^n) \exp\left(\frac{-3\kappa\alpha}{\rho_0 C}\left(\ln J(t = t^{n+1}) - \ln J(t = t^n)\right)\right) \tag{3.41}$$

In the framework of this thesis, a preliminary study will be considered on a simplified problem, where first we consider a weak coupling where the mechanical properties are independent of temperature, in this case we can use equation 3.41 if we wish to use the staggered scheme that will lead to unconditional stability. Afterward a strong coupling will be included to the thermo-mechanical problem by considering a strong dependence of mechanical properties on temperature, in this case, it is no longer possible to use the adiabatic temperature given by (3.41) if we wish to use staggered algorithm, the equation can be written under the following

$$\rho_0 C\dot{T} = T\left(\frac{\partial \mu}{\partial T}\frac{\mathbf{s}^{rev}}{\mu} + \left(\frac{\partial \kappa}{\partial T}\frac{1}{\kappa}\right)p\mathbf{I} - 3\kappa\alpha\mathbf{I}\right) : \dot{\boldsymbol{\epsilon}} \tag{3.42}$$

where μ is the shear modulus, κ the bulk modulus, $\mathbf{I} = \delta_{ij}$ is the identity tensor (of order 2), $\mathbf{s}^{rev}$ is the deviatoric reversible stress tensor, $p\mathbf{I}$ is the mean normal stress component

of the stress field (or mean hydrostatic stress tensor) that is defined as:

$$p = \frac{\sigma_{kk}}{3} \tag{3.43}$$

Equation 3.42 can be written in an alternative manner:

$$\rho_0 C\dot{T} = T\left(\frac{\partial\mu}{\partial T}\frac{\boldsymbol{\sigma}^{rev}}{\mu} + \left(\frac{\partial\kappa}{\partial T}\frac{1}{\kappa} - \frac{\partial\mu}{\partial T}\frac{1}{\mu}\right)p\mathbf{I} - 3\kappa\alpha\mathbf{I}\right) : \dot{\boldsymbol{\epsilon}} \tag{3.44}$$

In equation 3.44, $\dot{\boldsymbol{\epsilon}}$ is supposed constant in the time interval where integration is held.
In general the term $\left(\frac{\partial\kappa}{\partial T}\frac{1}{\kappa} - \frac{\partial\mu}{\partial T}\frac{1}{\mu}\right)$ is usually taken to zero, since only the Young modulus is temperature dependent (generally the Poisson's ratio exhibits no thermal dependence). In that case, we can rewrite equation 3.42 as

$$\rho_0 C\dot{T} = T\left(\frac{\partial\mu}{\partial T}\frac{\boldsymbol{\sigma}^{rev}}{\mu} - 3\kappa\alpha\mathbf{I}\right) : \dot{\boldsymbol{\epsilon}} \tag{3.45}$$

The adiabatic staggered scheme has a different feature from the simultaneous and isothermal scheme, since when we treat the adiabatic elasto-dynamic phase, a part of the thermo-mechanical coupling is used in order to evaluate the mechanical forces $\mathbf{F}^{int}$ *and* $\mathbf{F}^{ext}$. The second part of the split (heat conduction phase at fixed mechanical configuration) is similar to the isothermal staggered scheme since the thermal equilibrium is evaluated at fixed mechanical configuration.
The adiabatic staggered scheme in known as an alternative split of the thermo-mechanical problem which leads to unconditionally stable staggered algorithm, even in the full non-linear regime. Despite its theoretical unconditional stability, the adiabatic staggered algorithms is limited for a random time discretization and when a strong coupling is present. In fact, this scheme has the features of unconditional stability when considering time discretization characterized by a constant time step (see annex A).

3.6 Applications

3.6.1 Application of the FEM on a general thermal problem

Let us consider an isotropic body $\mathcal{B}_0$ with temperature-dependent heat transfer. Denote by ν the admissible thermal configurational space:

$$\nu = \left\{T : \mathcal{B}_0 \to \mathbb{R}_+ | T = \overline{T}(t_{n+1}) \text{ on } \partial_T\mathcal{B}_0; \mathbf{H} : \mathcal{B}_0 \to \mathbb{R}^3 | \mathbf{H}\cdot\mathbf{n} = \overline{\mathbf{H}}(t_{n+1})\mathbf{n} \text{ on } \partial_{\mathbf{H}}\mathcal{B}_0\right\} \tag{3.46}$$

We write equation (2.47) under the weak form:

$$\int_{\mathcal{B}_0}\left(\rho_0 C\dot{T} - \rho_0 r + \boldsymbol{\nabla}\cdot\mathbf{H}\right)\delta T dV = 0 \tag{3.47}$$

Using the divergence theorem, we can write:

$$\int_{\mathcal{B}_0} (\boldsymbol{\nabla} \cdot \mathbf{H})\, \delta T dV = -\int_{\mathcal{B}_0} \mathbf{H} \cdot \boldsymbol{\nabla} \delta T dV + \int_{\delta_H \mathcal{B}_0} \overline{\mathbf{H}} \cdot \mathbf{n} \delta T dA \tag{3.48}$$

Where $\mathbf{H}$ satisfies Fourier's law (eq.2.21).
Equation (3.47) becomes:

$$\int_{\mathcal{B}_0} \rho_0 C \dot{T} \delta T dV + \int_{\mathcal{B}_0} k \boldsymbol{\nabla} T \cdot \boldsymbol{\nabla} \delta T dV = \int_{\mathcal{B}_0} \rho_0 r \delta T dV - \int_{\partial_H \mathcal{B}_0} \overline{\mathbf{H}} \cdot \mathbf{n} \delta T dA \tag{3.49}$$

A domain $\mathcal{B}_0$ is divided into finite elements connected at nodes. We shall derive a finite element formulation via Galerkin approach.
Global equations for the domain can be assembled from finite element equations using connectivity information. Shape functions N_i *and* N_j are used for interpolation of temperature inside a finite element:

$$T(x) = \sum_i N_i(x) T_i \tag{3.50}$$

$$\delta T(x) = \sum_j N_j(x) \delta T_i \tag{3.51}$$

we obtain:

$$\sum_i^{N_{nodes}} \sum_j^{N_{nodes}} C_{ij} T_i \delta T_j + \sum_i^{N_{nodes}} \sum_j^{N_{nodes}} K_{ij} T_i \delta T_j = \sum_j^{N_{nodes}} q_j \delta T_j \quad \forall \delta T_j \tag{3.52}$$

where:

$$C_{ij} = \int_{\mathcal{B}_\prime} \rho_0 C N_i(x) N_j(x) dV \tag{3.53}$$

$$K_{ij} = \int_{\mathcal{B}_0} k \boldsymbol{\nabla} N_i(x) . \boldsymbol{\nabla} N_j(x) dV \tag{3.54}$$

$$q_j = \int_{\mathcal{B}_0} \rho_0 r N_j(x) dV - \int_{\partial_H \mathcal{B}_0} \overline{\mathbf{H}} \cdot \mathbf{n} N_j(x) dA \tag{3.55}$$

where C_{ij} and K_{ij} the entries of capacity and conductivity matrix, respectively. The system can be written in a matrix form:

$$[C] \left\{ \dot{T} \right\} + [K] \{T\} = \{q\} \tag{3.56}$$

The stationary problem is obtained by setting $\dot{T} = 0$, and leads to a problem similar to elasticity:

$$[K] \{T\} = \{q\} \tag{3.57}$$

For the discretization in time, we consider a temporal interval $[t_n, t_{n+1}]$, called time step Δt, as a part of sequences of steps covering the whole simulation time $[0, t_f]$, where the thermal state $[T_n, q_n]$ are supposed known at time $t = t_n$.

Generalized trapezoidal rule integration

$$\{T_{n+1}\} = \{T_n\} + (1-\alpha)\,\Delta t\left\{\dot{T}_n\right\} + \alpha\Delta t\left\{\dot{T}_{n+1}\right\} \tag{3.58}$$

We can write :

$$[C]\left\{\dot{T}_{n+1}\right\} + [K]\{T_{n+1}\} = \{q(t_{n+1})\} \tag{3.59}$$

If $\alpha = 0$ the scheme is called explicit, in this case:

$$\{T_{n+1}\} = \{T_n\} + \Delta t\left\{\dot{T}_n\right\} \tag{3.60}$$

and

$$\left\{\dot{T}_{n+1}\right\} = [C]^{-1}\left(\{q(t_{n+1})\} - [K]\{T_{n+1}\}\right) \tag{3.61}$$

Although the explicit scheme works well for first order elements, it encounters problems of stability. The solution (eq. 3.61) is trivial if $[C]$ is diagonal.

The Crank-Nicholson method, ($\alpha = \frac{1}{2}$) is unconditionally stable for many problem (ex. diffusion). However, the approximate solutions can still contain (decaying) spurious oscillations if the ratio of time step to the square of space step is large (typically larger than 1/2) [68]. For this reason, whenever large time steps or high spatial resolution is necessary, the less accurate backward Euler method is often used, for $\alpha = 1$, which is both stable and immune to oscillations.

Generalized mid point rule integration

$$\{T_{n+\alpha}\} = \{T_n\} + \alpha\Delta t\left\{\dot{T}_{n+\alpha}\right\} \tag{3.62}$$

Where

$$\{T_{n+\alpha}\} = (1-\alpha)\{T_n\} + \{\alpha T_{n+1}\} \tag{3.63}$$

The system becomes:

$$[C]\left\{\dot{T}_{n+\alpha}\right\} + [K]\{T_{n+\alpha}\} = \{q(t_{n+\alpha})\} \tag{3.64}$$

Where

$$\{q(t_{n+\alpha})\} = (1-\alpha)\{q(tn)\} + \alpha\{q(t_{n+1})\} \tag{3.65}$$

For stability purpose, the time step is limited by

$$\Delta t < \frac{1}{6\alpha}\frac{\rho_0 C h^2}{k} \tag{3.66}$$

where h is the element size. We remark that the time step decreases according to h^2, therefore refining the mesh leads to a small time step in numerical simulation (while in elasticity it is large).

3.6.2 Application to a thermo-elastic problem

In this application we will consider a linear thermo-elastic problem, we will show the finite element discretization for the monolithic solution, and a quick overview for the discretization solution for the staggered schemes described earlier.

We consider a body $\mathcal{B}$ under the action of a general system of external forces and prescribed temperatures, and $\partial\mathcal{B} = \partial\mathcal{B}_u \bigcup \partial\mathcal{B}_\sigma = \partial\mathcal{B}_\theta \bigcup \partial\mathcal{B}_H$.

The basic mechanical and energy balance equations for the linearized isotropic coupled thermo-elasticity theory are given by:

Balance equation of the linear momentum:

$$\rho_0 \dot{\mathbf{v}} = \boldsymbol{\nabla} \cdot \boldsymbol{\sigma} + \rho_0 \mathbf{b} \tag{3.67}$$

Energy balance equation:

$$T\dot{\eta} = -\boldsymbol{\nabla} \cdot \mathbf{H} + r \tag{3.68}$$

where

$$\mathbf{H} = -\mathbf{K} \cdot \boldsymbol{\nabla}\theta \tag{3.69}$$

where $\mathbf{K}$ is the thermal conduction tensor (of second order)
Under the assumption of small perturbation in temperature we can write

$$T = T^{ref} + \theta \tag{3.70}$$

with

$$\frac{\theta}{T^{ref}} \ll 1 \tag{3.71}$$

Under this assumption, we can write that

$$T\dot{\eta} \cong T^{ref}\dot{\eta} \tag{3.72}$$

We recall that for thermo-elastic problem, the stress and entropy are given by:

$$\boldsymbol{\sigma} = \frac{\partial \rho_0 W}{\partial \boldsymbol{\epsilon}} (\boldsymbol{\epsilon}, T) \tag{3.73}$$

and

$$\rho_0 \eta = -\rho_0 \frac{\partial W}{\partial T} (\boldsymbol{\epsilon}, T) \tag{3.74}$$

where

$$\rho_0 W (\boldsymbol{\epsilon}, T) = \frac{1}{2} \boldsymbol{\epsilon} : \overline{\overline{\overline{\mathbf{C}}}} : \boldsymbol{\epsilon} - \frac{1}{2} \frac{\rho_0 c}{T^{ref}} \theta^2 - \theta \boldsymbol{\alpha} : \overline{\overline{\overline{\mathbf{C}}}} : \boldsymbol{\epsilon} \tag{3.75}$$

where C is the heat capacity, and $\boldsymbol{\alpha}$ is the thermal dilatation tensor (of second order), and $\boldsymbol{\epsilon}$ is given by the following expression

$$\boldsymbol{\epsilon} = \boldsymbol{\nabla}^s \mathbf{u} = \frac{1}{2}\left(\boldsymbol{\nabla}\mathbf{u} + (\boldsymbol{\nabla}\mathbf{u})^T\right) \tag{3.76}$$

Expressions of stress and entropy become

$$\boldsymbol{\sigma} = \overline{\overline{\overline{\mathbf{C}}}} : (\boldsymbol{\epsilon} - \theta\boldsymbol{\alpha}) \tag{3.77}$$

and

$$\eta = c\frac{\theta}{T^{ref}} + \boldsymbol{\alpha} : \overline{\overline{\overline{\mathbf{C}}}} : \boldsymbol{\epsilon} \tag{3.78}$$

where $c = \rho_0 c$. Equations 3.78 and 3.72 lead to

$$T\dot{\eta} \cong c\dot{\theta} + T^{ref}\boldsymbol{\alpha} : \overline{\overline{\overline{\mathbf{C}}}}\dot{\boldsymbol{\epsilon}} = -\boldsymbol{\nabla}\cdot\mathbf{H} + \mathbf{b} \tag{3.79}$$

Arranging equation 3.79, we write

$$\dot{\theta} = \frac{1}{\tilde{c}}\boldsymbol{\nabla}\cdot\left[\tilde{\mathbf{K}}.\boldsymbol{\nabla}\theta\right] - \frac{1}{\tilde{c}}\boldsymbol{\alpha} : \overline{\overline{\overline{\mathbf{C}}}} : \boldsymbol{\nabla}^s\mathbf{v} + \frac{r}{c} \tag{3.80}$$

where

$$\tilde{c} = \frac{c}{T^{ref}} \tag{3.81}$$

and

$$\tilde{\mathbf{K}} = \frac{\mathbf{K}}{T^{ref}} \tag{3.82}$$

Therefore the problem of evolution for linearized thermo-elasticity can be written under the following

$$\begin{cases} \dot{\mathbf{u}} = \mathbf{v} \\ \dot{\mathbf{v}} = \dfrac{1}{\rho_0}\boldsymbol{\nabla}\cdot\left(\overline{\overline{\overline{\mathbf{C}}}} : (\boldsymbol{\nabla}^s\mathbf{u} - \theta\boldsymbol{\alpha})\right) + \mathbf{b} \\ \dot{\theta} = \dfrac{1}{\tilde{c}}\boldsymbol{\nabla}\cdot\left[\tilde{\mathbf{K}}.\boldsymbol{\nabla}\theta\right] - \dfrac{1}{\tilde{c}}\boldsymbol{\alpha} : \overline{\overline{\overline{\mathbf{C}}}} : \boldsymbol{\nabla}^s\mathbf{v} + \dfrac{r}{c} \end{cases} \tag{3.83}$$

The thermo-elastic problem defined by 3.83, can be written as

$$\dot{\mathcal{X}}(t) = \mathbf{A}\mathcal{X}(t) + \mathbf{f} \tag{3.84}$$

where

$$\mathcal{X}(t) = \begin{Bmatrix} \mathbf{u}(t) \\ \mathbf{v}(t) \\ \theta(t) \end{Bmatrix} \tag{3.85}$$

$$\mathbf{A}\mathcal{X}(t) = \left\{ \begin{array}{l} \mathbf{v} \\ \dfrac{1}{\rho_0}\boldsymbol{\nabla}\cdot\left(\overline{\overline{\overline{\mathbf{C}}}} : (\boldsymbol{\nabla}^s\mathbf{u} - \theta\boldsymbol{\alpha})\right) \\ \dfrac{1}{\tilde{c}}\boldsymbol{\nabla}\cdot\left[\tilde{\mathbf{K}}\cdot\boldsymbol{\nabla}\theta\right] - \dfrac{1}{\tilde{c}}\boldsymbol{\alpha} : \overline{\overline{\overline{\mathbf{C}}}} : \boldsymbol{\nabla}^s\mathbf{v} \end{array} \right\} \tag{3.86}$$

and

$$\mathbf{f} = \left\{ \begin{array}{c} 0 \\ \mathbf{b} \\ \dfrac{r}{c} \end{array} \right\} \tag{3.87}$$

The evolution equations (3.84) are supplemented by the following boundary conditions

$$u = \overline{u} \text{ on } \mathcal{B}_{\mathbf{u}} \qquad \theta = \overline{\theta} \text{ on } \mathcal{B}_{\theta} \tag{3.88}$$

$$\boldsymbol{\sigma}\cdot\mathbf{n} = \overline{t} \text{ on } \mathcal{B}_{\boldsymbol{\sigma}} \qquad \mathbf{H}\cdot\mathbf{n} = \overline{H} \text{ on } \mathcal{B}_{\mathbf{H}} \tag{3.89}$$

along with the initial conditions

$$\mathbf{u}(0) = \mathbf{u}_0 \qquad \theta(0) = \theta_0 \tag{3.90}$$

$$\dot{\mathbf{u}}(0) = \mathbf{v}_0 \qquad \dot{\theta}(0) = \dot{\theta}_0 \tag{3.91}$$

Monolithic scheme

Equations 3.84 and 3.83 are discretized in time with an implicit scheme

$$\frac{1}{\Delta t}\left(\boldsymbol{\chi}_{n+1} - \boldsymbol{\chi}_n\right) = \mathbf{A}\boldsymbol{\chi}_{n+\alpha} + \mathbf{f}(t_{n+\alpha}) \tag{3.92}$$

$$\left\{ \begin{array}{l} \dfrac{1}{\Delta t}\left(\mathbf{u}_{n+1} - \mathbf{u}_n\right) = \mathbf{v}_{n+\alpha} \\ \dfrac{1}{\Delta t}\left(\mathbf{v}_{n+1} - \mathbf{v}_n\right) = \dfrac{1}{\rho_0}\boldsymbol{\nabla}\cdot\left(\overline{\overline{\overline{\mathbf{C}}}} : (\boldsymbol{\nabla}^s\mathbf{u}_{n+\alpha} - \theta_{n+\alpha}\boldsymbol{\alpha})\right) + \mathbf{b}_{n+\alpha} \\ \dfrac{1}{\Delta t}\left(\theta_{n+1} - \theta_n\right) = \dfrac{1}{\tilde{c}}\boldsymbol{\nabla}\cdot\left[\tilde{\mathbf{K}}.\boldsymbol{\nabla}\theta_{n+\alpha}\right] - \dfrac{1}{\tilde{c}}\boldsymbol{\alpha} : \overline{\overline{\overline{\mathbf{C}}}} : \boldsymbol{\nabla}^s\mathbf{v}_{n+\alpha} + \dfrac{r_{n+\alpha}}{T_{ref}} \end{array} \right. \tag{3.93}$$

where

$$(.)_{n+\alpha} = (1-\alpha)(.)_n + \alpha(.)_{n+1} \tag{3.94}$$

For the displacement and velocity field

$$\mathbf{u}_{n+\alpha} = (1-\alpha)\,\mathbf{u}_n + \alpha\mathbf{u}_{n+1} \tag{3.95}$$

$$\begin{aligned}\mathbf{v}_{n+\alpha} &= (1-\alpha)\,\mathbf{v}_n + \alpha \mathbf{v}_{n+1} \\ &= \frac{\mathbf{u}_{n+1} - \mathbf{u}_n}{\Delta t}\end{aligned} \tag{3.96}$$

then

$$\begin{aligned}\mathbf{u}_{n+1} &= \mathbf{u}_n + \Delta t \mathbf{v}_{n+\alpha} \\ &= \mathbf{u}_n + \Delta t(1-\alpha)\boldsymbol{v}_n + \Delta t \alpha \mathbf{v}_{n+1}\end{aligned} \tag{3.97}$$

Equations 3.95 and 3.97 lead to

$$\mathbf{u}_{n+\alpha} = \mathbf{u}_n + \alpha\,(1-\alpha)\,\Delta t \mathbf{v}_n + \alpha^2 \Delta t \mathbf{v}_{n+1} \tag{3.98}$$

Now, we can discretize the differential equations (eq. 3.93) using the finite element methods.
Taking the weak form, we can write

$$\begin{cases} \dfrac{1}{\Delta t}\left\langle (\mathbf{u}_{n+1} - \mathbf{u}_n), \delta \mathbf{u} \right\rangle = \left\langle \mathbf{v}_{n+\alpha}, \delta \mathbf{u} \right\rangle \\ \dfrac{1}{\Delta t}\left\langle (\mathbf{v}_{n+1} - \mathbf{v}_n), \delta \mathbf{v} \right\rangle = \dfrac{1}{\rho_0}\left\langle \boldsymbol{\nabla} \cdot \left(\overline{\overline{\overline{\mathbf{C}}}} : (\boldsymbol{\nabla}^s \mathbf{u}_{n+\alpha} - \theta_{n+\alpha}\boldsymbol{\alpha}) \right) + \mathbf{b}_{n+\alpha}, \delta \mathbf{v} \right\rangle \\ \dfrac{1}{\Delta t}\left\langle (\theta_{n+1} - \theta_n), \delta \theta \right\rangle = \dfrac{1}{\tilde{c}}\left\langle \boldsymbol{\nabla} \cdot \left[\tilde{\mathbf{K}} \cdot \boldsymbol{\nabla} \theta_{n+\alpha} \right] - \dfrac{1}{\tilde{c}} \boldsymbol{\alpha} : \overline{\overline{\overline{\mathbf{C}}}} : \boldsymbol{\nabla}^s \mathbf{v}_{n+\alpha} + \dfrac{r_{n+\alpha}}{T_{ref}}, \delta \theta \right\rangle \end{cases} \tag{3.99}$$

where $< .,. >$ denotes the inner product which induces the natural norm $\sqrt{< .,. >}$, where

$$< A\mathcal{X}, \mathcal{X} >= \int_\Omega (\mathbf{A} \cdot \mathcal{X}) \cdot \mathcal{X} dV \tag{3.100}$$

For simplicity, we will consider the 1 D case for finite element analysis.
Neglecting body forces, we can write

$$\left\langle \frac{\mathcal{X}_{n+1} - \mathcal{X}_n}{\Delta t}, \delta \mathcal{X} \right\rangle = \left\langle \mathbf{A}\mathcal{X}_{n+\alpha}, \delta \mathcal{X} \right\rangle \tag{3.101}$$

$$\left\langle \frac{\mathcal{X}_{n+1} - \mathcal{X}_n}{\Delta t}, \delta \mathcal{X} \right\rangle = \int_\Omega \left(\frac{1}{\Delta t} (\boldsymbol{\epsilon}_{n+1} - \boldsymbol{\epsilon}_n) : \overline{\overline{\overline{\mathbf{C}}}} : \boldsymbol{\delta}\epsilon + \rho_0 \frac{\mathbf{v}_{n+1} - \mathbf{v}}{\Delta t} : \delta \boldsymbol{v} + \tilde{c} \frac{\theta_{n+1} - \theta_n}{\Delta t} \delta\theta \right) dV \tag{3.102}$$

$$\begin{aligned}\langle \mathbf{A}\mathcal{X}_{n+1}, \delta\mathcal{X}\rangle = \int_\Omega \Big(\boldsymbol{\nabla}^s \boldsymbol{u}_{n+\alpha} : \overline{\overline{\overline{\mathbf{C}}}} : \delta\boldsymbol{\epsilon} + \boldsymbol{\nabla}\cdot \left[\overline{\overline{\overline{\mathbf{C}}}} : (\boldsymbol{\epsilon}_{n+\alpha} - \theta_{n+\alpha}\boldsymbol{\alpha}) \right] \delta\mathbf{v} \\ + \left(\boldsymbol{\nabla}\cdot \left[\overline{\overline{\overline{\tilde{\mathbf{K}}}}} \cdot \boldsymbol{\nabla}\theta_{n+\alpha} \right] - \boldsymbol{\alpha} : \overline{\overline{\overline{\mathbf{C}}}} : \boldsymbol{\nabla}^s \mathbf{v}_{n+\alpha} \right) \delta\theta \Big) dV\end{aligned} \tag{3.103}$$

In a classical form, shape functions are defined on the connected node, and are set to zero elsewhere. For simplicity, the shape functions are taken the same for the mechanical and thermal field.

$$v(x,t) = \sum_{i=1}^{N^{node}} \phi^i(x) v^i(t) \tag{3.104}$$

$$\theta(x,t) = \sum_{i=1}^{N^{node}} \phi^i(x) \theta^i(t) \tag{3.105}$$

$$\delta v(x,t) = \sum_{j=1}^{N^{node}} \phi^j(x) \delta v^j(t) \tag{3.106}$$

$$\delta\theta(x,t) = \sum_{j=1}^{N^{node}} \phi^j(x) \delta\theta^j(t) \tag{3.107}$$

By discretizing the mechanical and thermal equations, in time and space, final weak form for the equation is given by

$$\begin{aligned}\frac{1}{\Delta t}\langle v_{n+1} - v_n, \delta v\rangle &= \int_\Omega \rho_0 \frac{v_{n+1} - v_n}{\Delta t} \delta\mathbf{v} dV \\ &= \int_\Omega \left(\rho_0 \sum_{i=1}^{N^{node}} \left(\phi^i(x) \frac{v^i_{n+1} - v^i_n}{\Delta t} \right) \sum_{j=1}^{N^{node}} \left(\phi_j(x) \delta v^j \right) \right) dV \\ &= \sum_{i=1}^{N^{node}} \sum_{j=1}^{N^{node}} \left(\int_\Omega \rho_0 \phi_i \phi_j dV \right) \frac{v^i_{n+1} - v^i_n}{\Delta t} \delta v^j\end{aligned} \tag{3.108}$$

$$
\begin{aligned}
\left\langle \boldsymbol{\nabla} \cdot \left[\overline{\overline{\overline{\mathbf{C}}}} : (\boldsymbol{\nabla}^s \mathbf{u}_{n+\alpha} - \theta_{n+\alpha}\boldsymbol{\alpha}) \right], \delta\mathbf{v} \right\rangle &= \int_\Omega \boldsymbol{\nabla} \cdot \left[\overline{\overline{\overline{\mathbf{C}}}} : (\boldsymbol{\nabla}^s \mathbf{u}_{n+\alpha} - \theta_{n+\alpha}\boldsymbol{\alpha}) \right] \delta\boldsymbol{v} dV \\
&= -\int_\Omega \boldsymbol{\nabla}^s \delta\mathbf{v} : \overline{\overline{\overline{\mathbf{C}}}} : (\boldsymbol{\nabla}^s \mathbf{u}_{n+\alpha} - \theta_{n+\alpha}\boldsymbol{\alpha})\, dV \\
&\qquad + \int_{\delta\Omega} \delta\mathbf{v} \left[\overline{\overline{\overline{\mathbf{C}}}} : (\boldsymbol{\nabla}^s \mathbf{u}_{n+\alpha} - \theta_{n+\alpha}\boldsymbol{\alpha}) \right] \mathbf{n} dA \\
&= -\int_\Omega \left(\sum_{j=1}^{N^{node}} \phi'_j \delta v^j \right) E \left(\sum_{i=1}^{N^{node}} \phi'_i u^i_{n+\alpha} - \sum_{i=1}^{N^{node}} \phi_i \theta^i_{n+\alpha} \alpha_0 \right) dV \\
&= -\sum_{i=1}^{N^{node}} \sum_{j=1}^{N^{node}} \left(\int_\Omega E\phi'_i\phi'_j dV \right) u^i_{n+\alpha} \delta v^j \\
&\qquad + \sum_{i=1}^{N^{node}} \sum_{j=1}^{N^{node}} \left(\int_\Omega \alpha_0 E \phi_i \phi'_j dV \right) \theta^i_{n+\alpha} \delta v^j
\end{aligned}
\tag{3.109}
$$

We can write equation 3.109 in matrix form

$$
\begin{aligned}
\frac{1}{\Delta t} [\mathbf{M}] (\{\mathbf{v}_{n+1}\} - \{\mathbf{v}_n\}) = &- \left[\mathbf{K}^{mechanical} \right] \left(\{\mathbf{u}_n\} + \alpha (1-\alpha) \Delta t \{\mathbf{v_n}\} + \alpha^2 \Delta t \{\mathbf{v}_{n+1}\} \right) \\
&+ \left[\mathbf{G}^{mechanical} \right] \left((1-\alpha) \{\theta_n\} + \alpha \{\theta_{n+1}\} \right)
\end{aligned}
\tag{3.110}
$$

where the mass matrix $\mathbf{M}_{ij}$, mechanical stiffness matrix $\boldsymbol{K}^{mechanical}_{ij}$ and thermo-elastic coupling matrix $\boldsymbol{G}^{mechanical}_{ij}$ are defined as

$$
\boldsymbol{M}_{ij} = \int_\Omega \rho_0 \phi_i(x) \phi_j(x) dV \tag{3.111}
$$

$$
\boldsymbol{K}^{mechanical}_{ij} = \int_\Omega E \phi'_i(x) \phi'_j(x) dV \tag{3.112}
$$

and

$$
\boldsymbol{G}^{mechanical}_{ij} = \boldsymbol{G}_{ij} = \int_\Omega \alpha_0 E \phi_i \phi'_j dV \tag{3.113}
$$

Discretizing the heat equation (equation 3.93), we can write

$$
\begin{aligned}
\frac{\tilde{c}}{\Delta t} \langle \theta_{n+1} - \theta_n, \delta\theta \rangle &= \int_\Omega \tilde{c} \frac{\theta_{n+1} - \theta_n}{\Delta t} \delta\theta dV \\
&= \int_\Omega \tilde{c} \left(\sum_{i=1}^{N^{node}} \phi_i \frac{\theta^i_{n+1} - \theta^i_n}{\Delta t} \right) \left(\sum_{j=1}^{n+1} \phi_j \delta\theta^j \right) dV \\
&= \sum_{i=1}^{N^{node}} \sum_{j=1}^{N^{node}} \left(\int_\Omega \tilde{c} \phi_i \phi_j dV \right) \left(\frac{\theta^i_{n+1} - \theta^i_n}{\Delta t} \delta\theta^j \right)
\end{aligned}
\tag{3.114}
$$

and

$$\begin{aligned}\left\langle \boldsymbol{\nabla}\cdot\left[\tilde{\mathbf{K}}\cdot\boldsymbol{\nabla}\theta\right],\delta\theta\right\rangle &= \int_{\Omega}\boldsymbol{\nabla}\cdot\left[\mathbf{K}\cdot\boldsymbol{\nabla}\theta\right]\delta\theta dV \\ &= -\int_{\Omega}\boldsymbol{\nabla}\delta\theta\cdot\boldsymbol{K}\cdot\boldsymbol{\nabla}\theta dV+\int_{\delta\Omega}\boldsymbol{K}\boldsymbol{\nabla}\theta\delta\theta\boldsymbol{n}dA\end{aligned} \tag{3.115}$$

where

$$\int_{\partial\Omega}\boldsymbol{K}\boldsymbol{\nabla}\theta\delta\theta\boldsymbol{n}dA=0 \tag{3.116}$$

then

$$\begin{aligned}\left\langle \boldsymbol{\nabla}\cdot\left[\tilde{\mathbf{K}}\cdot\boldsymbol{\nabla}\theta\right],\delta\theta\right\rangle &= -\int_{\Omega}\boldsymbol{\nabla}\delta\theta\cdot\boldsymbol{K}\cdot\boldsymbol{\nabla}\theta dV \\ &= -\int_{\Omega}\left(\sum_{j=1}^{N^{node}}\phi'_j\delta\theta^j\right)K\left(\sum_{i=1}^{N^{node}}\phi'_i\theta^i_{n+\alpha}\right)dV \\ &= -\sum_{i=1}^{N^{node}}\sum_{j=1}^{N^{node}}\left(\int_{\Omega}\tilde{K}\phi'_i\phi'_jdV\right)\left(\theta^i_{n+\alpha}\delta\theta^i\right)\end{aligned} \tag{3.117}$$

$$\begin{aligned}\left\langle \boldsymbol{\alpha}:\overline{\overline{\overline{\mathbf{C}}}}:\boldsymbol{\nabla}^s\mathbf{v}_{n+\alpha},\delta\theta\right\rangle &= \int_{\Omega}\left(\boldsymbol{\alpha}:\overline{\overline{\overline{\mathbf{C}}}}:\boldsymbol{\nabla}^s\boldsymbol{v}_{n+\alpha}\right)\delta\theta dV \\ &= \int_{\Omega}\alpha_0E\sum_{i=1}^{N^{node}}\phi'_iv^i_{n+\alpha}\sum_{j=1}^{N^{node}}\phi_j\delta\theta^jdV \\ &= \sum_{i=1}^{N^{node}}\sum_{j=1}^{N^{node}}\left(\int_{\Omega}\alpha_0E\phi'_i\phi_jdV\right)v^i_{n+\alpha}\delta\theta^j\end{aligned} \tag{3.118}$$

We can write then the heat equation of the thermo-elastic problem under a matrix form

$$\frac{1}{\Delta t}\left[\tilde{\boldsymbol{C}}\right](\{\theta_{n+1}-\theta_n\})=-\left[\tilde{\boldsymbol{K}}\right]^{thermal}((1-\alpha)\{\theta_n\}+\alpha\{\theta_{n+1}\})-\left[\boldsymbol{G}^{thermal}\right]((1-\alpha)\{\mathbf{v}_n\}+\alpha\{\mathbf{v}_{n+1}\}) \tag{3.119}$$

where the capacity matrix $\tilde{\boldsymbol{C}}_{ij}$, thermal conductivity $\tilde{\boldsymbol{K}}^{thermal}_{ij}$ and the thermo-elastic coupling matrix $\mathbf{G}^{thermal}_{ij}$ are defined as

$$\tilde{\boldsymbol{C}}_{ij}=\int_{\Omega}\tilde{K}\phi'_i(x)\phi'_j(x)dV \tag{3.120}$$

$$\tilde{\boldsymbol{K}}^{thermal}_{ij}=\int_{\Omega}\tilde{K}\phi'_i(x)\phi'_j(x)dV \tag{3.121}$$

and

$$\mathbf{G}^{thermal}_{ij}=\mathbf{G}^{mechanical}_{ji}=\mathbf{G}^T_{ij}=\int_{\Omega}\alpha_0E\phi_i(x)\phi'_j(x)dV \tag{3.122}$$

Combining equations 3.110 and 3.119, we can write the basic solution of both mechanical and thermal

$$\begin{bmatrix} \frac{1}{\Delta t}[\mathbf{M}] + \alpha^2 \Delta t \left[\mathbf{K}^{mechanical}\right] & -\alpha[\mathbf{G}] \\ \alpha[\mathbf{G}]^T & \frac{1}{\Delta t}\left[\tilde{\mathbf{C}}\right] + \alpha\left[\tilde{\mathbf{K}}^{thermal}\right] \end{bmatrix} \begin{Bmatrix} \{\mathbf{v}_{n+1}\} \\ \{\boldsymbol{\theta}_{n+1}\} \end{Bmatrix} = \begin{Bmatrix} \frac{1}{\Delta t}[\mathbf{M}]\{\mathbf{v}_n\} - \left[\mathbf{K}^{mechanical}\right](\{\mathbf{u}_n\} + \alpha(1-\alpha)\Delta t\{\mathbf{v}_n\}) + (1-\alpha)[\mathbf{G}]\{\boldsymbol{\theta}_n\} \\ \frac{1}{\Delta t}\left[\tilde{\mathbf{C}}\right]\{\boldsymbol{\theta}_n\} - (1-\alpha)\left[\tilde{\mathbf{K}}^{thermal}\right]\{\boldsymbol{\theta}_n\} - (1-\alpha)\left[\mathbf{G}^{thermal}\right]\{\mathbf{v}_n\} \end{Bmatrix} \tag{3.123}$$

Equation 3.123 is the basic solution of the thermo-elastic problem, in the absence of body forces and gravity, only initial conditions are considered.
The obtained system 3.123 is relatively costly computationalwise especially for the evaluation of the tangent matrix. In the next paragraph we will consider two types of staggered scheme that will reduce system 3.123, thus the computational time cost.

Isothermal staggered scheme

Now the full thermo-elastic problem of evolution will be split into two:

- Isothermal phase
- Heat conduction phase at fixed mechanical configuration

Therefore, the operator defined for the full problem will be split into two

$$\mathbf{A} = \mathbf{A}_1 + \mathbf{A}_2 \tag{3.124}$$

where

$$\mathbf{A}_1\mathcal{X} = \begin{Bmatrix} \mathbf{v} \\ \frac{1}{\rho_0}\boldsymbol{\nabla}\cdot\left[\overline{\overline{\overline{\mathbf{C}}}} : (\boldsymbol{\nabla}^s\mathbf{u} - \theta\boldsymbol{\alpha})\right] \\ 0 \end{Bmatrix} \qquad \text{Problem 1: isothermal phase} \tag{3.125}$$

$$\mathbf{A}_2\mathcal{X} = \begin{Bmatrix} 0 \\ 0 \\ \frac{1}{\tilde{c}}\boldsymbol{\nabla}\cdot\left[\tilde{\mathbf{K}}\cdot\boldsymbol{\nabla}\theta_{n+\alpha}\right] - \frac{1}{\tilde{c}}\boldsymbol{\alpha} : \overline{\overline{\overline{\mathbf{C}}}} : \boldsymbol{\nabla}^s\mathbf{v}_{(n+\alpha)\ or\ (n+1)} \end{Bmatrix} \qquad \text{Problem 2: Heat conduction phase} \tag{3.126}$$

The obtained system has been reduced considerably ($ndof^{mechanical} \times ndof^{mechanical}$) for the first phase and ($ndof^{thermal} \times ndof^{thermal}$) for the second phase. In that case the result is directly obtained with a simple discretization, which is the advantage of this

split, but at the expense of unconditional stability
By assuming that the temperature θ is not changing in the first phase, we can write

$$\frac{1}{\Delta t}\left[\mathbf{M}\right]\left(\{\mathbf{v}_{n+1}\}-\{\mathbf{v}_n\}\right)=-\left[\mathbf{K}^{mechanical}\right]\left(\{\mathbf{u}_n\}+\alpha\left(1-\alpha\right)\Delta t\{\mathbf{v_n}\}+\alpha^2\Delta t\{\mathbf{v}_{n+1}\}\right)+\left[\mathbf{G}^{mechanical}\right]\{\theta_n\} \tag{3.127}$$

while the second phase leads to

$$\frac{1}{\Delta t}\left[\tilde{\boldsymbol{C}}\right]\left(\{\theta_{n+1}-\theta_n\}\right)=-\left[\tilde{\boldsymbol{K}}^{thermal}\right]\left(\left(1-\alpha\right)\{\theta_n\}+\alpha\{\theta_{n+1}\}\right)-\left[\boldsymbol{G}^{thermal}\right]\{\mathbf{v}_{(n+\alpha)\ or\ (n+1)}\} \tag{3.128}$$

In the latter equation we can use $\mathbf{v}_{n+\alpha}$ or $\mathbf{v}_{n+1}$.
The linear thermo-elastic problem of evolution can be written under the following system

$$\begin{bmatrix} \frac{1}{\Delta t}\left[\mathbf{M}\right]+\alpha^2\Delta t\left[\mathbf{K}^{mechanical}\right] & 0 \\ \left[\mathbf{G}\right]^T & \left(-\frac{1}{\Delta t}\left[\tilde{\mathbf{C}}\right]+\alpha\left[\tilde{\mathbf{K}}^{thermal}\right]\right) \end{bmatrix}\begin{Bmatrix} \{\mathbf{v}_{n+1}\} \\ \{\boldsymbol{\theta}_{n+1}\} \end{Bmatrix}= \begin{Bmatrix} \frac{1}{\Delta t}\left[\mathbf{M}\right]\{\mathbf{v}_n\}-\left[\mathbf{K}^{mechanical}\right]\left(\{\mathbf{u}_n\}+\alpha\left(1-\alpha\right)\Delta t\{\mathbf{v}_n\}\right)+\left[\mathbf{G}\right]\{\boldsymbol{\theta}_n\} \\ \frac{1}{\Delta t}\left[\tilde{\mathbf{C}}\right]\{\boldsymbol{\theta}_n\}-\left(1-\alpha\right)\left[\tilde{\mathbf{K}}^{thermal}\right]\{\boldsymbol{\theta}_n\} \end{Bmatrix} \tag{3.129}$$

Adiabatic split

In the case of adiabatic staggered algorithm, the thermo-mechanical problem is split into an adiabatic elasto-dynamic phase followed by a heat conduction phase at fixed configuration. Under these conditions, we can write the split as

$$\mathbf{A}_1\mathcal{X}=\begin{Bmatrix} \mathbf{v} \\ \frac{1}{\rho_0}\boldsymbol{\nabla}\cdot\left[\overline{\overline{\overline{\mathbf{C}}}}:\left(\boldsymbol{\nabla}^s\mathbf{u}-\theta\boldsymbol{\alpha}\right)\right] \\ -\frac{1}{c}\boldsymbol{\alpha}:\overline{\overline{\overline{\mathbf{C}}}}:\boldsymbol{\nabla}^s\mathbf{u} \end{Bmatrix} \qquad \text{Problem 1: Elasto-dynamic phase} \tag{3.130}$$

$$\mathbf{A}_2\mathcal{X}=\begin{Bmatrix} 0 \\ 0 \\ \frac{1}{\tilde{c}}\boldsymbol{\nabla}\cdot\left[\tilde{\mathbf{K}}\cdot\boldsymbol{\nabla}\theta_{n+\alpha}\right] \end{Bmatrix} \qquad \text{Problem 2: Heat conduction phase} \tag{3.131}$$

We can remark in the first phase that the term $-\frac{1}{c}\boldsymbol{\alpha}:\overline{\overline{\overline{\mathbf{C}}}}:\boldsymbol{\nabla}^s\mathbf{u}$ is the source term of the elasto-dynamic phase, where the temperature is no longer constant, but the entropy is.

Basing on the discretization done in the previous paragraph, the adiabatic split of the thermo-elastic problem, is written as

$$\begin{aligned}\frac{1}{\Delta t}\left[\mathbf{M}\right]\left(\{\mathbf{v}_{n+1}\}-\{\mathbf{v}_n\}\right) = &-\left[\mathbf{K}^{mechanical}\right]\left(\{\mathbf{u}_n\}+\alpha\left(1-\alpha\right)\Delta t\{\mathbf{v_n}\}+\alpha^2\Delta t\{\mathbf{v}_{n+1}\}\right)\\ &+\left[\mathbf{G}\right]\left(\left(1-\alpha\right)\{\theta_n\}+\alpha\{\theta_{n+1}^{adiabatic}\}\right)\end{aligned} \tag{3.132}$$

where the adiabatic temperature is computed through the following equation

$$\frac{1}{\Delta t}\left[\tilde{\boldsymbol{C}}\right]\left(\{\theta_{n+1}^{adiabatic}-\theta_n\}\right) = -\left[\boldsymbol{G}\right]^T\left((1-\alpha)\{\mathbf{v}_n\}+\alpha\{\mathbf{v}_{n+1}\}\right) \tag{3.133}$$

where the second phase leads to

$$\frac{1}{\Delta t}\left[\tilde{\boldsymbol{C}}\right]\left(\{\theta_{n+1}-\theta_{n+1}^{adiabatic}\}\right) = -\left[\tilde{\boldsymbol{K}}^{thermal}\right]\left(\left(1-\alpha\right)\{\theta_{n+1}^{adiabatic}\}+\alpha\{\theta_{n+1}\}\right) \tag{3.134}$$

Adiabatic temperature is computed through equation 3.133, It can be written as follow

$$\left\{\theta_{n+1}^{adiabatic}\right\} = \{\theta_n\}-\Delta t\left[\tilde{\mathbf{C}}\right]^{-1}\left[\boldsymbol{G}\right]^T\left((1-\alpha)\{\mathbf{v}_n\}+\alpha\{\mathbf{v}_{n+1}\}\right) \tag{3.135}$$

By injecting equation 3.135 into 3.132, we can determine the mechanical configuration of the current step

$$\begin{aligned}\left[\frac{1}{\Delta t}\left[\mathbf{M}\right]+\alpha^2\Delta t\left(\left[\boldsymbol{K}^{mechanical}\right]+\left[\boldsymbol{G}\right]\left[\tilde{\boldsymbol{C}}\right]^{-1}\left[\boldsymbol{G}\right]^T\right)\right]\{\mathbf{v}_{n+1}\} &= \frac{1}{\Delta t}\left[\mathbf{M}\right]\{\mathbf{v}_n\}\\ &-\left[\boldsymbol{K}^{mechanical}\right]\left(\{\mathbf{u}_n\}+\alpha\left(1-\alpha\right)\Delta t\{\mathbf{v}_n\}\right)+\left(1-\alpha\right)\left[\mathbf{G}\right]\{\theta_n\}\\ &+\alpha\left[\mathbf{G}\right]\left(\{\theta_n\}-(1-\alpha)\Delta t\left[\tilde{\boldsymbol{C}}\right]^{-1}\left[\boldsymbol{G}\right]^T\{\mathbf{v}_n\}\right)\\ =\frac{1}{\Delta t}\left[\mathbf{M}\right]\{\mathbf{v}_n\}-\left[\mathbf{K}^{mechanical}\right]\{\mathbf{u}_n\}+\alpha(1-\alpha)\Delta t&\left(\left[\mathbf{K}^{mechanical}\right]+\left[\mathbf{G}\right]\left[\tilde{\mathbf{C}}\right]^{-1}\left[\mathbf{G}\right]^T\right)\{\mathbf{v}_n\}+\left[\mathbf{G}\right]\{\theta_n\}\end{aligned} \tag{3.136}$$

The temperature of the current step in determined by a simple injection of equation 3.135 into the equation of heat conduction phase (equation 3.134), we get

$$\begin{aligned}\frac{1}{\Delta t}\left[\tilde{\mathbf{C}}\right]\left(\{\theta_{n+1}\}-\{\theta_n\}\right)+\left[\mathbf{G}\right]^T\left((1-\alpha)\{\mathbf{v}_n\}-\alpha\{\mathbf{v}_{n+1}\}\right)+\left[\tilde{\mathbf{K}}^{thermal}\right]\left(\alpha\{\theta_{n+1}\}+(1-\alpha)\theta_n\right)&\\ -(1-\alpha)\Delta t\left[\tilde{\mathbf{K}}^{thermal}\right]\left[\tilde{\mathbf{C}}\right]^{-1}\left[\mathbf{G}\right]^T\left((1-\alpha)\{\mathbf{v}_n\}+\alpha\{\mathbf{v}_{n+1}\}\right)=0&\end{aligned} \tag{3.137}$$

The condensation in equations 3.136 and 3.137 may be surprising at first, but in fact the Schur complement is not computed.
The local adiabatic problem that we have treated here avoid the condensation, in fact equation 3.133 is solved point by point, although we have showed it in a matrix form.

Comparison to thermo-visco-elastic problem

From basic mechanical and energy balance equations for the coupled thermo-visco-elasticity, the problem of evolution can be written under the following form

$$\begin{cases} \dot{\mathbf{u}} = \mathbf{v} \\ \dot{\mathbf{v}} = \dfrac{1}{\rho_0}\boldsymbol{\nabla}\cdot\left(\overline{\overline{\mathbf{C}}} : (\boldsymbol{\nabla}^s\mathbf{u} - \theta\boldsymbol{\alpha}) + \underbrace{\overline{\overline{\mathbf{C}^v}} : \boldsymbol{\nabla}^s\mathbf{v}}\right) + \mathbf{b} \\ \dot{\theta} = \dfrac{1}{\tilde{c}}\boldsymbol{\nabla}\cdot\left[\tilde{\mathbf{K}}.\boldsymbol{\nabla}\theta\right] - \dfrac{1}{\tilde{c}}\boldsymbol{\alpha} : \overline{\overline{\mathbf{C}}} : \boldsymbol{\nabla}^s\mathbf{v} + \underbrace{\dfrac{1}{\tilde{c}}\boldsymbol{\nabla}^s\mathbf{v} : \dfrac{\overline{\overline{\mathbf{C}^v}}}{T_{ref}} : \boldsymbol{\nabla}^s\mathbf{v}} + \dfrac{r}{c} \end{cases} \tag{3.138}$$

From the above system of equations, two additional terms as compared to thermo-elasticity ($\overline{\overline{\mathbf{C}^v}} : \boldsymbol{\nabla}^s\mathbf{v}$ and $\frac{1}{\tilde{c}}\boldsymbol{\nabla}^s\mathbf{v} : \frac{\overline{\overline{\mathbf{C}^v}}}{T_{ref}} : \boldsymbol{\nabla}^s\mathbf{v}$)
These terms are non-linear in nature, we can discretize them and use some stable scheme. In this application we are not going to skim into the details, but we will write the problem of evolution in the case of isothermal and adiabatic split.

If we use an isothermal split, it can be written as

$$\begin{cases} \dot{\mathbf{u}} = \mathbf{v} \\ \dot{\mathbf{v}} = \dfrac{1}{\rho_0}\boldsymbol{\nabla}\cdot\left(\overline{\overline{\mathbf{C}}} : (\boldsymbol{\nabla}^s\mathbf{u} - \theta^p\boldsymbol{\alpha}) + \underbrace{\overline{\overline{\mathbf{C}^v}} : \boldsymbol{\nabla}^s\mathbf{v}}\right) + \mathbf{b} \\ \dot{\theta} = 0 \end{cases} \quad \text{Problem 1: isothermal phase} \tag{3.139}$$

$$\begin{cases} \dot{\mathbf{u}} = 0 \\ \dot{\mathbf{v}} = 0 \\ \dot{\theta} = \dfrac{1}{\tilde{c}}\boldsymbol{\nabla}\cdot\left[\tilde{\mathbf{K}}\cdot\boldsymbol{\nabla}\theta\right] - \dfrac{1}{\tilde{c}}\boldsymbol{\alpha} : \overline{\overline{\mathbf{C}}} : \boldsymbol{\nabla}^s\mathbf{v} \\ \quad + \underbrace{\dfrac{1}{\tilde{c}}\boldsymbol{\nabla}^s\mathbf{v} : \dfrac{\overline{\overline{\mathbf{C}^v}}}{T_{ref}} : \boldsymbol{\nabla}^s\mathbf{v}} + \dfrac{r}{c} \end{cases} \quad \text{Problem 2: Heat conduction phase} \tag{3.140}$$

Better results can be obtained if we applied the adiabatic split, in this case the system

of equations can be split into

$$\begin{cases} \dot{\mathbf{u}} = \mathbf{v} \\ \dot{\mathbf{v}} = \dfrac{1}{\rho_0}\boldsymbol{\nabla}\cdot\left(\overline{\overline{\overline{\mathbf{C}}}} : \left(\boldsymbol{\nabla}^s\mathbf{u} - \theta^{ad}\boldsymbol{\alpha}\right) + \underbrace{\overline{\overline{\overline{\mathbf{C}^v}}} : \boldsymbol{\nabla}^s\mathbf{v}}\right) + \mathbf{b} \\ \dot{\theta} = -\dfrac{1}{\tilde{c}}\overline{\overline{\boldsymbol{\alpha}}} : \overline{\overline{\overline{\mathbf{C}}}} : \boldsymbol{\nabla}^s\mathbf{v} \qquad (\dot{\eta} = 0) \end{cases}$$

Problem 1: Adiabatic elasto-dynamic phase

(3.141)

$$\begin{cases} \dot{\mathbf{u}} = 0 \\ \dot{\mathbf{v}} = 0 \\ \dot{\theta} = \dfrac{1}{\tilde{c}}\boldsymbol{\nabla}\cdot\left[\tilde{\mathbf{K}}\cdot\boldsymbol{\nabla}\theta\right] - \dfrac{1}{\tilde{c}}\boldsymbol{\alpha} : \overline{\overline{\overline{\mathbf{C}}}} : \boldsymbol{\nabla}^s\mathbf{v} + \dfrac{r}{c} \end{cases}$$

Problem 2: Heat conduction phase

(3.142)

Those two problems are both linear, where time step plays an important rule. Stability is not assured if the problem is not well posed.

Adiabatic formulation are not used in commercial codes, by the term $-\frac{1}{\tilde{c}}\overline{\overline{\boldsymbol{\alpha}}} : \overline{\overline{\overline{\mathbf{C}}}} : \boldsymbol{\nabla}^s\mathbf{v}$.

In the next chapter we will expose variational approach strategy for coupled thermo-mechanical problems that will be the base of our work.

Chapter 4

Energy consistent variational approach to coupled thermo-mechanical problems

Résumé

Dans ce chapitre, on expose la formulation du principe variationnel qui caractérise le problème aux conditions limites thermo-mécanique couplé pour des solides dissipatifs. Cette approche variationnelle permet d'écrire les équations d'équilibre mécanique et thermique sous la forme d'un problème d'optimisation d'une fonctionelle scalaire de type énergie.
Cet approche variationnelle présente plusieurs avantages dont:

- *une formulation numérique à structure symétrique, qui fait défaut aux formulations couplées thermo-mécaniques alternatives que l'on peut trouver dans la littérature*
- *la possibilité de dériver des algorithmes étagés*
- *elle est utile pour des approches adaptives (maillage, temps)*
- *elle permet l'utilisation d'algorithmes d'optimisation, en particulier pour les problèmes fortement couplées*

Ce principe consiste en la minimisation d'une énergie incrémentale, afin d'obtenir une approximation consistante de l'état thermomécanique, et le principe variationnel s'écrit

$$\inf_{\varphi_{n+1}} \sup_{T_n+1} \Phi_n^{**}(\varphi_{n+1}, T_{n+1}) \tag{4.1}$$

On montre également que les conditions de stationnarité conduisent aux équations discrétisées d'équilibre mécanique et thermique.

Dans la deuxième partie de ce chapitre on introduit les différents schémas algorithmiques afin de résoudre le problème thermo-mécanique.
Le problème thermo-mécanique est résolu d'une manière itérative jusqu'à ce que l'équilibre soit atteint (equations de stationarité) par des procédures Newton-Raphson, schéma alterné et enfin un schéma de type Uzawa.
Le schéma alterné consiste à effectuer la minimisation par rapport au déplacement, en gardant la température constante, ensuite la maximisation par rapport à la température, tout en gardant le déplacement constant, jusqu'à convergence. Tandis que l'algorithme de type Uzawa consiste à limiter la maximisation par rapport à la température à une seule itération.
Dans cette dernière approche, on considère deux types d'algorithme, le premier utilisant le complément de Schur, et le deuxième avec une expression simplifiée.

On termine ce chapitre par une application sur un cas simplifié en traitant un problème consistant en un volume élémentaire de matière soumis à un chargement en contrainte, avec un comportement thermo-visco-élastique de type Kelvin-Voigt. On considère deux cas: couplage faible où on peut comparer avec une solution analytique, et le couplage fort (en incluant la dépendance des coefficients mécaniques par rapport à la température). Dans ce dernier cas la dérivation d'une solution analytique est difficile, et la solution de référence sera établie via une discrétisation temporelle très fine.
Ce cas simplifié permet de tirer deux résultats intéressant :

- *L'algorithme de type Uzawa semble offrir un coût de calcul intéressant*
- *La fonctionnelle présente un point de selle dans les deux cas envisagés*

Cependant, ces résultats ont été obtenus sur un cas très particulier, et il reste à les vérifier dans des conditions plus générales.

4.1 Introduction

In this chapter, we will introduce the formulation of variational principles characterizing the solutions of the coupled thermo-mechanical problem for general dissipative solids, here understood as the static equilibrium problem of an inelastic deformable solid to which the heat conduction problem is added.
Following the pioneering work of Biot [20, 64], the variational form of the coupled thermo-elastic and thermo-visco-elastic problems has been extensively investigated ([88][107][116][72][65]). In addition, at present there are well-developed variational principles for the equilibrium problem of general dissipative solids in the absence of heat conduction (Han *et al.*[23, 26], Ortiz and Stainier [6]). By contrast, the case of thermo-mechanical coupling in dissipative materials has received comparatively less attention [108].

When the equilibrium and heat conduction problems for general dissipative solids are combined, the resulting coupled problem lacks an obvious variational structure. This lack of variational structure reveals itself upon linearization of the coupled problem, which results in a non-symmetric operator.
A new variational formulation of coupled thermo-mechanical boundary-value problems has been recently proposed by Yang *et al.* [115] leading to a symmetric structure.
It allows to write mechanical and thermal balance equation under the form of an optimisation problem of a scalar energy-type functional. This formulation can be implemented for a wide range of materials including generalized standard material [28].
This variational approach has many advantages especially that it leads to a symmetric numerical formulation, allows to derive staggered or simultaneous schemes, is useful for adaptive approach (adaptive time, mesh), and allows the use of optimization algorithms, in particular for strongly coupled problems [115, 79]

4.2 Variational formulation

We consider a time increment $[t_n, t_{n+1}]$, where the thermo-mechanical state variables $(\boldsymbol{\varphi}_n, T_n, \boldsymbol{\xi}_n)$ are known at $t = t_n$. We recall that $\boldsymbol{\varphi}_n, T_n, \boldsymbol{\xi}_n$ are the displacement mapping, temperature, and internal variables depending on the modeled material behavior, respectively. It has been shown [115, 73], that thermo-mechanical state variables at $t = t_{n+1}$ are obtained through the minimization of an incremental energy of the following variational principle

$$\inf_{\varphi_{n+1}} \sup_{T_n+1} \Phi_n^{**}(\varphi^{n+1}, T^{n+1}) \tag{4.2}$$

where

$$\begin{aligned} \Phi_n^{**}\left(\boldsymbol{\varphi}_{n+1}, T_{n+1}; \boldsymbol{\varphi}_n, T_n, \xi_n\right) &= \int_{\mathcal{B}_0} \left[\mathcal{W}_n - \Delta t \chi\left(\mathbf{G}_{n+1}\right)\right] dV + \int_{\mathcal{B}_0} \Delta t \frac{T_{n+1}}{T_n} \rho_0 r\left(t_{n+1}\right) dV \\ -\int_{\partial_H \mathcal{B}_0} \Delta t \frac{T_{n+1}}{T_n} \overline{\mathbf{H}}\left(t_{n+1}\right) \mathbf{n} dA &- \int_{\mathcal{B}_0} \rho_0 \mathbf{b}(t_{n+1}) \cdot \Delta \boldsymbol{\varphi} dV - \int_{\partial_\sigma \mathcal{B}_0} \overline{\mathbf{t}}(t_{n+1}) \cdot \Delta \boldsymbol{\varphi} dA \end{aligned} \tag{4.3}$$

$$\boldsymbol{\varphi} = \overline{\boldsymbol{\varphi}}(t_{n+1}) \text{ on the boundary } \partial_u \mathcal{B}_0 \tag{4.4}$$

$$T = \overline{T}(t_{n+1}) \text{ on the boundary } \partial_T \mathcal{B}_0 \tag{4.5}$$

and

- $\mathcal{W}_n$: Incremental potential
- $\rho_0 r$: Volumic heat supply
- $\overline{\mathbf{H}}$: imposed heat flux on the boundary $\partial_H \mathcal{B}_0$

- χ : conduction potential
- $\mathbf{b}$: body force
- $\bar{\mathbf{t}}$: imposed surface forces on the boundary

The nominal heat flux is a function of Fourier's conduction potential $\chi(\mathbf{G})$, also called Biot dissipation function [54], and is given by the following expression

$$\mathbf{H} = \frac{\partial \chi}{\partial \mathbf{G}}(\mathbf{G}) \tag{4.6}$$

where

$$\mathbf{G} = -\frac{\boldsymbol{\nabla} T}{T} \tag{4.7}$$

The local incremental potential $\mathcal{W}_n\left(\mathbf{F}_{n+1}, T_{n+1}; \mathbf{F}_n, T_n, \boldsymbol{\xi}_n\right)$ is given by

$$\begin{aligned} \mathcal{W}_n(\mathbf{F}_{n+1}, T_{n+1}; \mathbf{F}_n, T_n, \boldsymbol{\xi}_n) = \inf_{\boldsymbol{\xi}_{n+1}} \Bigg[& W_{n+1} - W_n + \rho_0 \eta_n (T_{n+1} - T_n) \\ & + \Delta t \psi^* \left(\frac{T_{n+1}}{T_n} \frac{\Delta \boldsymbol{\xi}}{\Delta t} \right) \Bigg] + \Delta t \phi^* \left(\frac{T_{n+1}}{T_n} \frac{\Delta \mathbf{F}}{\Delta t} \right) \end{aligned} \tag{4.8}$$

$$\rho_0 \eta_n = -\frac{\partial W_n}{\partial T} \tag{4.9}$$

$$\delta \boldsymbol{\xi} = \boldsymbol{\xi}_{n+1} - \boldsymbol{\xi}_n \tag{4.10}$$

$$\delta \mathbf{F} = \mathbf{F}_{n+1} - \mathbf{F}_n \tag{4.11}$$

where $\mathbf{F}$, $W(\mathbf{F}, T, \boldsymbol{\xi})$, $\psi^*(\dot{\boldsymbol{\xi}})$ and $\phi^*(\dot{\mathbf{F}}, \mathbf{F})$ are the gradient of transformation, Helmholtz free energy density, internal dissipation pseudo-potential and external viscous dissipation pseudo-potential, respectively.
The specific details relative to the formulation of the incremental potentiel for particular constitutive models can be found in [61] and [62, 86, 85] for large transformation in plasticity, and in [1] for non-linear visco-elasticity with large transformation.

4.3 Finite element approach for the variational formulation

As defined before, we consider an admissible thermo-mechanical configurational space of a continuum body $\mathcal{B}_0$, denoted by $\boldsymbol{\nu}$, where $\partial \mathcal{B}_0$ is its smooth boundary.

$$\begin{aligned} \boldsymbol{\nu} = \Big\{ & \boldsymbol{\varphi} : \mathcal{B}_0 \to \mathbb{R}^3 | \boldsymbol{\varphi} = \overline{\boldsymbol{\varphi}} \text{ on } \partial_{\mathbf{u}} \mathbf{B}_0 \times [0,t]; \boldsymbol{\sigma} : \mathcal{B}_0 \to \mathbb{R}^6 | \boldsymbol{\sigma} \mathbf{n} = \bar{\mathbf{t}}_0 \text{ on } \partial_{\sigma} \mathbf{B}_0 \times [0,t] \\ & T : \mathcal{B}_0 \to \mathbb{R}_+ | T = \overline{T} \text{ on } \partial_T \mathbf{B}_0 \times [0,t]; \mathbf{H} : \mathcal{B}_0 \to \mathbb{R}^3 | \mathbf{H} \mathbf{n} = \overline{\mathbf{H}} \text{ on } \partial_H \mathbf{B}_0 \times [0,t] \Big\} \end{aligned} \tag{4.12}$$

From the variational principle defined above (eq. 4.2, 4.33 and 4.8) we can derive a finite element formulation via Ritz-Galerkin approach.
In a classical form, shape functions are defined on the connected nodes, and are set to zero elsewhere. For simplicity, the shape function are taken the same for the mechanical and thermal field. Eventually, we consider the sub-space of admissible functions $\boldsymbol{\nu}_h$ constructed at the element mesh $\mathcal{E}_h$ of the domain $\mathcal{B}_0$

$$\boldsymbol{\nu} = \left\{ \boldsymbol{\varphi}_h : \mathcal{B}_0 \to \mathbb{R}^3 \mid \boldsymbol{\varphi}_h(\mathbf{X}) = \sum_{i=1}^{N^{node}} N_i(\mathbf{X})\mathbf{x}_i(t); T : \mathcal{B}_0 \to \mathbb{R}_+ \mid T_h(\mathbf{X},t) = \sum_{i=1}^{N^{node}} N_i(\mathbf{X})T_i(t) \right\} \tag{4.13}$$

Discretized gradients of deformation and temperature are given by the following expressions

$$\mathbf{F}_h(\mathbf{X},t) = \sum_{i=1}^{N^{node}} \boldsymbol{x}_i(t) \boldsymbol{\nabla} N_i(\mathbf{X}) \tag{4.14}$$

$$\boldsymbol{G}_h(\mathbf{X},t) = -\frac{\sum_{i=1}^{N^{node}} T_i(t) \boldsymbol{\nabla} N_i(\mathbf{X})}{\sum_{i=1}^{N^{node}} T_i(t) N_i(\boldsymbol{X})} \tag{4.15}$$

where $\boldsymbol{x}_i = \boldsymbol{\varphi}(\mathbf{X}_i, t_{n+1})$ are the positions of the N^{nodes} in the current configuration, and $T_i = T(\mathbf{X}_i, t_{n+1})$ are the temperatures on these same nodes. h index refer to the mesh element $\mathcal{T}_h$.
We can rewrite the variational principle on each sub-domain $\boldsymbol{\nu}_h$

$$\inf_{\boldsymbol{\varphi}_h \in \boldsymbol{\nu}_h} \sup_{T_h \in \boldsymbol{\nu}_h} \Phi_{n^{**}} \left(\boldsymbol{\varphi}_{h_{n+1}}, T_{h n+1}; \varphi_n, T_n, \boldsymbol{\xi}_n \right) \tag{4.16}$$

and the stationary equations (min-max) of the variational principle can be written as

$$\begin{aligned} \sum_{i=1}^{Nelt} f_i^{mechanical} \cdot \delta x_i &= \sum_{i=1}^{Nelt} \{ \int_{\mathcal{B}_0} \left[\frac{\partial \mathcal{W}_n}{\partial \mathbf{x}_i} - \rho_0 \mathbf{b} N_i \right] - \int_{\partial_\sigma \mathcal{B}_0} \overline{\mathbf{t}} N_i dA \} \delta x_i = 0 \quad \forall \cdot \delta x_i \\ \sum_{i=1}^{Nelt} f_i^{thermal} \cdot \delta T_i &= \sum_{i=1}^{Nelt} \{ \int_{\mathcal{B}_0} \left[\frac{\partial \mathcal{W}_n}{\partial T} + \Delta t \frac{\partial \chi}{\partial T_i} + \Delta t \rho_0 r \frac{N_i}{T_n} \right] dV \\ &- \int_{\partial_H \mathcal{B}_0} \Delta t \overline{\boldsymbol{H}} \cdot \frac{N_i}{T_n} \mathbf{n} dA \} \cdot \delta T_i = 0 \qquad \forall \, \partial T_i \end{aligned} \tag{4.17, 4.18}$$

$$\begin{aligned} \frac{\partial \mathcal{W}_n}{\partial \mathbf{x}_i} &= \frac{\partial \mathcal{W}_n}{\partial \mathbf{F}} \cdot \frac{\partial \mathbf{F}}{\partial \mathbf{x}_i} \\ &= \mathbf{P}_h \cdot \boldsymbol{\nabla} N_i \end{aligned} \tag{4.19}$$

where the stress tensor $\mathbf{P}_h$ is defined as

$$\mathbf{P}_h = \frac{\partial \mathcal{W}_n}{\partial \mathbf{F}} (\mathbf{F}_{n+1_h}, T_{n+1_h}; \mathbf{F}_n, T_n, \boldsymbol{\xi}_n) \tag{4.20}$$

$$\begin{aligned}\frac{\partial \mathcal{W}_n}{\partial T_i} &= \frac{\partial \mathcal{W}_n}{\partial T} \cdot \frac{\partial T}{\partial T_i} \\ &= -\rho_0 \Delta \eta_h^{eff} N_i\end{aligned} \tag{4.21}$$

where effective entropy variation $\Delta \eta_h^{eff}$ is defined as

$$\rho_0 \Delta \eta_h^{eff} = -\frac{\partial \mathcal{W}_n}{\partial T}(\mathbf{F}_{h_{n+1}}, T_{h_{n+1}}; \mathbf{F}_n, T_n, \boldsymbol{\xi}_n) \tag{4.22}$$

$$\begin{aligned}\frac{\partial \chi}{\partial T_i} &= \frac{\chi}{\partial \mathbf{G}} \cdot \frac{\partial \mathbf{G}}{\partial T_i} \\ &= \mathbf{H}_h \cdot \left(\frac{\boldsymbol{\nabla} N_i}{T_h} + \frac{\mathbf{G}_h}{T_h} N_i \right)\end{aligned} \tag{4.23}$$

where the heat flux $\boldsymbol{H}_h$ is defined as

$$\boldsymbol{H}_h = \frac{\partial \chi}{\partial \mathbf{G}}(\mathbf{G}_h; \mathbf{F}_n, T_n, \boldsymbol{\xi}_n) \tag{4.24}$$

The stationary equations can be written as

$$\sum_{i=1}^{Nelt} f_i^{mechanical} \cdot \delta x_i = \sum_{i=1}^{Nelt} \{ \int_{\mathcal{B}_0} [\mathbf{P}_h \cdot \boldsymbol{\nabla}(N_i) - \rho_0 \mathbf{b} N_i] \, dV - \int_{\partial_\sigma \mathcal{B}_0} \overline{\mathbf{t}} N_i dA \} \delta x_i = 0 \quad \forall \, \delta x_i \tag{4.25}$$

$$\begin{aligned}\sum_{i=1}^{Nelt} f_i^{thermal} \cdot \delta T_i &= \sum_{i=1}^{Nelt} \{ \int_{\mathcal{B}_0} \left[-\rho_0 \Delta \eta_h^{eff} N_i + \Delta t \mathbf{H}_h \cdot \left(\frac{\boldsymbol{\nabla}(N_i)}{T_h} + \frac{\mathbf{G}_h}{T_h} N_i \right) + \Delta t \rho_0 r \frac{N_i}{T_n} \right] dV \\ &- \int_{\partial_H \mathcal{B}_0} \Delta t \overline{\boldsymbol{H}} \cdot \frac{N_i}{T_n} \mathbf{n} dA \} \cdot \delta T_i = 0 \qquad \forall \, \delta T_i\end{aligned} \tag{4.26}$$

Stationary conditions (eq. 4.25 and 4.26) lead to discretized equations for mechanical and thermal equilibrium that can be written in an alternative manner:

$$\mathbf{F}_i^{int} - \mathbf{F}_i^{ext} = 0 \qquad where \; i = 1, ..., N^{nodes} \tag{4.27}$$

where

$$\mathbf{F}_{int}^{mechanical} = \bigcup_{e=1}^{Nelt} \int_{\mathcal{B}_0^e} \mathbf{P}_h \cdot \boldsymbol{\nabla} N_i dV \tag{4.28}$$

$$\mathbf{F}_{ext}^{mechanical} = \bigcup_{e=1}^{Nelt} \int_{\mathcal{B}_0^e} \rho_0 \mathbf{b} N_i dV + \bigcup_{e=1}^{Nelt} \int_{\partial_\sigma \mathcal{B}_0^e} \overline{\mathbf{t}} N_i dA \tag{4.29}$$

$$\mathbf{F}_{int}^{thermal} = \bigcup_{=1}^{Nelt} \int_{\mathcal{B}_0^e} \left[\rho_0 \Delta \eta_h^{eff} N_i - \Delta t \mathbf{H}_h \cdot \left(\frac{\boldsymbol{\nabla} N_i}{T_h} + \frac{\mathbf{G}_h}{T_h} N_i \right) \right] dV \tag{4.30}$$

$$\mathbf{F}_{ext}^{thermal} = \bigcup_{e=1}^{Nelt} \int_{\mathcal{B}_0^e} \Delta t \frac{\rho_0}{T_n} N_i dV - \bigcup_{e=1}^{Nelt} \int_{\partial_H \mathcal{B}_0^e} \Delta t \frac{\overline{\mathbf{H}} \cdot \mathbf{n}}{T_n} N_i dA \tag{4.31}$$

where $\bigcup$ is the assembly operator of the elements at each node, and $\mathcal{B}_0^e$ is the elementary domain.
Note that the thermo-mechanical problem (eq. 4.27) features a non-linear quasi-static problem, even thought heat capacity effects are included in the term $\rho_0 \Delta \eta_h^{eff}$. Thermal equilibrium that is used in the variational formulation, is based on the balance of entropy, evaluated on a (current) temporal increment, where as in classical approaches , thermal equilibrium is based on the instantaneous flux equilibrium equation.
Implicit schemes (implicit backward Euler) are typically used in this framework for the resolution of the equilibrium equations 4.27, as a mean of achieving unconditional stability, and the evaluation of derivatives of expressions 4.20, 4.22 and 4.24 with respect to the variation of nodal unknowns is necessary.
To note a interesting or fundamental feature of the variational approach that it leads to a symmetric tangent matrix (the tangent matrix is linked to the second derivative of the incremental potential (eq. 4.8)).

4.4 Mixed boundary conditions

The variational formulation developed so far, does not take into account mixed boundary conditions (heat exchange with the environmental surrounding).
Thus the convection term can be written by analogy with the conduction potential, therefore an additional term in the variational formulation (eq. 4.33) is added

$$-\Delta t \int_{\partial_H \mathcal{B}_0} \frac{1}{2} h T_{ref} \left(\frac{T_{n+1} - T_{ext}}{T_{n+1}} \right)^2 J_{n+1} dA \tag{4.32}$$

where h is the convection coefficient and J_{n+1} is the jacobian of the element (surface).

Therefore we can write the incremental energy as

$$\begin{aligned} \Phi_n^{**} \left(\boldsymbol{\varphi}_{n+1}, T_{n+1}; \boldsymbol{\varphi}_n, T_n, \xi_n \right) &= \int_{\mathcal{B}_0} \left[\mathcal{W}_n - \Delta t \chi \left(\mathbf{G}_{n+1} \right) \right] dV + \int_{\mathcal{B}_0} \Delta t \frac{T_{n+1}}{T_n} \rho_0 r \left(t_{n+1} \right) dV \\ - \int_{\partial_H \mathcal{B}_0} \Delta t \frac{T_{n+1}}{T_n} \overline{\mathbf{H}} \left(t_{n+1} \right) \mathbf{n} dA &- \int_{\mathcal{B}_0} \rho_0 \mathbf{b}(t_{n+1}) \cdot \Delta \boldsymbol{\varphi} dV - \int_{\partial_\sigma \mathcal{B}_0} \overline{\mathbf{t}}(t_{n+1}) \cdot \Delta \boldsymbol{\varphi} dA \\ &- \Delta t \int_{\partial_H \mathcal{B}_0} \frac{1}{2} h T_{ref} \left(\frac{T_{n+1} - T_{ext}}{T_{n+1}} \right)^2 J_{n+1} dA \end{aligned} \tag{4.33}$$

4.5 Solution schemes

The variational formulation described above, allows to write mechanical and thermal balance equation under the form of an optimisation problem of a scalar functional, thus allows the use of optimization algorithms.

In the framework of this thesis, we are interested to validate the energetic formulation

of the coupled thermo-mechanical problems considering different algorithmic schemes, the goal being to obtain a good compromise between the following aspects: precision, stability and computational cost.
Wy setting $\mathbf{F}_{o-b} = \mathbf{F}_{int} - \mathbf{F}_{ext}$, we can write

$$\mathbf{F}_{o-b}(\mathbf{z}^{k+1}) = \mathbf{F}_{o-b}(\mathbf{z}^{k}) + \left(\frac{\partial \mathbf{F}_{o-b}(\mathbf{z}^{k})}{\partial \mathbf{z}^{k}} \right) \Delta \mathbf{z} \tag{4.34}$$

4.5.1 Newton scheme

Newton scheme consist of iterating on the generalized displacement $\mathbf{z}$ until equilibrium is achieved (equation (4.27)), in other words until $\mathbf{F}_{o-b}(\mathbf{z}^{k+1})$, this will lead to the following system

$$\begin{bmatrix} \mathbf{K}_{UU} & \mathbf{K}_{UT} \\ \mathbf{K}_{TU} & \mathbf{K}_{TT} \end{bmatrix} \begin{bmatrix} \delta U \\ \delta T \end{bmatrix} = - \begin{bmatrix} R_U \\ R_T \end{bmatrix} \tag{4.35}$$

In this case the total matrix of size $\left(ndof^{mechanical} + ndof^{thermal}\right) \times \left(ndof^{mechanical} + ndof^{thermal}\right)$ (see table 4.1)

Table 4.1: Newton scheme

1	If k=0 $\mathbf{z} = \mathbf{z}^n$	else $\mathbf{z} = \mathbf{z}^{k+1}$
2	If $\mathbf{F}_{o-b}^{k+1}(\mathbf{z}) \approx 0$ then move to next time step $t = t + \Delta t$	else (k=k+1) & move to 3
3	$\mathbf{z}^{k+1} = \mathbf{z}^{k} - (\mathbf{K})^{-1}\mathbf{F}_{o-b}^{k}(\mathbf{z}^{k})$ & loop to 1	

4.5.2 Alternated scheme

To compare with Newton scheme, we apply the alternated algorithm that consists in minimizing with respect to displacement, at a constant temperature, then maximizing with respect to temperature at a constant displacement, until convergence. (see table 4.2)

The alternated algorithm reduces the size of the system at a defined step but not necessarily the global time step, therefore it is interesting to compare it with Newton schemes to see which algorithm exhibits more interesting time cost results.

Table 4.2: Alternated algorithm (Uzawa-like scheme: only 1 iteration in step 3)

1	Prediction on temperature field	eg. $T_{n+1^p} = T_n$
2	Solving the optimisation problem for the displacement field	$\inf_{\varphi_{n+1}} \Phi_n^{**}(\varphi_{n+1}, T_{n+1}^p)$
3	Solving the temperature field	$\sup_{T_{n+1}} \Phi_n^{**}(\varphi_{n+1}, T_{n+1})$
4	Loop to 2 until convergence	$\|T_{n+1} - T_{n+1}^p\| < \eta$

4.5.3 Uzawa-like algorithm

The idea of this scheme consists of minimizing with respect to displacement, at a constant temperature, then maximizing with respect to temperature at a constant displacement but limiting the maximization on temperature to only one iteration.

After many investigations of such kind of schemes, various Uzawa-like schemes are considered in the application chapter. In this paragraph we will consider two types of Uzawa schemes, the first one with an enhanced Jacobian, and the second one with a simpler expression. Those schemes will be compared to the two others defined above.

The Uzawa-like scheme will be defined by decomposing the thermo-mechanical problem obtained previously (eq. 3.30 into two)

Problem 1: mechanical problem.

$$[K_{UU}]\{\delta U\} = -\{R_U\} \tag{4.36}$$

when the mechanical equilibium is achieved ($\{R_U\} \simeq 0$), we solve problem 2 defined as follow:

Problem 2: thermal problem

$$\begin{aligned} [K_{UU}]\{\delta U\} + [K_{UT}]\{\delta T\} &= 0 & (4.37)\\ [K_{TU}]\{\delta U\} + [K_{TT}]\{\delta T\} &= -\{R_T\} & (4.38) \end{aligned}$$

Combining equations 4.36, 4.37 *and* 4.38, we can write

$$\left([K_{TT}] - [K_{TU}][K_{UU}]^{-1}[K_{UT}]\right)\{\delta T\} = -\{R_T\} \tag{4.39}$$

Since the incremental variational formulation lead to a symmetric structure [115] we can write

$$K_{UT} = K_{TU}^{T} \tag{4.40}$$

A simpler alternative scheme is

$$[K_{TT}]\{\delta T\} = -\{R_T\} \tag{4.41}$$

Note that is also possible to solve the thermal problem using equations (4.37) and (4.38) instead of the Schur complement (4.39).

4.6 Preliminary analysis

We consider, in this application, a simplified problem consisting of an infinitesimal control volume under compressive load, having a visco-elastic behavior satisfying Kelvin-Voigt model (creep).
The goal being to validate the energetic variational thermo-mechanical formulation of the coupled problem, we consider two types of coupling, weak and strong coupling. For the weak coupling, an analytical solution can be found (under certain simplification), and compared to the variational formulation, but it is not the case for the second case (strong coupling), the analytical solution cannot be provided, thus a numerical reference solution will be suggested in this case.
In each case, we show an important property of the variational thermo-mechanical coupled problem, the solution of the scalar energy-like functional is a saddle point (*note that proof or existence conditions of the saddle point solution of the variational formulation are difficult and have not yet been established, but in this simplified case, we can show graphically that the solution is a saddle point*).
Note that since we consider an infinitesimal control volume, only time discretization is considered (no FEM).
The effects of heat capacity, intrinsic dissipation and the heat exchange with the environment are included in the model.
By neglecting body force, heat supply field, and taking into account the assumption of small displacement, the variational problem for the elementary control volume can be written under the following form

$$\inf_{\epsilon^{n+1}} \sup_{T_{n+1}} \Big[W(\epsilon_{n+1}, T_{n+1}) - W(\epsilon_n, T_n) + \rho_0 \eta_n (T_{n+1} - T_n) + \Delta t \phi^* \left(\frac{T_{n+1}}{T_n} \frac{\epsilon_{n+1} - \epsilon_n}{\Delta t} \right) - \Delta t \chi \left(\frac{T_{n+1} - T_{ext}}{T_{n+1}} \right) - \sigma \left(\epsilon_{n+1} - \epsilon_n \right) \Big] \tag{4.42}$$

where

$$W(\epsilon, T) = \frac{1}{2} E \epsilon^2 - \frac{1}{2} C \frac{(T - T_0)^2}{T_0} \tag{4.43}$$

$$\phi^*(\dot{\epsilon}) = \frac{1}{2} E_v \dot{\epsilon}^2 \tag{4.44}$$

$$\chi\left(\frac{\Delta T}{T}\right) = \frac{1}{2} h T^{ext} \left(\frac{\Delta T}{T}\right)^2 \tag{4.45}$$

and

$$\rho_0 \eta_n = -\frac{\partial W}{\partial T}(\epsilon_n, T_n) = C\frac{\theta_n}{T_0} \tag{4.46}$$

Thermo-visco-elastic characteristics of the material are given in table 4.3

Table 4.3: Material characteristics of the problem

Characteristic	Value	Unit
Young modulus (E)	2×10^9	Pa
Visco-elastic modulus (E^v)	5×10^{13}	$Pa.s$
Density (ρ_0)	1450	$Kg.m^{-3}$
Specific heat capacity (C)	148	$J.Kg^{-1}.C^{-1}$
Convective heat coefficient (h)	25	$W.m^{-2}.C^{-1}$

Temperature small perturbation Under the assumption of small perturbation in temperature, and by setting $T_{ext} = T_0$, we can deduce the following expressions

$$\frac{T_{n+1}}{T_n} \approx 1 + \frac{\theta_{n+1} - \theta_n}{T_0} \tag{4.47}$$

and

$$\frac{T_{n+1} - T_{ext}}{T_n} \approx \frac{\theta_{n+1}}{T_0} \tag{4.48}$$

4.6.1 Weak coupling

At first, we consider constant mechanical properties thus leading to a weak coupling (mechanical coefficients not dependent on the temperature). The variational problem is solved via the 3 types of algorithms described above, and compared to the derived analytical solution. In this case, we see no difference between the efficiency of different algorithms, thus the results we be exposed using one algorithm (Newton Raphson). Figures 4.1 and 4.2 show the evolution of the temperature and strain fields.

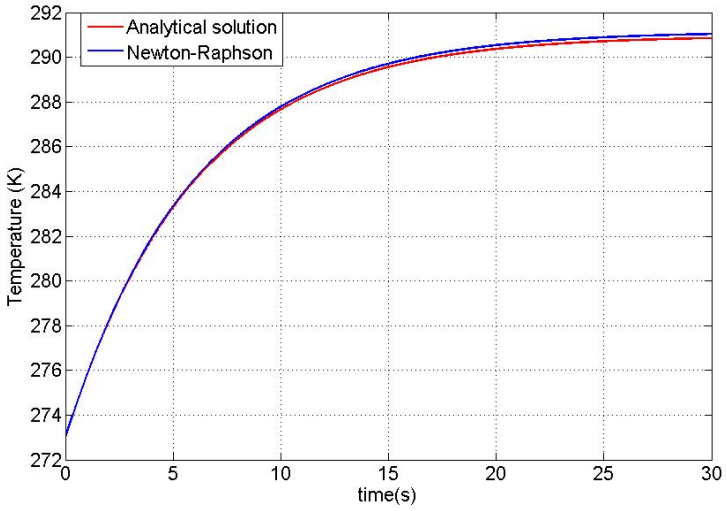

Figure 4.1: Evolution of the temperature field

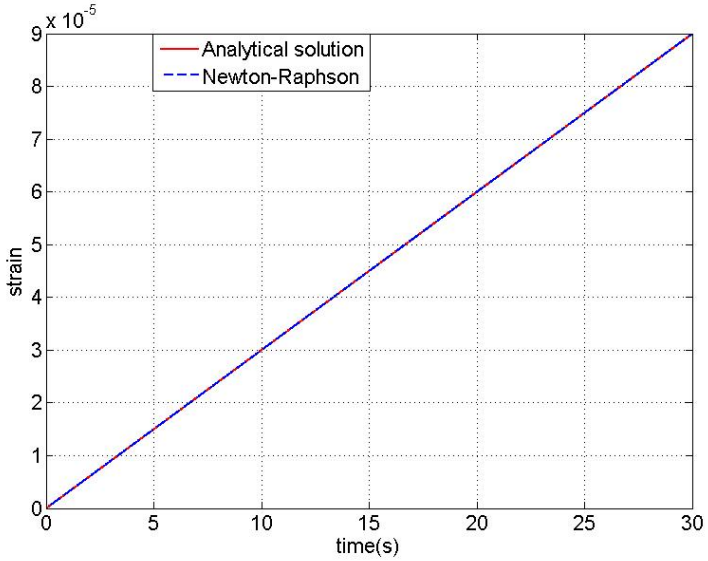

Figure 4.2: Evolution of the strain field

Figures 4.1 and 4.2 clearly show that the results of variational problem and the analytical solution coincide.
The properties of the scheme are given in figures 4.3, and 4.4. They show clearly the precision of the scheme, the smallest the time step is, the more precise the scheme is, with convergence of order 1.

Figure 4.5 show clearly the saddle point property, the functional is convex with re-

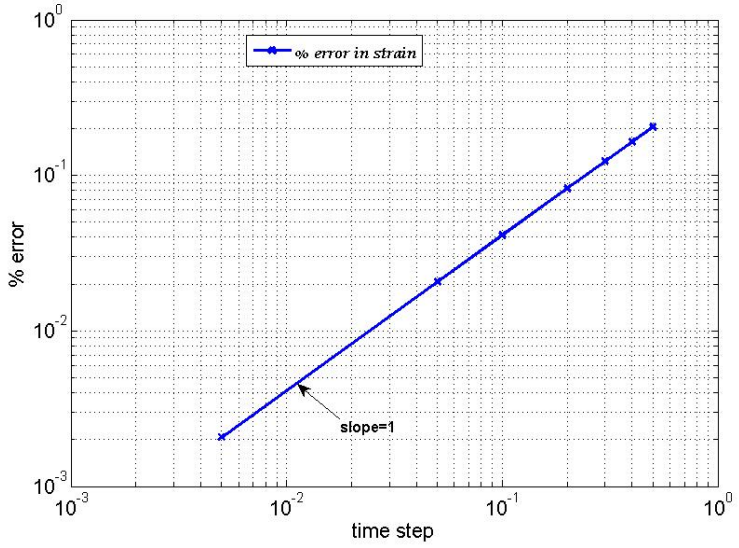

Figure 4.3: Convergence of the Newton-Raphson algorithm in strain field

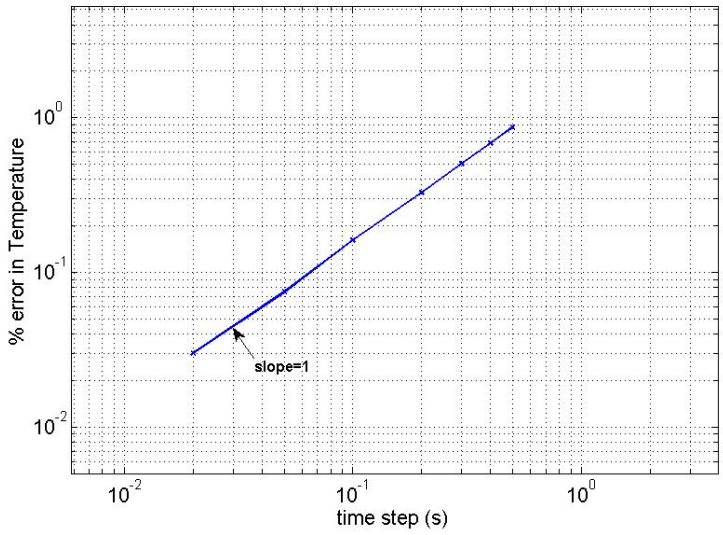

Figure 4.4: Convergence of Newton scheme in temperature

spect to strain and concave with respect to temperature, thus the solution $(\epsilon_{solution}, T_{solution})$ is a saddle point, and this is verified for different simulation times t.

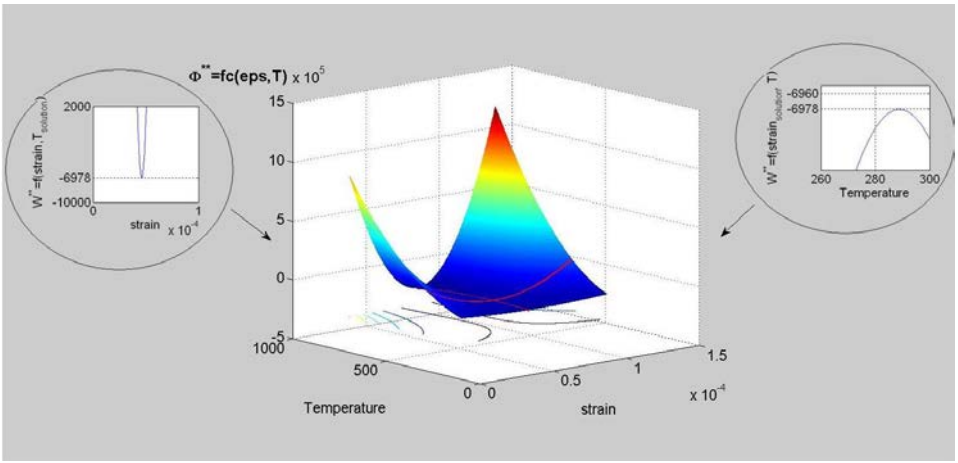

Figure 4.5: Saddle point property of the functional

4.6.2 Strong coupling

In a second phase, we take into account the thermal softening phenomenon where mechanical coefficients are dependent on temperature, thus creating a strong coupling. In our simulation we consider only Young modulus (E) and viscous modulus (E^v) dependent on temperature [99], this is shown in figure 4.6. In fact, the material being thermo-sensible, it has a strong dependency on temperature. The evolution of mechanical coefficients has been observed experimentally (figure 4.7) [27]

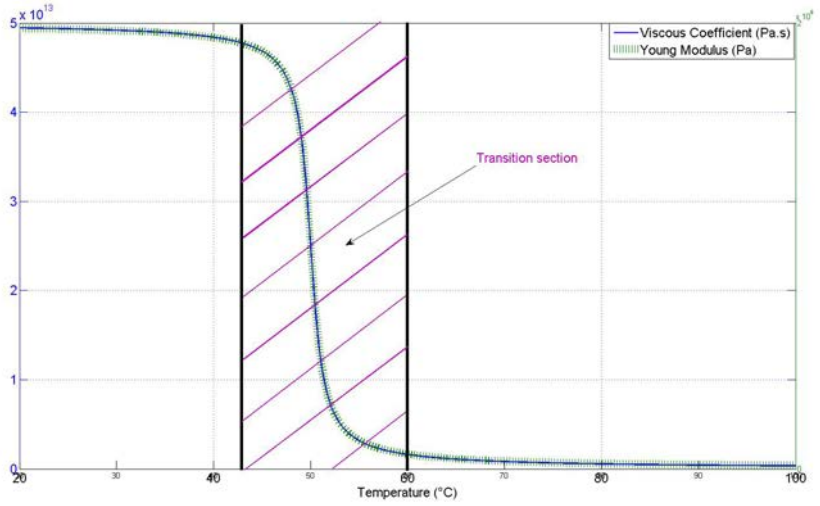

Figure 4.6: Evolution of Young modulus and visco-elastic modulus function of temperature

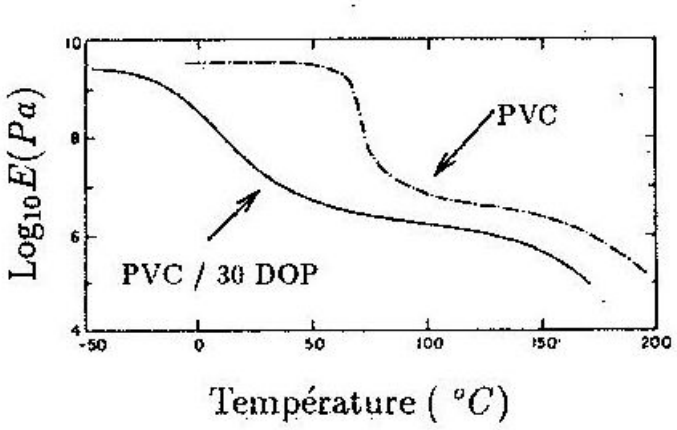

Figure 4.7: Experimental evolution of mechanical properties of a PVC

Figure 4.6 show a sudden drop of mechanical moduli, the temperature interval where the sudden drop occur is called transition section area, which will have a strong effect on the convergence of the algorithmic scheme. This temperature dependency will create a strong coupling. Our goal is to mesure its effect in our numerical simulation for the thermo-mechanical problem, especially when the temperature reach the transition section.
The thermal softening phenomenon will lead to the impossibility of deriving an analytical solution. Initially, we will apply the algorithm of Newton-Raphson for solving the thermo-visco-elastic problem. The reference solution is discretized at small time step ($\Delta t = 10^{-6}s$). We verify as well, the conservation of the saddle point property of the energetic variational formulation.

Numerical simulations show sudden increase of temperature in the transition section area (see Fig. 4.8), the same behavior is observed for the strain field.

Different algorithmic schemes are compared at different time steps, and convergence has been analyzed. In this case, we find that alternated optimization algorithm offers more interesting results in time cost than Newton-Raphson (simultaneous optimization). First tests have been also achieved by limiting the maximisation on the temperature to one iteration, leading to an algorithm of the type of Uzawa's algorithm. This approach seems to reduce more the global time cost (table 4.4). Nevertheless, these results have been obtained within a very particular case, and in the next chapter we will expose a more general coupled thermo-mechanical boundary-value problem case.

Figure 4.9 shows the comparisons between the three algorithms for the temperature field. In this case, these three algorithms almost coincide in term of precision. This has

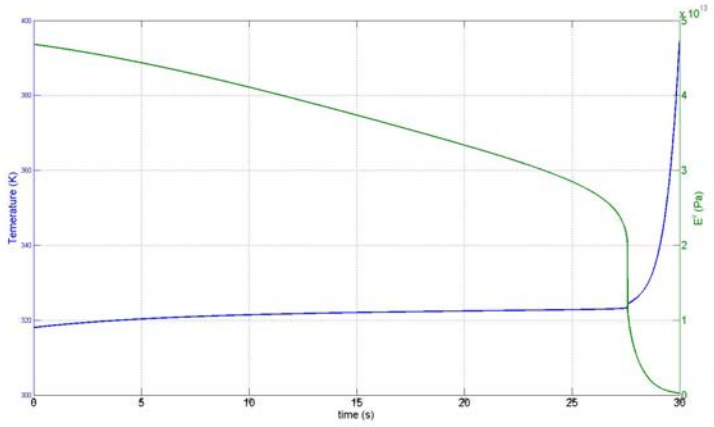

Figure 4.8: Sudden increase of temperature in the transition section area

Table 4.4: Comparison between the three algorithmic schemes, with a precision of 10^{-8} and a simulation time of 30 s

Algorithm	Iteration nb.	time cost (s)
Newton	19 921	3.873
Alternate	120 321	3.205
Uzawa	131 674	3.024

been verified as well for the strain field (figure 4.10).

Eventually, it is important to verify if the saddle point property is still verified in the case of strong coupling, especially when the temperature reaches the transition section interval.
Figure 4.11 shows that the structure at saddle point is always conserved, and this is verified for different time steps.

4.6.3 Conclusion

In this simplified application we have presented the monolithic energetic variational formulation applied to a coupled thermo-mechanical problem, consisting of an elementary control volume, satisfying Kelvin-Voigt model. Initially, we consider a weak coupling where mechanical coefficients are constant. Afterward, we take into account, the temperature dependency, of the mechanical coefficients, leading to a strong coupling, where

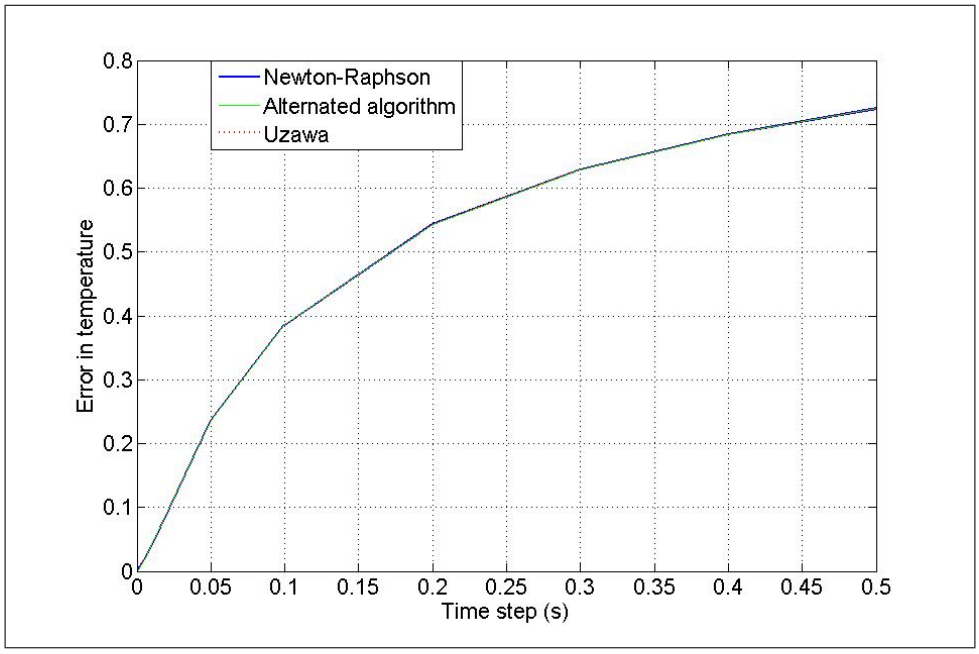

Figure 4.9: Comparaison between the three different types of algorithm for the temperature field

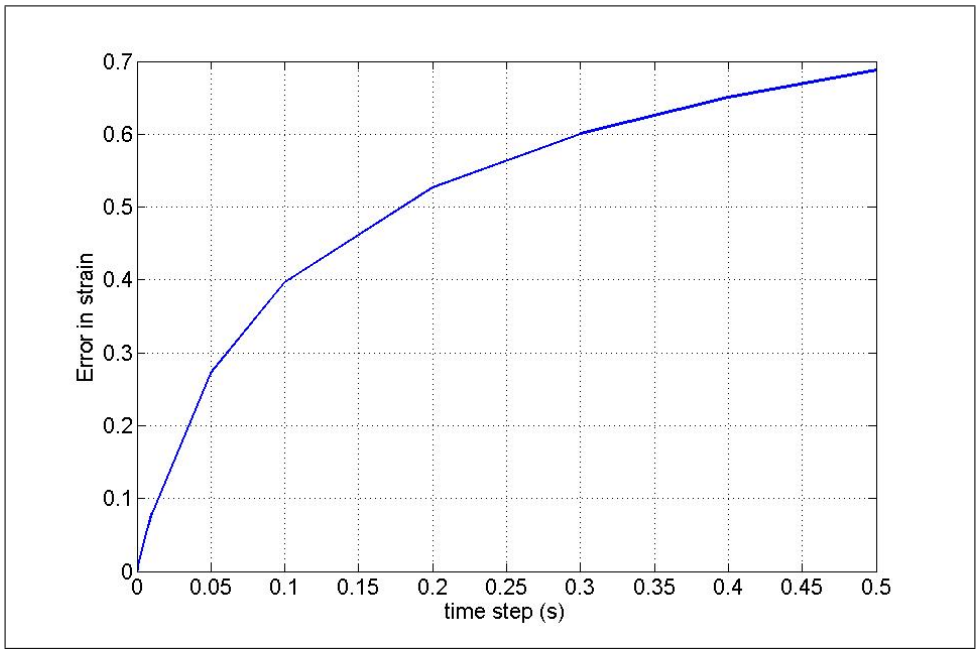

Figure 4.10: Relative error for the strain field

the goal is to measure its effect in our numerical simulation. Uzawa-like algorithm seems to offer an interesting computational cost in comparison with other type of algorithms.

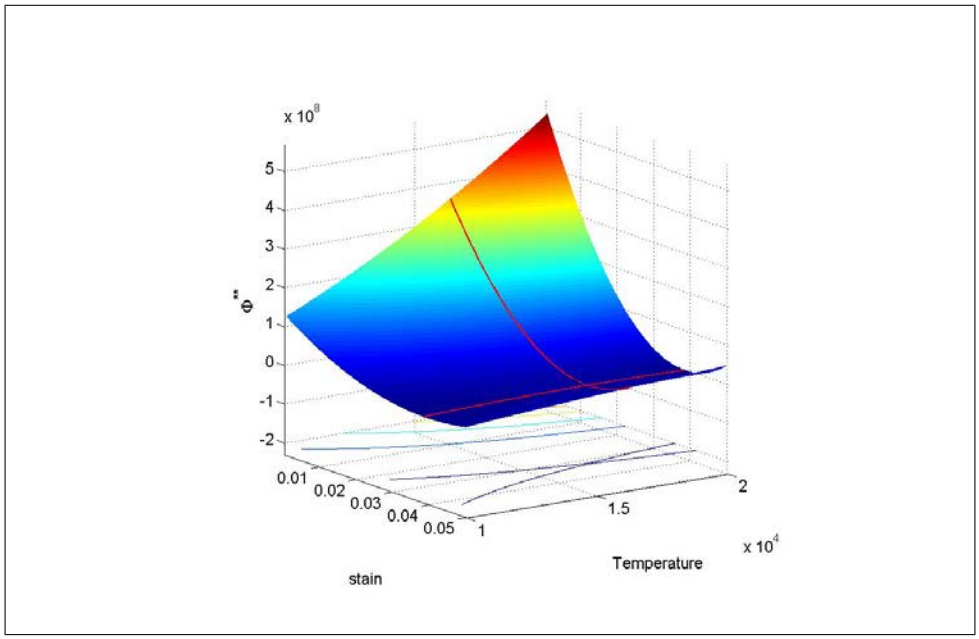

Figure 4.11: Conservation of the structure at saddle point for strong coupling

We obtain as well a second interesting result, the solution point is a saddle point in both cases. However, these results are obtained for a very particular case and we still need to verify them to a more general coupled thermo-mechanical boundary-value problem, which is the goal of the next chapter.

Chapter 5

Applications to coupled thermo-mechanical boundary-value problem

Résumé

Ce dernier chapitre est consacré à l'application de la formulation variationnelle au problème aux condition limites thermo-mécanique.
La première application sera une extension du problème simplifié défini dans le chapitre 4, et consiste en une plaque rectangulaire (2D) trouée en son centre, soumise à un chargement en compression appliqué sur les deux extrêmes, avec un comportement thermoviscoélastique de type Kelvin-Voigt.
Les effect de capacité thermique, de dissipation intrinsèque et d'échange de chaleur avec l'environnement sont inclus dans le modèle. Le couplage thermomécanique est complété en incluant une dépendance forte des coefficients mécaniques par rapport à la température.
Pour comparer, on considère 3 types de maillage différents, et on choisi un pas de temps adaptatif selon le nombre d'itérations effectués au pas précédent.
Le résultat montre la propagation d'une zone de déformation localisée, accompagnée d'une zone de localisation de la température. L'évolution de ces bandes explique bien le phénomène d'auto-échauffement. Les concentrations de contrainte au bord du trou, associées aux termes de couplage thermo-mécanique, conduisent à un échauffement local du matériau, puis à son adoucissement. La perte de rigidité qui en résulte autorise une déformation locale plus importante, qui à son tour accroît les mécanismes de dissipation. Lorsque l'échauffement correspond à la largeur de la zone de transition, les modules de rigidité décroissent rapidement avec l'augmentation de la température ce qui cause une diminution des phénomènes dissipatifs. Lorsque le niveau de la température est au delà de la zone de transition, les phénomènes dissipatifs deviennent négligeables sur le plan thermique. A noter que les zones de propagation localisée ne dépendent pas du maillage suite à la prise en compte de la conduction.

En comparant les différents algorithmes, l'algorithme de type Uzawa montre sa difficulté de converger, tandis que les deux autres montrent un bon résultat. Par suite un schéma alternatif de type Uzawa est prise en compte, en limitant la minimisation sur le champs de déplacement à une seule itération, puis des itérations de type Newton sur le champs de température, jusqu'a convergence. Ce schéma alternatif de type Uzawa semble réduire le temps global, et donne une meilleur performance.

La $2^{\text{ème}}$ application est une extension du cas $2D$. En effet on considère la même plaque mais en $3D$ avec les mêmes conditions que le cas précédent. Les résultats montrent toujours la propagation d'une zone de localisation de déformation accompagnée par une zone de localisation de température. Le schéma alternatif de type Uzawa offre de nouveau un temps de calcul réduit, et des meilleurs performances.

Dans notre $3^{\text{ème}}$ application, on considère le problème de striction d'une barre rectangulaire, avec un comportement élasto-plastique. La striction de la barre est due à la non-homogénéité dans le champs de température, qui se produit suite à la combinaison de l'échauffement uniforme de la barre dû à la création de déformations plastiques et du refroidissement causé par les conditions limites de convection appliquées sur la surface libre. Cette combinaison conduit à un champ de température non homogène dont le point chaud se situe au centre de la barre. La température influence le comportement du matériau, en particulier sa limite élastique. La barre est par suite affaiblie en son centre conduisant à une concentration de déformation, et donc sa striction au centre.

Le résultat de la simulation montre que même si la déformation, donc l'échauffement associé est initialement homogène, l'échange de chaleur avec le milieu extérieur crée une inhomogénéité dans le champ de température.
En comparant les trois algorithmes, le schéma de Newton apparait supérieur aux deux autres schémas, et par suite offre un meilleur temps de calcul.
Une conclusion importante peut être donc tirée à partir de ces applications, que le schéma qui peut être robuste dans un cas particulier, ne le sera pas forcément dans un autre cas de couplage.

5.1 Thermo-visco-elastic behaviour of a rectangular plate with a hole in 2D

We consider a rectangular plate of dimension 50×32 (mm), with a hole in the center of diameter $5mm$. A compression loading is applied on its two extreme sides, and the heat exchange with the environment is performed through the free sides and the hole (Figure 5.1).

The considered material of the rectangular plate is a PVC, satisfying a thermo-visco-elastic behavior of type Kelvin-Voigt. The material characteristics of a PVC are given

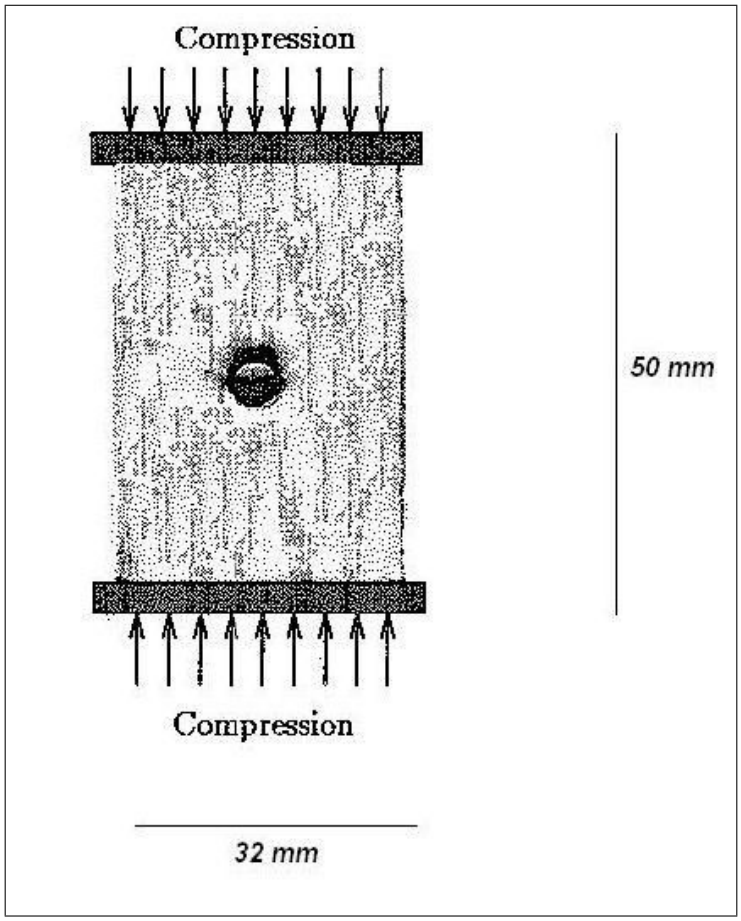

Figure 5.1: Rectangular plate under compressive loading [99]

by table 5.1. This example is taken from the thesis of Meissonnier [99].

An experiment has shown that bands appear on the specimen, initiating on the border of the hole and propagating at a direction of 45° with a symmetric pattern (see figure 5.2). On the mechanical scale, these bands correspond to localisation of deformation. An infrared thermography has shown that those bands also appear on a thermal scale, and correspond to the localization of temperature [99, 93].

As done in the previous chapter, a strong coupling is included due to strong temperature dependency of mechanical properties (figure 4.6) and displacement dependent thermal effects (source term in the heat equation that is dependent on the strain rate).

Boundary conditions The compression on the rectangular plate's sides, is simulated by imposing a vertical displacement $u(t)$ on its two extreme sides. Numerically this

Table 5.1: Thermoviscoelastic characteristics of a PVC at $23°C$

Characteristic	Value	Unit
Young modulus (E)	2×10^9	Pa
Visco-elastic modulus (E^v)	5×10^{13}	$Pa.s$
Poisson coefficient (ν)	0.35	-
Viscous Poisson coefficient (ν^v)	0.35	-
Specific heat capacity (C)	148	$J.kg^{-1}.C^{-1}$
Convective heat coefficient (h)	25	$W.m^{-2}.C^{-1}$
Thermal dilatation (α_0)	6×10^{-5}	$°C^{-1}$

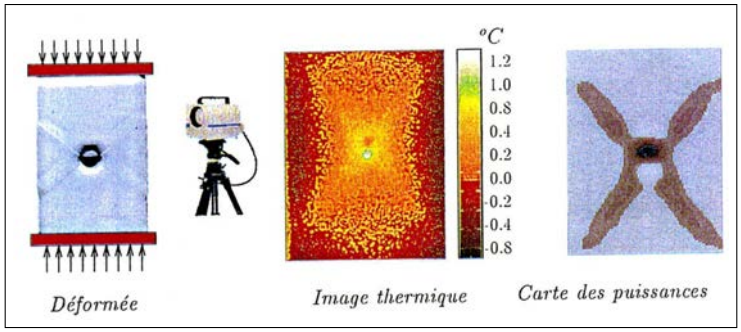

Figure 5.2: Compressive test on the speciment, we see on the left the localized deformation, on the middle the thermal image by infrared, and on the right the thermal power by infrared [99]

compression is simulated by imposing the following Dirichlet condition in displacement

$$u(t) = -4 \times 10^{-5} t \ (ms^{-1}) \tag{5.1}$$

The lateral sides are free from mechanical constraints, whereas a convective heat exchange is performed on the hole and all free sides, and the convection coefficient is supposed constant of value

$$h = 25 W.m^{-2}.C^{-1} \tag{5.2}$$

By symmetry we consider one fourth of the geometry. Displacements and fluxes are set to zero on the axes corresponding to symmetry, whereas the mixed boundary condition is set on the sides and the hole (see figure (5.1).

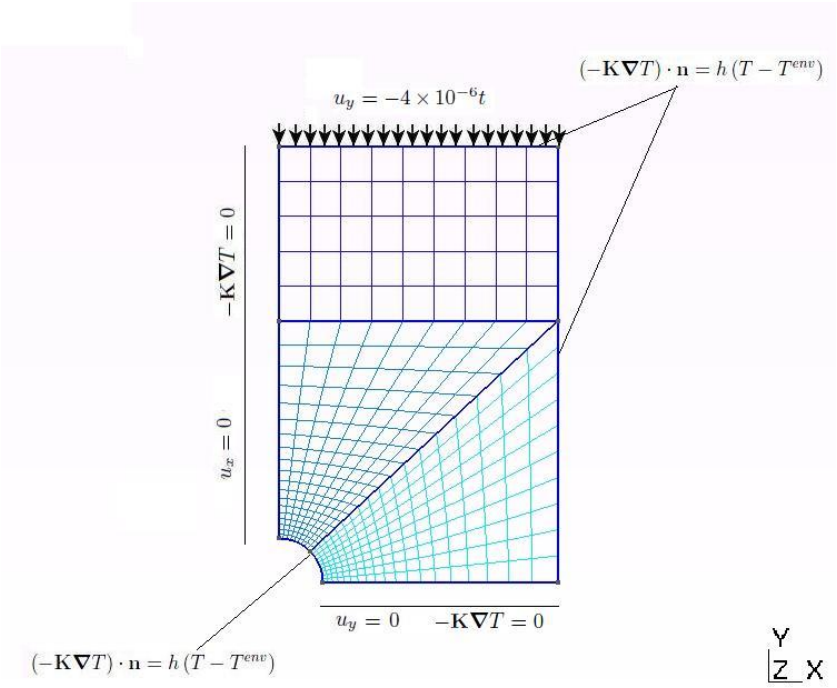

Initial conditions We suppose that the plate has a uniform temperature at $t = 0s$ of value $293K$, the initial condition are given by

$$\begin{cases} u(0) = 0\ m \\ \dot{u}(0) = 0\ m.s^{-1} \\ \theta(0) = 0K \\ \dot{\theta}(0) = 0K.s^{-1} \end{cases} \tag{5.3}$$

Note that in our simulation is done in plane strain, although the original problem was in plane stress, that will serve later as a reference solution.

Mesh To compare we chose three types of mesh for our simulation, shown in figure 5.3 and their characteristics in table 5.2. We denote by mesh 1, mesh 2 and mesh 3, the meshed plates shown (figure 5.3) on the left, middle and right, respectively.

The meshes are finely refined on the hole's border and the direction of 45° in order to obtain a better precision of the results and to show clearly the propagated band .
Note that mesh number 3 is more refined on the direction of 45° than the others.

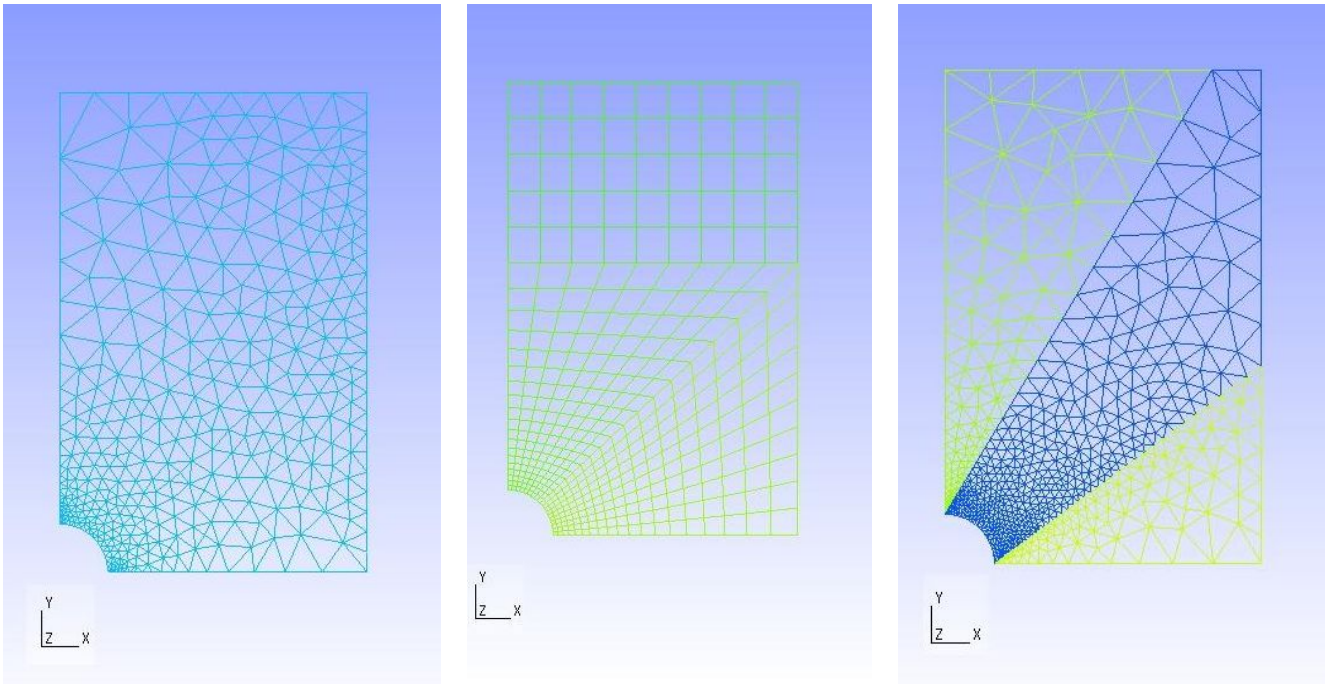

Figure 5.3: Three different types of mesh chosen for our simulation

Table 5.2: Characteristics for each mesh

	node's number	element's number (2^{nd} degree)
Mesh 1	1506	800
Mesh 2	1711	492
Mesh 3	2718	1398

5.1.1 Adaptive time step

After many tests, we have decided to choose an optimized adaptive time step according to the number of iterations till convergence of the previous step, following a rule summarized in table 5.3
The termination criteria is determined by the minimum time step allowed and the maximum number of iterations. If the algorithm did not converge after the maximum number of iterations allowed, the time step is divided as defined by table 5.3, and if after many divisions of the time step the algorithm still not converge, while the time step is at its minimum value, we suppose that the algorithm has not converged, and the simulation is interrupted.

Algorithmic parameters have been chosen as follows:

Table 5.3: Chosen adaptive time step for the simulation of the problem

Number of iterations	Time step
0	$2 \times \Delta t$
1	$1.5 \times \Delta t$
< 4	$1.25 \times \Delta t$
< 6	Δt
> 6	$\Delta t/(number\ of\ iteration)^{\frac{1}{2}}$

1. $\Delta t_{max} = 0.1$ sec
2. $\Delta t_{min} = 10^{-6}$ sec
3. Maximum number of iterations = 20

5.1.2 Results

We apply the three types of algorithms described in the previous chapter (section 4.5): Newton, Alternated and Uzawa-like schemes. The following figures (fig. 5.4, 5.5, 5.6, 5.7, 5.8, 5.9 and 5.10) show the evolution of temperature, displacement, strain and reaction force considering different meshes (and using different algorithms that show the same results choosing the same characteristics and the same mesh). The other results (Velocities and Heat Flux) are shown in Annex II.

These results (figures 5.4, 5.6, 5.7, 5.6) show an evolution and propagation of a localized deformation zone that is accompanied by a localized temperature zone. The width of this localization zone is independent of mesh refinement due to taking into account the conduction process in the material.
Physically, this can be explained by the fact that the plate under compressive loading will generates stress concentration (on the hole borders) and therefore deformation localisation due to a local heating linked to thermo-mechanical coupling. This heating though small, is enough to alter mechanical properties causing thermal softening and therefore localized material flow. This will result to an increase in dissipative effect that leads to an increase in temperature; an autocatalytic cycle is then initiated.

5.1.3 Reference solution

The results have been validated by considering for a particular case, 2D plane stress frame, where we consider the plate with a thickness of $5mm$, and the heat exchange with the environment is performed through free sides. The imposed displacement is set

equal to 4×10^6 (mm).
Figures 5.11 and 5.13 show the validation of the thermo-visco-elastic problem via variational approach (right side of the figure), results are compared to the work done by Meissonnier [99] in plane stress considering the classical approach (left side of the figure).

5.1.4 Algorithmic analysis

The three types of algorithms described previously (section 4.5) are applied on the three different meshes (figure 5.3), and in this paragraph we will analyse the performance of each scheme.

Newton scheme Although Newton scheme exhibits good performance in the beginning, it encounters convergence difficulties when coupling becomes stronger and localization develops. Table 5.4 shows the limitation of physical time of simulation in function of the precision taken in each case. This limitation is caused by the non-convergence at the minimal time step allowed.
In fact, the maximum iteration number being set to 20, after a simulation time, Newton

Table 5.4: Limitation of Newton scheme(sec)

Precision	mesh 1	mesh 2	mesh 3
10^{-3}	26.2	36.4	49.4
10^{-4}	18.7	31.7	25.2
10^{-5}	22.6	9.9	23.9
10^{-6}	10.1	9.6	17.2
10^{-7}	9.2	11	14.7

scheme do not converge after 20 iterations, the time step in then divided by the square root of the iteration number ($\frac{\Delta t}{\sqrt{number of iteration}}$), and then Newton iterations are applied again. In case of continued lack of convergence, the time step is divided until a minimum value (set to $10^{-6}s$ in this case). If no convergence occurs at Δt_{min} then the scheme is called being limited.

Alternated scheme The alternated scheme offers more interesting results since it has overcome the limitation for low precision, and allows better performance for higher ones (table 5.5). On top of that, the alternated scheme performs with better computational cost, especially for high precision and long simulation time.

Table 5.5: Alternated algorithm shows a better performance in term of limitation of physical time (sec)

Precision	mesh 1	mesh 2	mesh 3
10^{-3}	∞	∞	∞
10^{-4}	∞	∞	∞
10^{-5}	63.8	58.6	66
10^{-6}	33.9	37.6	44.6
10^{-7}	13	12.6	19.5

Uzawa scheme In this paragraph we will consider two types of Uzawa scheme, the first one with an enhanced Jacobian, and the second one with a simpler expression. Both schemes performances will be compared in order to chose the most efficient one, that will be compared to the two other algorithms.

Problem with enhanced Jacobian During our simulation, some problems have been encountered with the Uzawa schemes especially with the enhanced Jacobian: since we need to extract the two coupled sub-matrix K_{UT} and K_{TU} from the total matrix, in order to evaluate the enhanced Jacobian term, and both of these two operations influence considerably the computational cost. Indeed in the previous schemes, we have used a skyline storage, that reduces considerably the size of the system, and the computational cost, while this is not possible when extracting off-diagonal sub-matrices.
Therefore we consider two types of Uzawa's scheme as defined beneath.

1. The mechanical part remains the same $[K_{UU}]\{\delta U\} = -\{R_U\}$
2. The mechanical part differs
   (a) Uzawa 1 : $\left([K_{TT}] - [K_{TU}][K_{UU}]^{-1}[K_{UT}]\right)\{\delta T\} = -\{R_T\}$
   (b) Uzawa 2 : $[K_{TT}]\{\delta T\} = -\{R_T\}$

To compare between these two types of schemes, we consider the mesh nb. 2 for the thermo-visco-elastic 2D problem. Simulation is ran for 2 sec with a constant time step $\Delta t = 0.1$ *sec*. Table 5.6 summarizes the results. Both schemes gave the same simulation results, but scheme Uzawa 2 seems more interesting results since the extraction from the total matrix and the evaluation of K_{TT} is less costly than the jacobian, on top of that we can extract K_{TT} from the skyline matrix, which allows to reduce more the global computational cost.
For comparison between the three different schemes, a constant time step is chosen of value $\Delta t = 0.1$, and mesh nb.2 is selected as defined in the previous section. This choice of a constant time step =0.1 was decided after many tests on Uzawa schemes choosing

Table 5.6: Comparison between the two Uzawa schemes

	Total iteration	Elapsed computational time
Uzawa 1	274	25 hr 10 min 56 sec
Uzawa 2	244	25 min 52 sec

Table 5.7: Comparison between the three different schemes for the coupled thermo-visco-elastic 2D problem with a precision of 10^{-4}

	Newton	Alternated scheme	Uzawa 2
Total iteration	177	80	1021
Elapsed computational time	$4m:39s$	$5m:12s$	$1h:07m:37s$

different adaptive time steps and constant ones. Table 5.7 shows a comparison between the 3 different schemes, it gives the total number of iterations needed for each algorithm for 5 sec of simulations at a constant time step $\Delta t = 0.1s$ and a maximum number of iterations allowed by each algorithm is set to 40 iterations. The simulation shows shows for that case that the alternated scheme has the least number of general iterations (but not the total ones), on the other hand the total computational cost that we show is not comparable with Uzawa scheme since in Newton and the Alternated scheme matrices are stored in a skyline matrix, while the Uzawa 3 scheme matrices is stored in the total matrix, where it has a bigger size and therefore extraction of sub-matrices is more costly. Note that for small physical time Newton has better performance than the Alternated scheme, because the localization still didn't develop enough to increase the strength of coupling.

Alternative Uzawa-like algorithm From what we have exposed so far, Uzawa's algorithm was not the best choice to reduce computational costs (at least for this problem), for this we will try to proceed in another manner by imposing one iteration on the mechanical problem instead of the thermal one.

The Uzawa 2 algorithm used to apply Newton iterations on the mechanical problem until convergence while only one iteration for the thermal problem. Now the problem is inverted, so we consider an alternative Uzawa-like algorithm denoted by Uzawa 3, defined by table 5.8
To compare with the two other Uzawa algorithms considered earlier, we take the same thermo-visco-elastic 2D problem as defined before, and we consider again the same mesh

Table 5.8: One general iteration of Uzawa 3 scheme; (note: "n" denotes the time step, and "k" denotes the iteration number)

1	If k=0 $\{U,T\}_{k+1}^{T} = \{U,T\}_{n}^{\mathcal{T}}$	else $\{U,T\}_{k+1}^{\mathcal{T}} = \{U,T\}_{k}^{\mathcal{T}}$
2	only one iteration on the mechanical problem	$\Delta u = [\mathbf{K}_{uu}]^{-1}\{-\mathbf{R}_u\}$
3	Newton iterations on the Thermal problem	$\Delta T = [\mathbf{K}_{TT}]^{-1}\{-\mathbf{R}_T\}$
4	If total residual $< \varepsilon$ then move to the next step Loop to 1	If total residu $> \varepsilon$, $k = k+1$

Table 5.9: Comparison between the three Uzawa schemes

	Number of iteration
Uzawa 1	274
Uzawa 2	244
Uzawa 3	75

(mesh 2). Simulation is run again for 2sec (table 5.9)
By trying to limit both thermal and mechanical problem to one iteration until convergence, the results don't change much with respect to Uzawa2 (too many iterations until convergence).

Now, if we try to use the Uzawa 3 algorithm but starting with thermal iteration in step 2, and then mechanical iterations in step 3, this modification is given by table 5.10.

With the modified Uzawa 3 the results will change significantly only by inverting the mechanical and thermal iterations. The same test is made for 2D thermo-visco-elastic problem for different algorithms, and simulation is run for 15 sec with the adaptive time step as described above, with a precision of 10^{-6}.

Table 5.11 shows well that the modified Uzawa 3 scheme give the best result. Aiming to enhance it, we will consider another Uzawa-like scheme with an enhanced Jacobian. For this we will consider the same thermo-mechanical problem defined previously (equation

Table 5.10: Modified Uzawa 3

1	If k=0 $\{U,T\}_{n+1}^{T} = \{U,T\}_{n}^{\mathcal{T}}$	else $\{U,T\}_{k+1}^{\mathcal{T}} = \{U,T\}_{k}^{\mathcal{T}}$
2	Newton iterations on the Thermal problem	$\Delta T = [\mathbf{K}_{TT}]^{-1}\{-\mathbf{R}_T\}$
3	only one iteration on the mechanical problem	$\Delta u = [\mathbf{K}_{uu}]^{-1}\{-\mathbf{R}_u\}$
4	If total residual $< \varepsilon$ then move to the next step Loop to 1	If total residu $> \varepsilon$, $It = It + 1$

Table 5.11: Comparison between different algorithms for 15 sec of total simulation

	Iteration number	Elapsed computational time
Uzawa 3	2434	4 hr 14 min 09 sec
Modified Uzawa 3	167	13 min 03 sec
Newton	9491	2 hr 23 min 22 sec
Alternated	1428	2 hr 55 min 15 sec

3.30).
By decomposing equation 3.30 into two problems, we can write:

Problem 1 : thermal problem

$$\{\mathbf{R}_T\} = 0 \tag{5.4}$$

Newton iterations are applied to problem 1 until thermal equilibrium is achieved, then we solve the mechanical problem defined by

Problem 2 : mechanical problem

$$[K_{UU}]\{\delta U\} + [K_{UT}]\{\delta T\} = -\{R_U\} \tag{5.5}$$
$$[K_{TU}]\{\delta U\} + [K_{TT}]\{\delta T\} = 0 \tag{5.6}$$

$5.5 \cup 5.6 \Rightarrow$

$$\left([K_{UU}] - [K_{UT}][K_{TT}]^{-1}[K_{TU}]\right)\{\delta U\} = -\{R_U\} \tag{5.7}$$

where $K_{UT} = K_{TU}^T$.

The problem defined by equations 5.4 & 5.7 constitutes the Uzawa4 scheme defined in the same manner as modified Uzawa3 scheme, this means Newton iteration on the thermal problem first as defined by equation 5.4, and then one iteration only to the mechanical problem as defined by equation 5.7.
The same thermo-visco-elastic 2D problem has been tested and results shows that 15 sec of simulation took 154 iterations for Uzawa 4, with an average of one general iteration per unit step. We didn't show the computational time taken for 15 sec of simulation because the extracted sub-matrices $\mathbf{K}_{UT}$ and $\mathbf{K}_{TU}$ influence considerably the computational cost since the extraction is done from the full matrix, therefore this kind of storage is not optimized and we cannot compare it to skyline storage.

To compare the limitation of different Uzawa schemes, as done previously, we consider the 2D thermo-visco-elastic problem, we set the following parameter:

- $\Delta t_{max} = 0.1$ sec
- $\Delta t_{min} = 10^{-6}$ sec
- Maximum iteration = 10
- Maximum total number of steps = 10 000
- Precision = 10^{-6}

Many tests have been made choosing different meshes, and all results have shown that Uzawa4 scheme exhibits the best performance in term of limitation of physical time. Table 5.12 show the results choosing mesh nb.1 defined previously

Table 5.12: Limitation of physical time between different algorithms for precision of 10^{-7}

	Limitation of physical time (sec)
Uzawa 3, 4	> 55
Newton	9.6
Alternated	37.6

5.1.5 Conclusion

In this application we have validated the energetic variational formulation for a $2D$ thermo-visco-elastic coupled problem including a strong coupling. Many algorithmic

scheme where tested, Newton scheme exhibit good performance in the beginning (for low precisions), but it ends of being limited. An alternative scheme has overcome the limitation for lower precision, and exhibits a better performance on higher ones, but still limited. Different Uzawa-like algorithm were suggested in order to enhance the limitation encountered in the other two schemes previously mentioned. The algorithm that showed best performance consisted of maximizing with respect to temperature, at constant displacement, then minimizing with respect to displacement at constant temperature, until convergence, but limiting the minimization on displacement to only one iteration.
These results have been validated on a $2D$ coupled boundary-value problem, and in the next section we will extend the same problem to a $3D$ coupled thermo-visco-elastic coupled boundary-value problem.

5.2 Extension of the thermo-visco-elastic rectangular plate with a hole to 3D

In this section we will consider the same previous problem of a plate with a hole in its center, but this time in 3 dimensions.
The thickness of the rectangular plate is set to 5 mm, the visco-elastic behaviour is taken of Kelvin-Voigt type. A compressive loading is applied on the two extremes, and is simulated by imposing a Dirichlet condition in displacement.

$$u2(t) = -10^{-4}t \quad (ms^{-1}) \tag{5.8}$$

Since we have taken into account the heat exchange of the top surface with the environment, the temperature of the plate does not evolve significantly if we take the same value of displacement as taken in the 2D case. Therefore, to make a clear comparison, the loading is increased (eq. 5.8). The two lateral surfaces of the plate are free from mechanical constraints. We simulate the heat exchange with the environment by simulating a mixed boundary conditions in temperature as before

$$(-\mathbf{K}\boldsymbol{\nabla}T)\cdot\mathbf{n} = h(T - T^{env}) \tag{5.9}$$

where T^{env} is the environmental temperature set equal to $30°C$.
By symmetry, we chose to take the one eighth of the rectangular plate. A tetrahedral mesh is chosen for the numerical simulation (figure 5.14)

Results The evolutions of temperature and strain fields are given by figures 5.15, 5.16 and 5.17. We can always see the localization of deformation that is followed by the localization of temperature.

To compare between different algorithms, a simulation is ran for 50 sec. We consider the modified Uzawa 3 algorithm instead of Uzawa 4 since off-diagonal extraction increases

Table 5.13: comparison in 3D case between different algorithms

	Total number of iterations	Elapsed computational time
Uzawa3	324	54h:34m:07
Alternated	521	$77h20m43s$
Newton	no convergence	

significantly the computational time, resulting a practical impossibility of computing the Schur complement.
The same adaptive time step as before (2D case) is chosen (see table 5.3). Newton-Raphson being limited, it does not achieve 50 seconds of simulation in 10 000 step. The results are summarized through table 5.13, Newton scheme has shown great difficulties of convergence, while Uzawa 3 and Alternated schemes have overcome this difficulty. Once again Uzawa 3 scheme exhibits the best performance. Note that extension to $3D$ were aimed to check if the performances of different algorithms are limited only to $2D$ case or can also be applied for $3D$ case.
We are still interested in applying these different algorithmic schemes to other types of problems that behave differently in order to check the conservation of algorithmic performances. For this we will expose the problem of necking in a rectangular bar with a elasto-plastic behaviour.

5.3 Necking in a $3D$ elasto-plastic rectangular bar

In this application we will simulate the necking of a bar that is due to non-homogeneity of the temperature field. The non-homogeneity occurs due to the combination of uniform heating of the bar due to the creation of plastic deformation, and cooling thereof via a convective boundary condition applied on its outer surface. Therefore, this combination leads to an inhomogeneous temperature field in which the hot spot is located in the center of the bar (farthest point of the convective boundary condition). The temperature influences the material behavior, including the limit of elasticity, the bar is therefore weakened in its center which induces a concentration of deformation, and thus the necking of the bar at this location.
Note that this application is treated in various papers and conference proceedings, considering monolithic or staggered schemes, or both (see in [50], [40],[84] [114]) etc ...

5.3.1 Elasto-plastic model

The elasto-plastic model chosen for this simulation is exposed in detail in section (2.6.3). Experimental observations showed that the heat capacity of metals is not influenced by work hardening, therefore W^p is dependent on the temperature T [44, 46].
Although both experimental observations and theoretical analysis indicate a linear de-

pendence of elastic constants with respect to the temperature (Weiner, 2002), we decide to use, for simplicity, constant elastic moduli (constant Young and bulk *moduli*). We will consider the following free energies W^e, W^p and W^h defined by

$$W^e(\mathbf{C}^e;T) = \frac{1}{2}\kappa(tr[\boldsymbol{\epsilon}^e])^2 + E\left(dev[\boldsymbol{\epsilon}^e] : dev[\boldsymbol{\epsilon}^e]\right) - 3\kappa\alpha(T-T_0)logJ \tag{5.10}$$

where the third term accounts for thermo-elastic coupling (thermal dilatation coefficient α).
The plastic free energy W^p is composed of a power-law term and an exponential saturation term, it is given by the following expression:

$$W^p(\bar{\epsilon}^p,T) = \frac{n}{n+1}\frac{\sigma_0}{b}\left(1+b\bar{\epsilon}^p\right)^{\frac{1}{n}+1} + \hat{\sigma}_0\left[\bar{\epsilon}^p + \frac{1}{d}exp(-d\bar{\epsilon}^p)\right] \tag{5.11}$$

and the thermal free energy

$$W^h(T) = \rho_0 CT\left(1 - log\frac{T}{T_0}\right) \tag{5.12}$$

where $\mathbf{C}^e$ is the elastic right Cauchy-Green strain tensor

$$\mathbf{C}^e = \mathbf{F}^{e^T}\mathbf{F}^e \tag{5.13}$$

where $\mathbf{F}^e$ denotes the elastic deformation.

$$\boldsymbol{\epsilon}^e = log\left[\sqrt{\mathbf{C}^e}\right] \tag{5.14}$$

$$J = det\left[\sqrt{\mathbf{C}^e}\right] = det\left[\mathbf{F}\right] \tag{5.15}$$

The dissipation potential ψ^* for the elasto-plastic problem is given by the following expression

$$\psi^*(\dot{\bar{\epsilon}}^p;\bar{\epsilon}^p,T) = \sigma_y(\bar{\epsilon}^p,T)\dot{\bar{\epsilon}}^p \tag{5.16}$$

where

$$\sigma_y(\bar{\epsilon}^p,T) = \sigma_1(T)\left(1+b'\bar{\epsilon}^p\right)^{\frac{1}{n'}} \tag{5.17}$$

where the critical stress σ_1 is given by the following expression

$$\sigma_1(T) = \sigma_1(T_0)\left[1 - 0.0007(T-T_0)\right] \tag{5.18}$$

Note that dissipation pseudo-potential ψ^* is composed of a rate-independent term (homogeneous of order 1 in $\dot{\bar{\epsilon}}^p$), where for the case visco-plasticity a rate dependent term (power law) can be added [61].

For details about the thermodynamic framework for plasticity see [73, 30, 29, 52, 59, 71, 58]

5.3.2 Simulation

We consider a rectangular bar of a cross section area $20 \times 2 \quad mm^2$ and a length of $L = 100mm$.
The rectangular bar is made up of an aluminium alloy *Al2024-T3* with an elasto-plastic behaviour, strain rate independent, for which it has been possible to identify the constitutive parameters from the stress-strain curves and adiabatic heating obtained by Hodowany et al. [15], who conducted tests both in the quasi-static range and the dynamic range.

A simple identification procedure, consisting in fitting numerical stress-strain and temperature-strain curves to experimental ones (figure 5.18 and 5.19), yields to the identification of constitutive parameters of the alloy listed in table 5.14.

Boundary conditions The metallic rectangular bar is under traction loading on each side of the plate, which is simulated by imposing a vertical displacement $u(t)$ on its two extreme sides. Numerically this traction is simulated by imposing the following Dirichlet condition in displacement

$$u(t) = 0.5 \times 10^{-3} t \quad (ms^{-1}) \tag{5.19}$$

Since we are interested in the coupled thermo-mechanical behavior, it is necessary to apply thermal boundary conditions. Taking into account the symmetries of the problem, only one eighth of the bar is being modeled. Heat fluxes are set to zero on the entries corresponding to symmetry (axes x and y, see figure 5.20), and a mixed boundary condition is set on the free sides .
The mixed boundary condition is modeled as a convective heat exchange with a convective coefficient of value

$$h = \begin{cases} 25W.m^{-2}.C^{-1} & \text{On the side where the displacement is imposed} \\ 15W.m^{-2}.C^{-1} & \text{elsewhere on the other free sides} \end{cases} \tag{5.20}$$

Table 5.14: Material properties for rate-independent 2024-T3 aluminium alloy at $T = 293K$

Characteristic	**Value**	**Unit**
Initial temperature T_0	293	K
Mass density ρ_0	2780	$kg.m^{-3}$
Elastic properties		
Young modulus E	73.1×10^9	Pa
Poisson coefficient (ν)	0.33	–
Thermo-elastic properties		
Thermal dilatation coefficient α_0	24.7×10^{-6}	K^{-1}
Plastic properties		
Initial yield stress	$380.0e6$	Pa
Hardening coefficient	66.7	–
Hardening exponent	5.8	–
Thermoplastic properties		
Initial yield stress stored σ_0	275.0×10^6	Pa
Hardening coefficient stored b	-1.9	–
Hardening exponent stored n	1	–
Saturation yield stress stored $\hat{\sigma}_0$	170×10^6	Pa
Hardening saturation coefficient stored d	14	–
Initial yield stress dissipated σ_1	100×10^6	Pa
Hardening coefficient dissipated b'	8.5	–
Hardening exponent dissipated n'	1	–
Thermal properties		
Conductivity coefficient k	121	$W.m^{-1}K^{-1}$
Specific heat capacity C	875	$J.kg^{-1}K^{-1}$

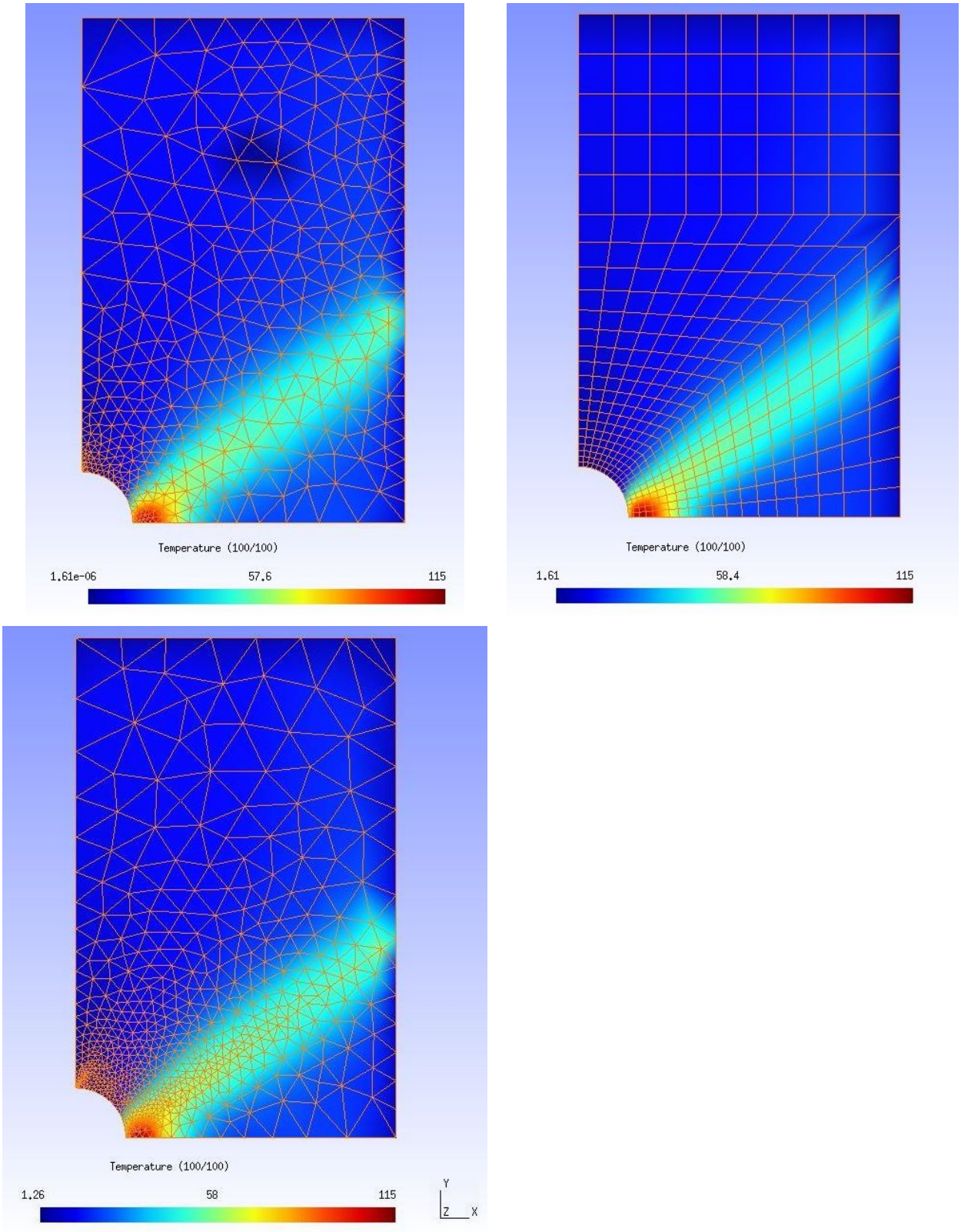

Figure 5.4: Temperature increase (K) at time $t = 10sec$, showing different meshes, on the top left "mesh 1", on the top right "mesh 2" and on the bottom "mesh 3"

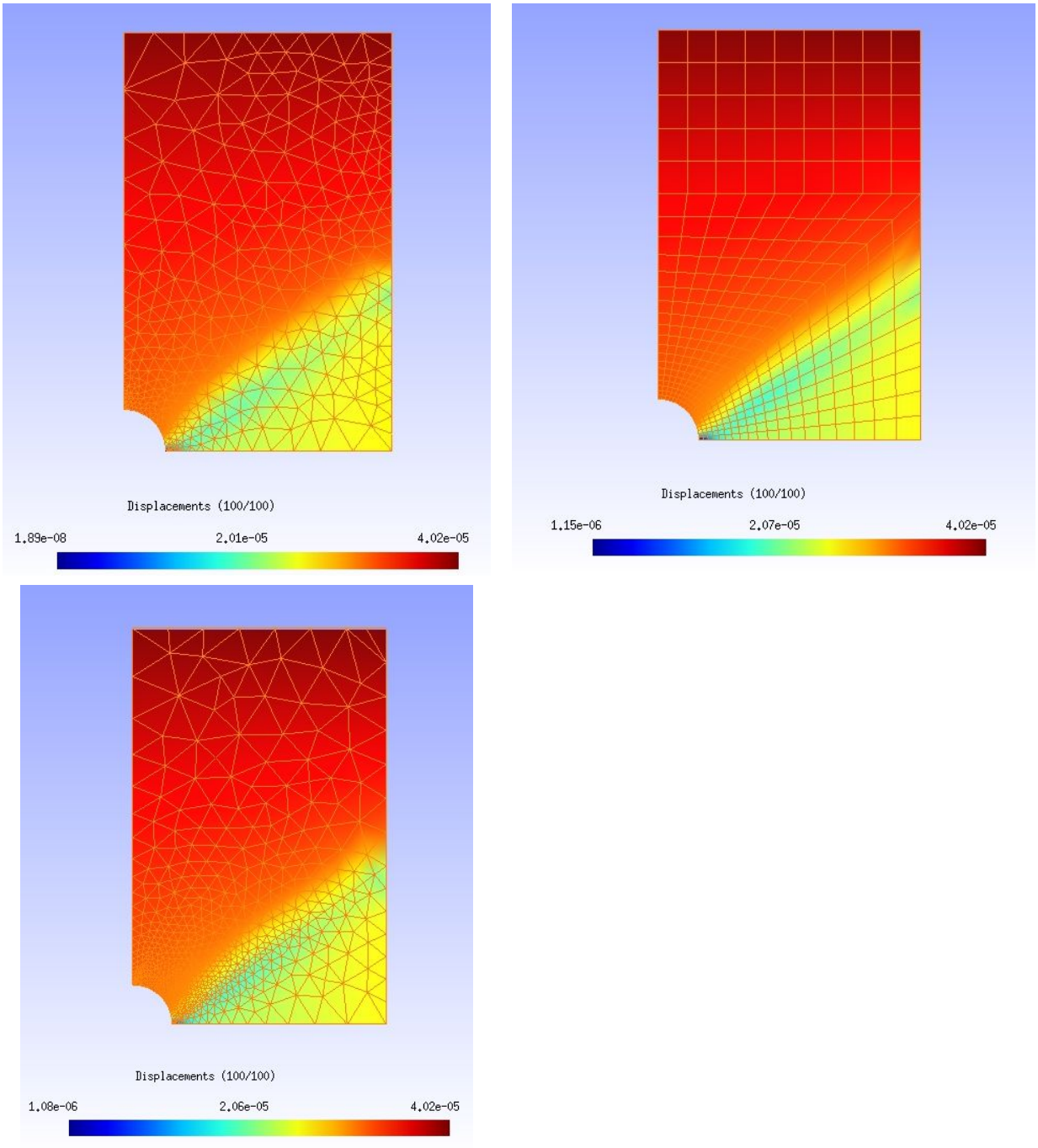

Figure 5.5: Displacement (m) at time $t = 10sec$, showing different meshes, on the top left "mesh 1", on the top right "mesh 2" and on the bottom "mesh 3"

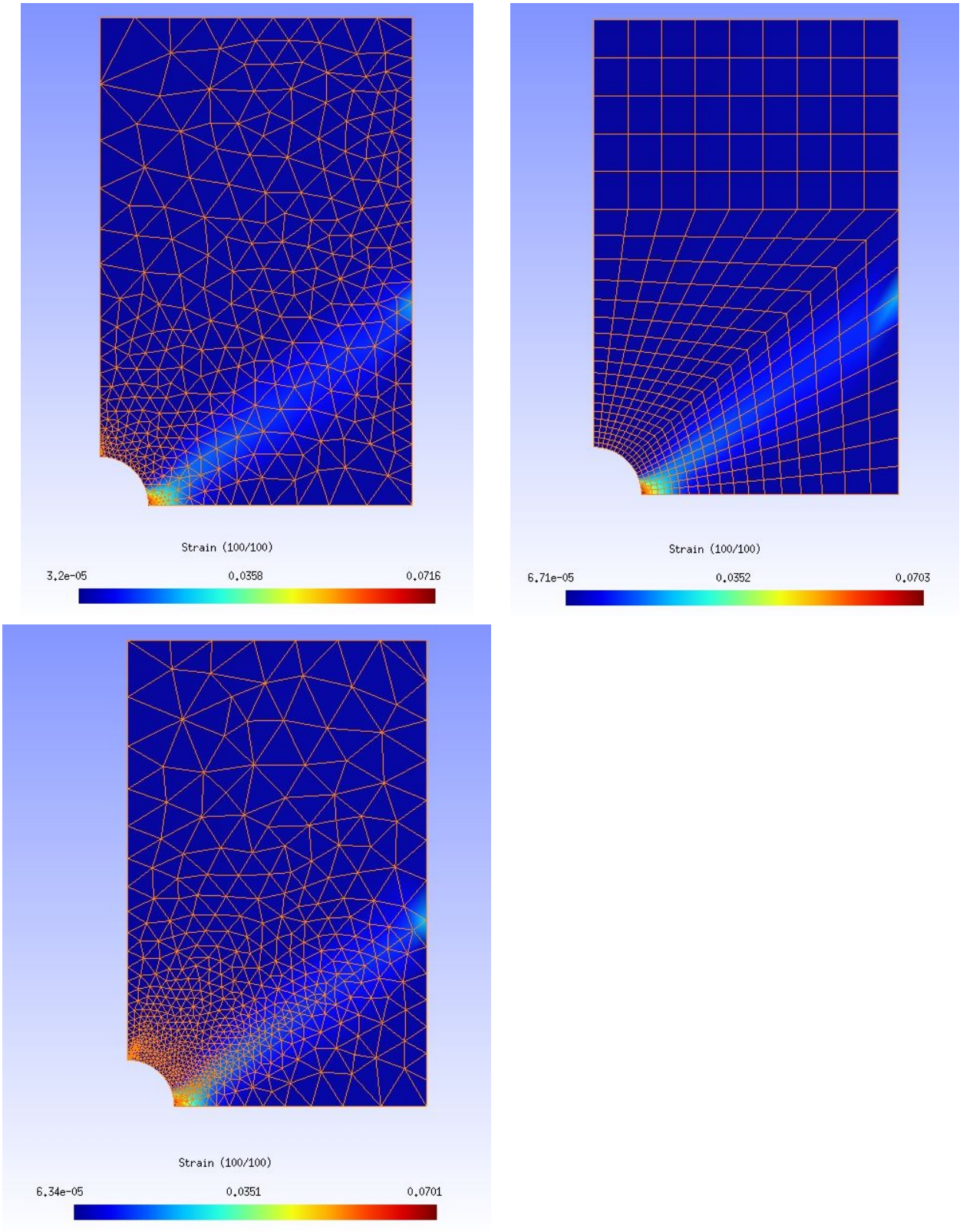

Figure 5.6: Strain at time $t = 10sec$, showing different meshes, on the top left "mesh 1", on the top right "mesh 2" and on the bottom "mesh 3"

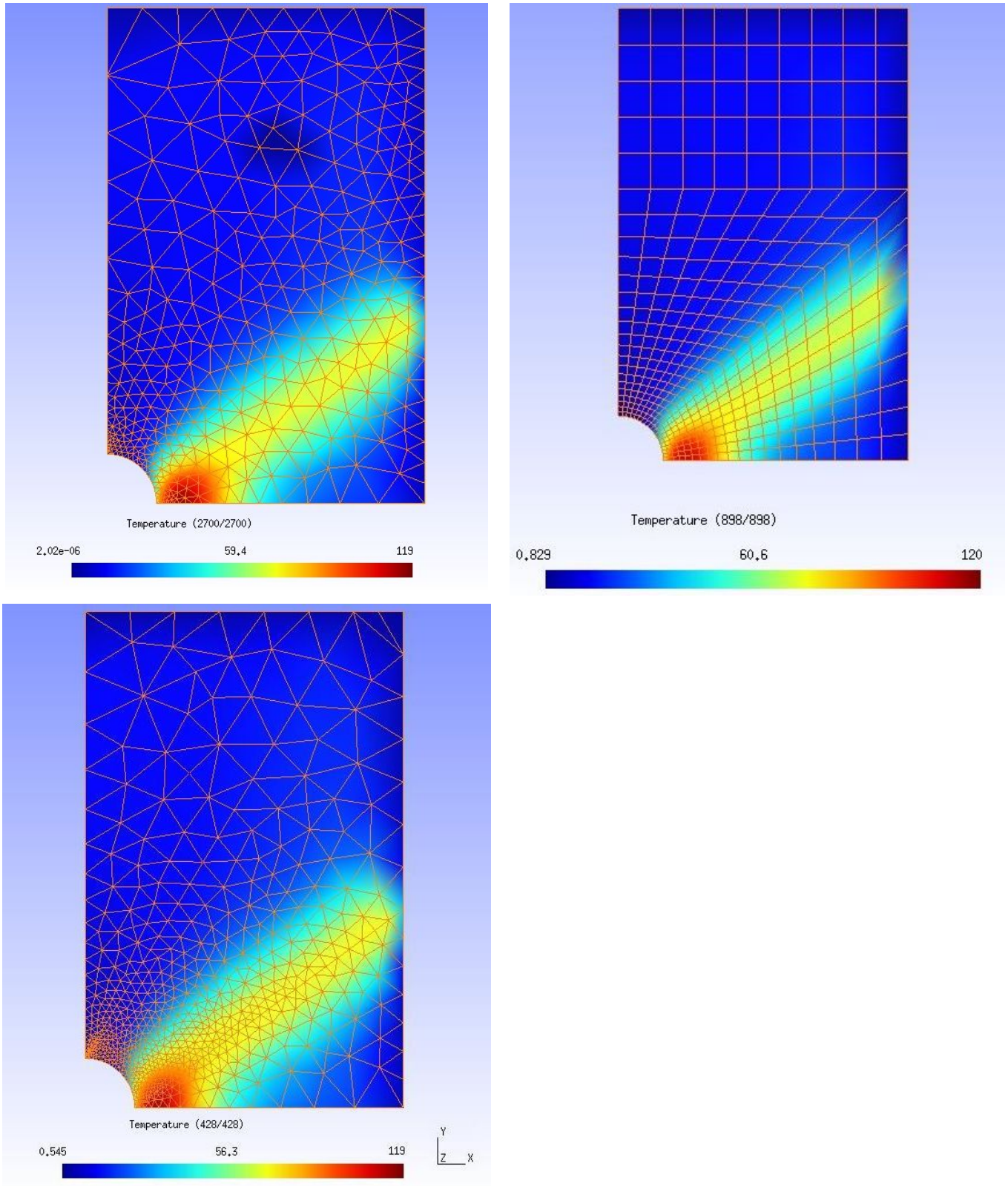

Figure 5.7: Temperature increase (K) at time $t = 30sec$, showing different meshes, on the top left "mesh 1", on the top right "mesh 2" and on the bottom "mesh 3"

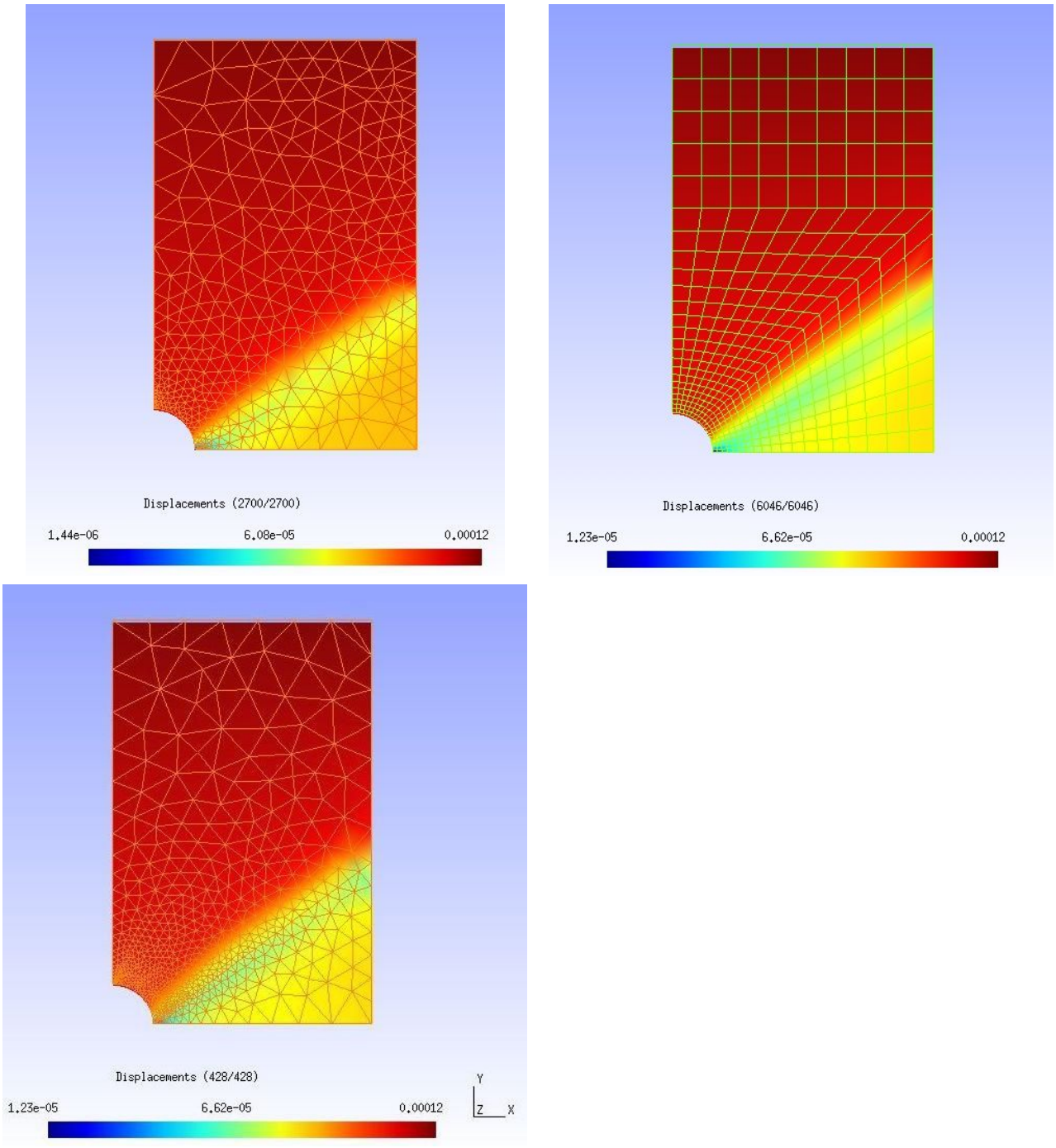

Figure 5.8: Displacement (m) at time $t = 30sec$, showing different meshes, on the top left "mesh 1", on the top right "mesh 2" and on the bottom "mesh 3"

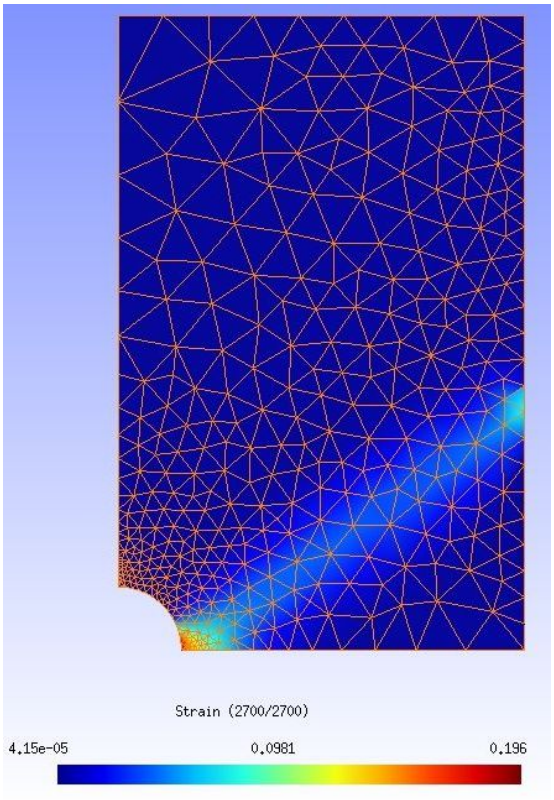

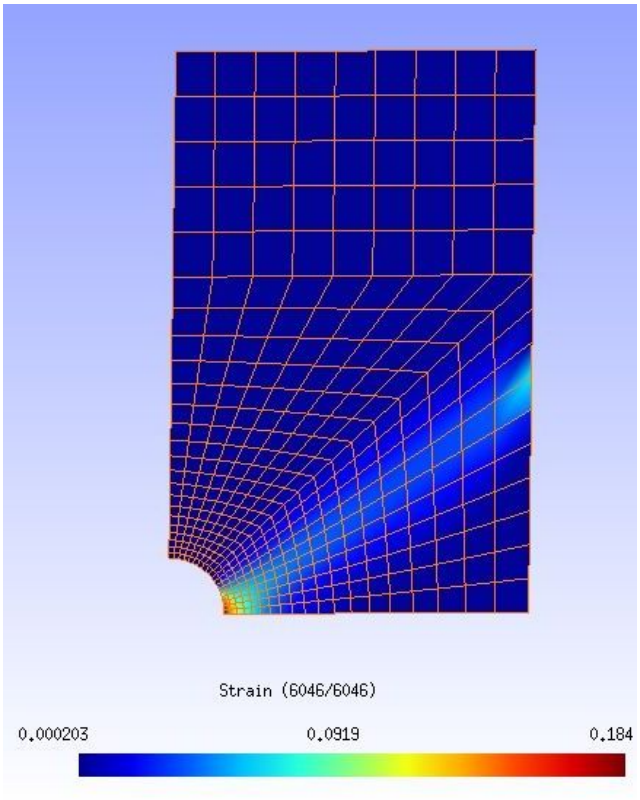

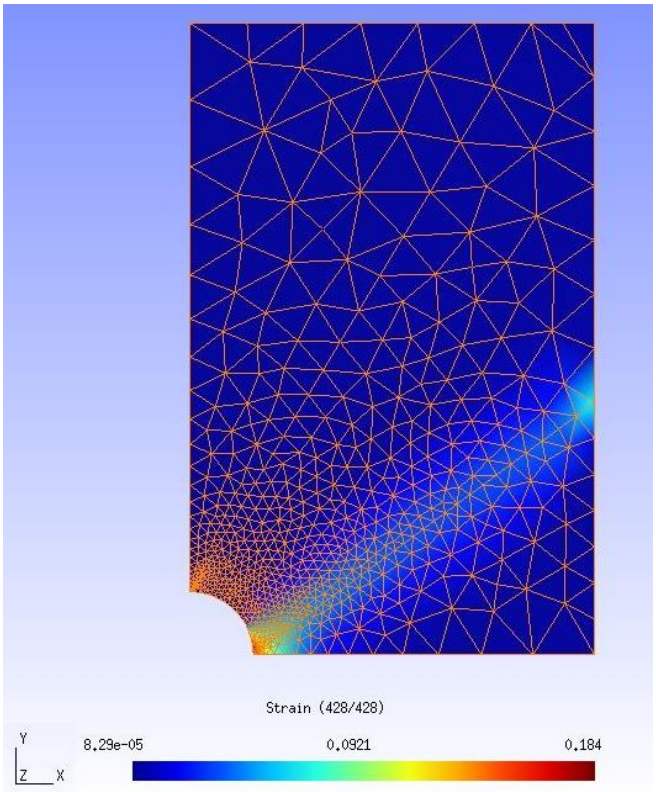

Figure 5.9: Strain at time $t = 30sec$, showing different meshes, on the top left "mesh 1", on the top right "mesh 2" and on the bottom "mesh 3"

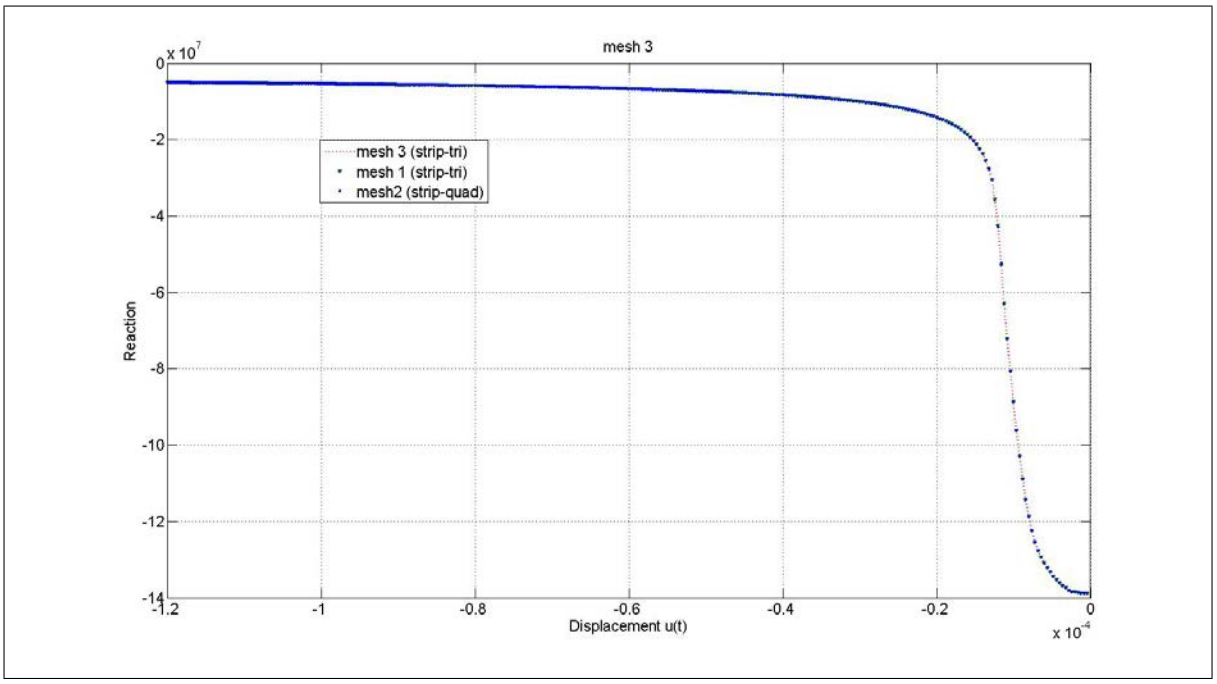

Figure 5.10: Evolution of reaction ($in\ N$) function of displacement ($in\ m$), for the three different meshes

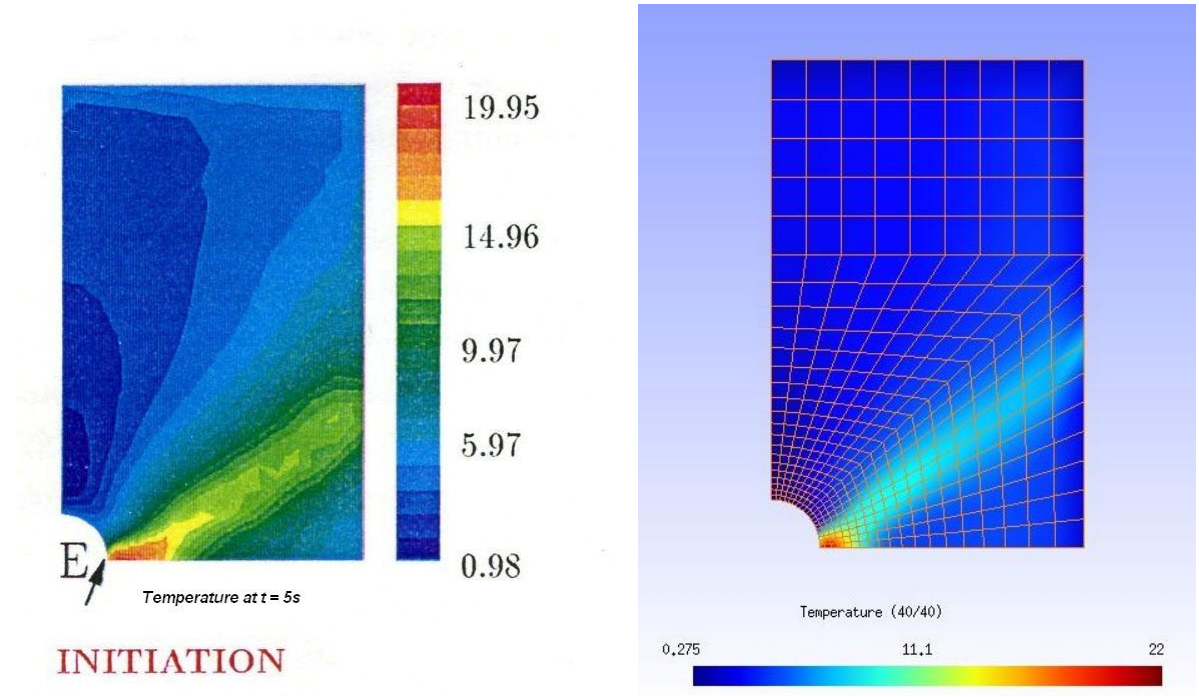

Figure 5.11: Reference solution of the 2D thermo-visco-elastic problem, temperature increase (K) at $t = 5s$

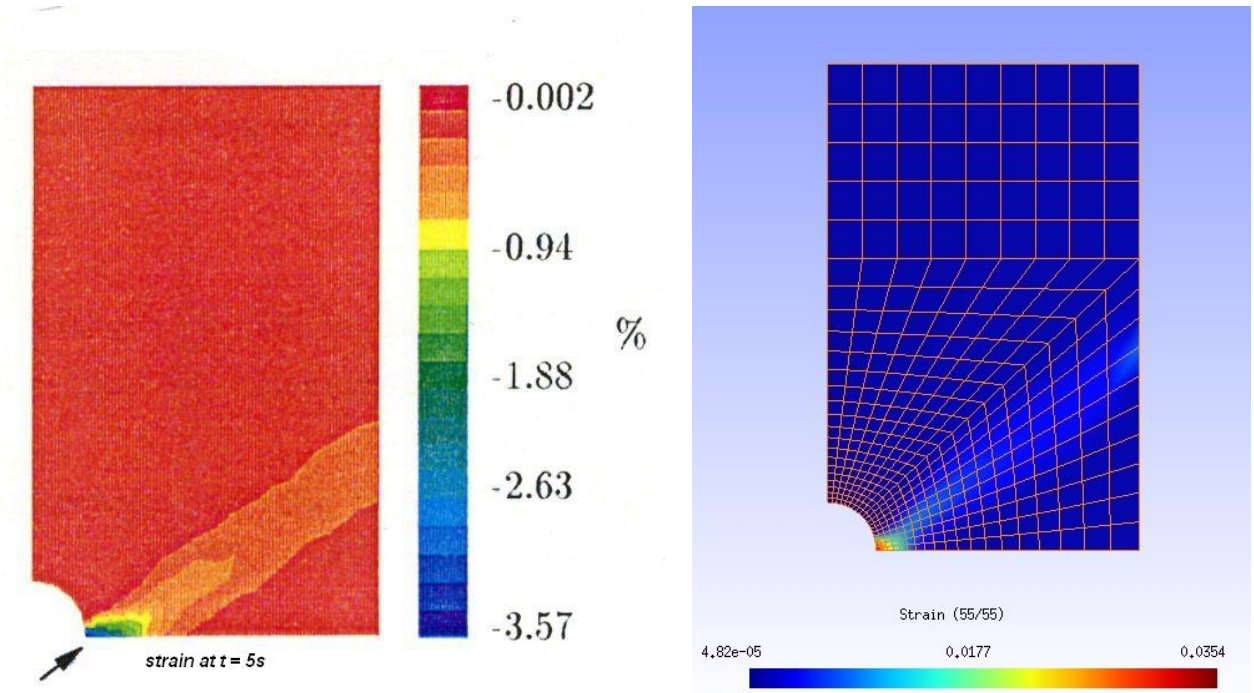

Figure 5.12: Reference solution of the 2D thermo-visco-elastic problem, strain evolution at $t = 5s$

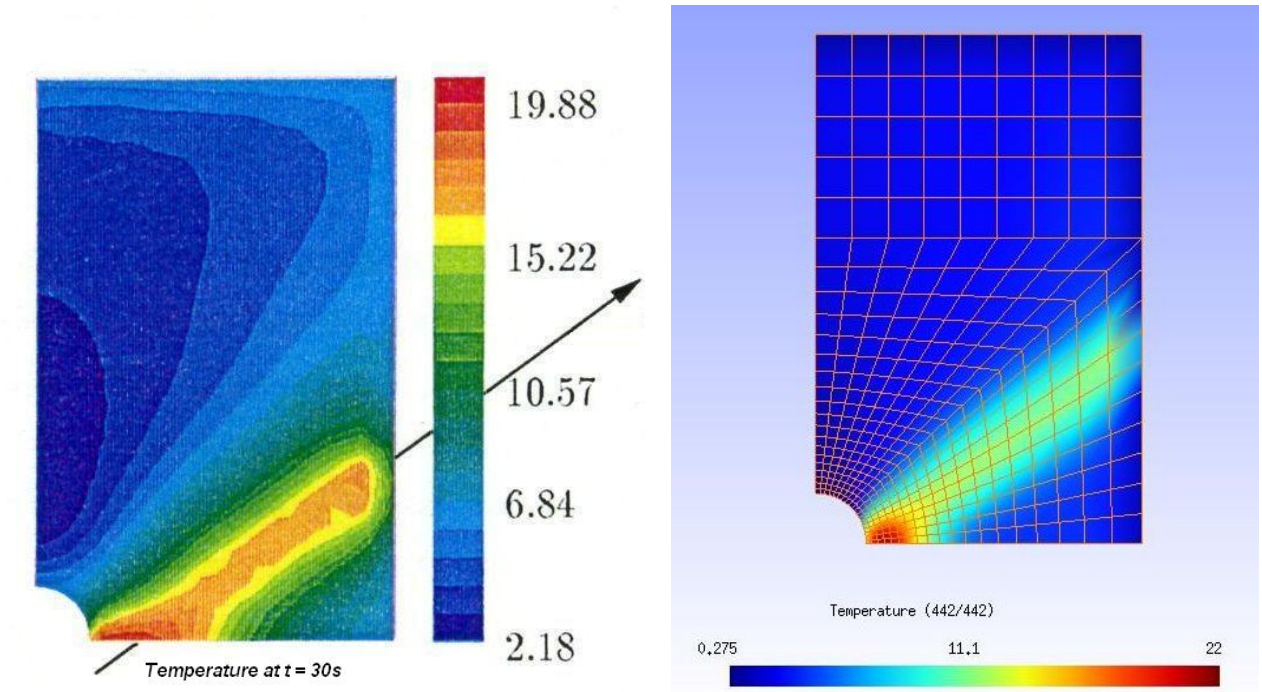

Figure 5.13: Reference solution of the 2D thermo-visco-elastic problem, temperature increase (K) at $t = 30s$

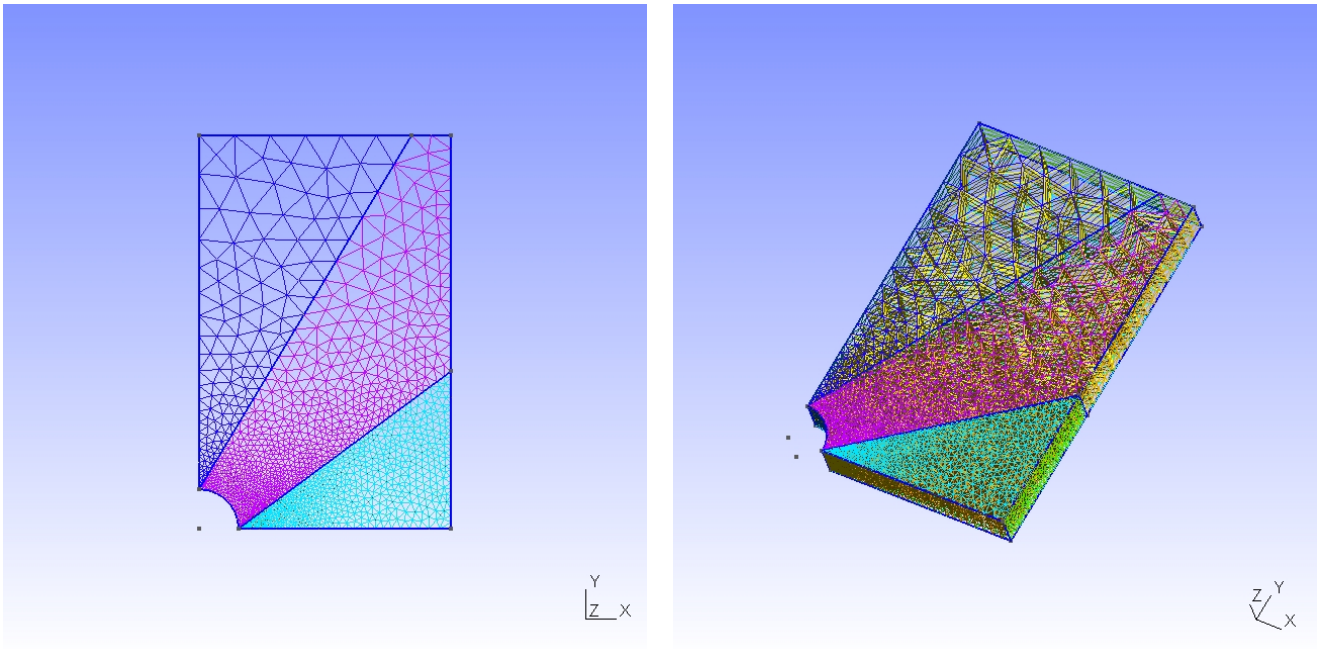

Figure 5.14: 3D mesh of the rectangular plate

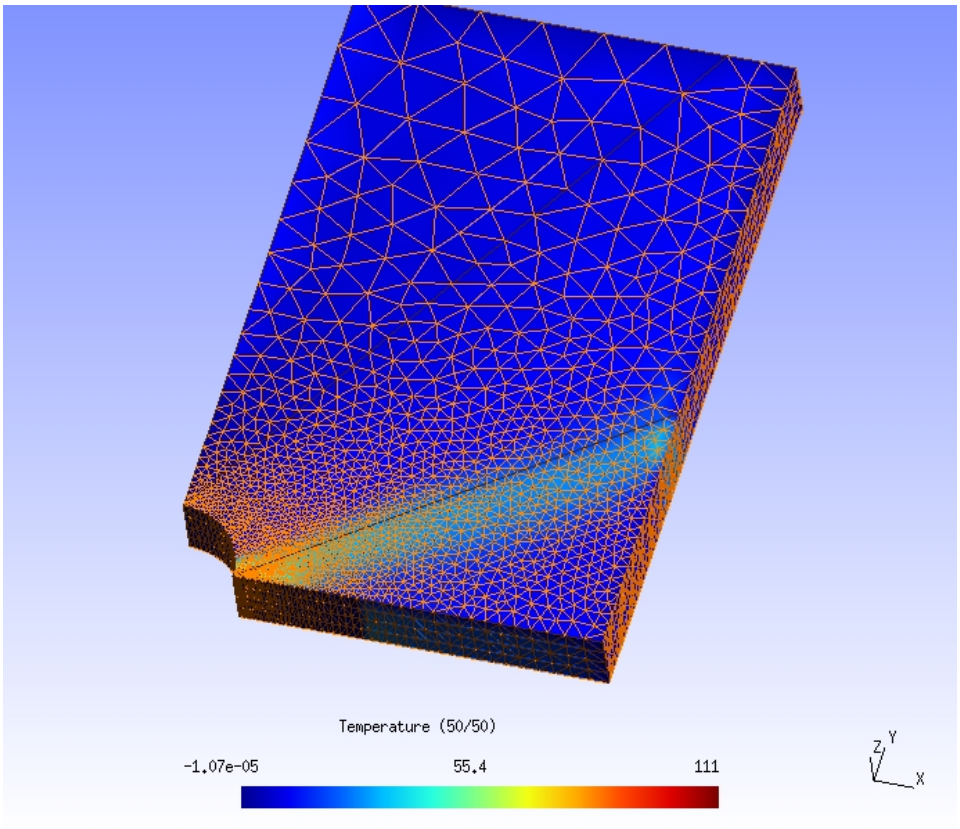

Figure 5.15: Temperature increase (K) at time $t = 50s$

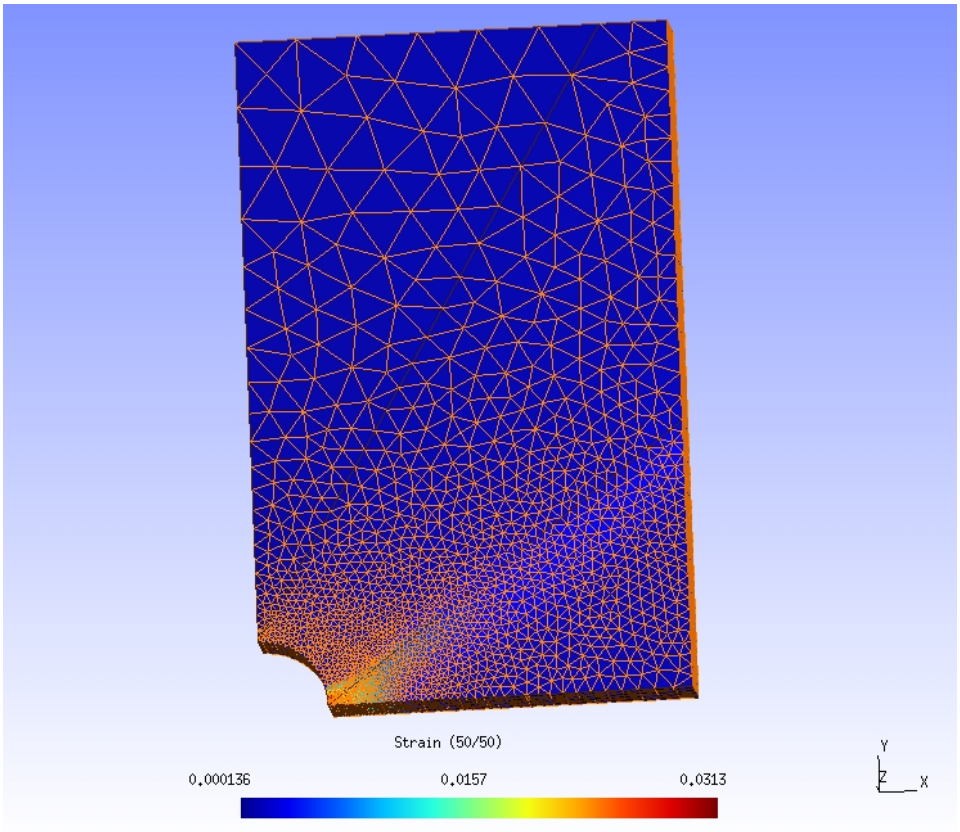

Figure 5.16: Evolution of strain for time $t = 50s$

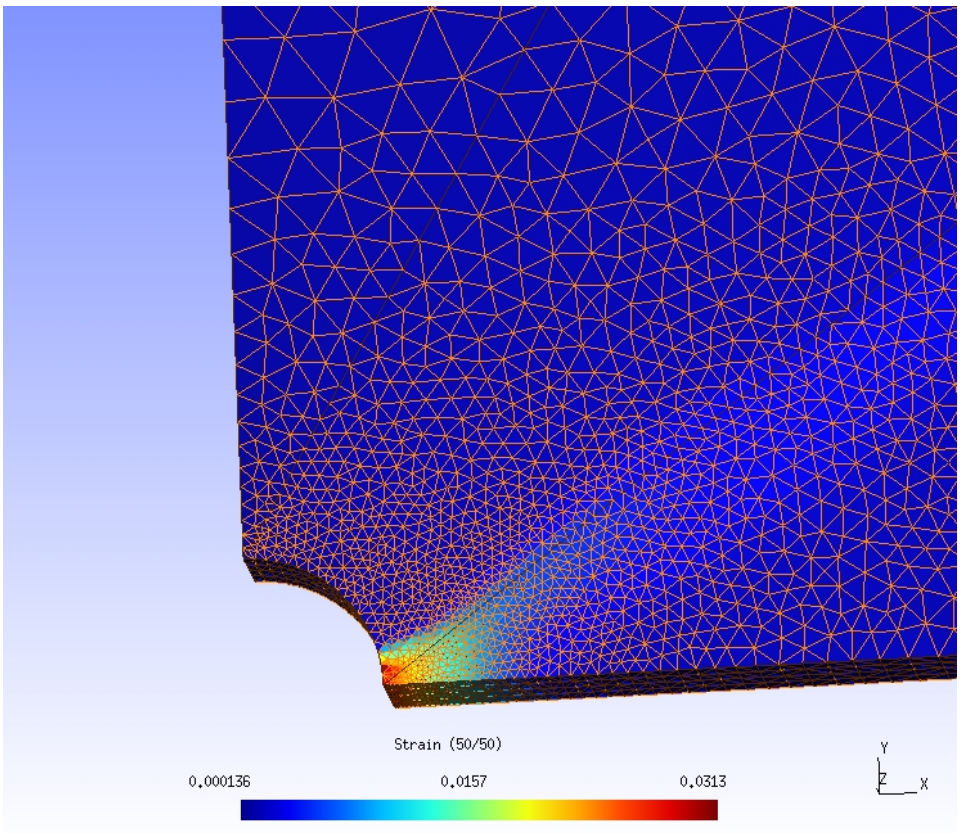

Figure 5.17: Zoom on the strain field at time $t = 50s$

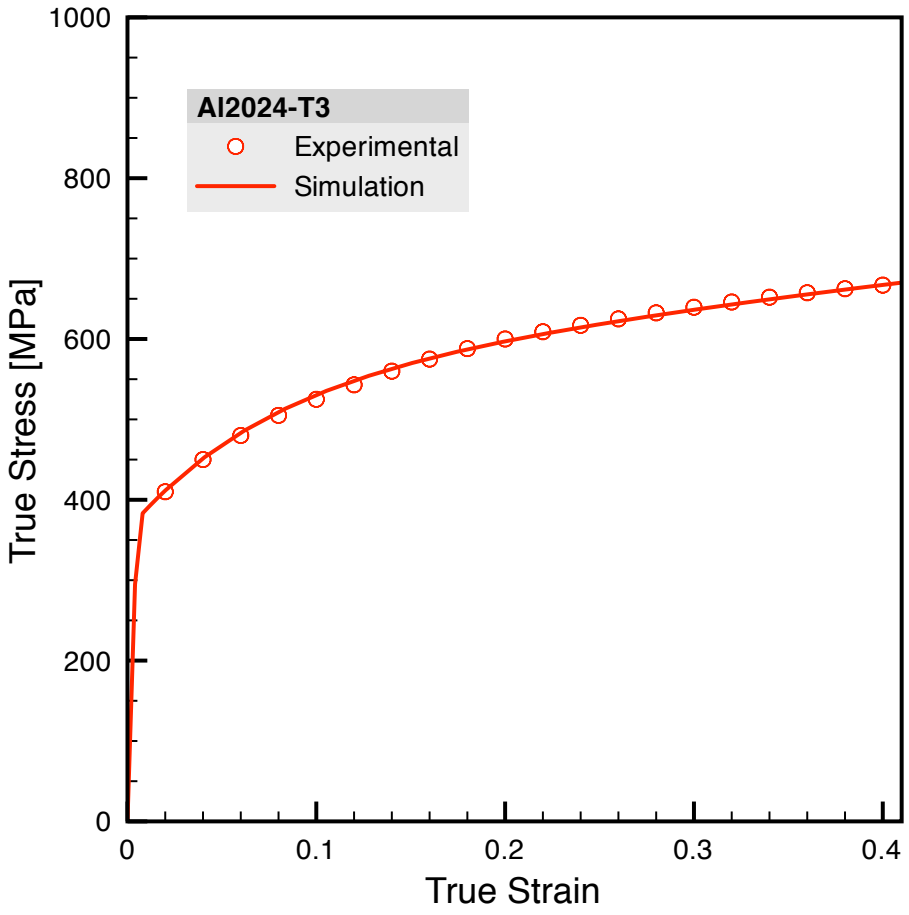

Figure 5.18: Stress-strain curve for rate-independent 2023-T3 aluminum alloy

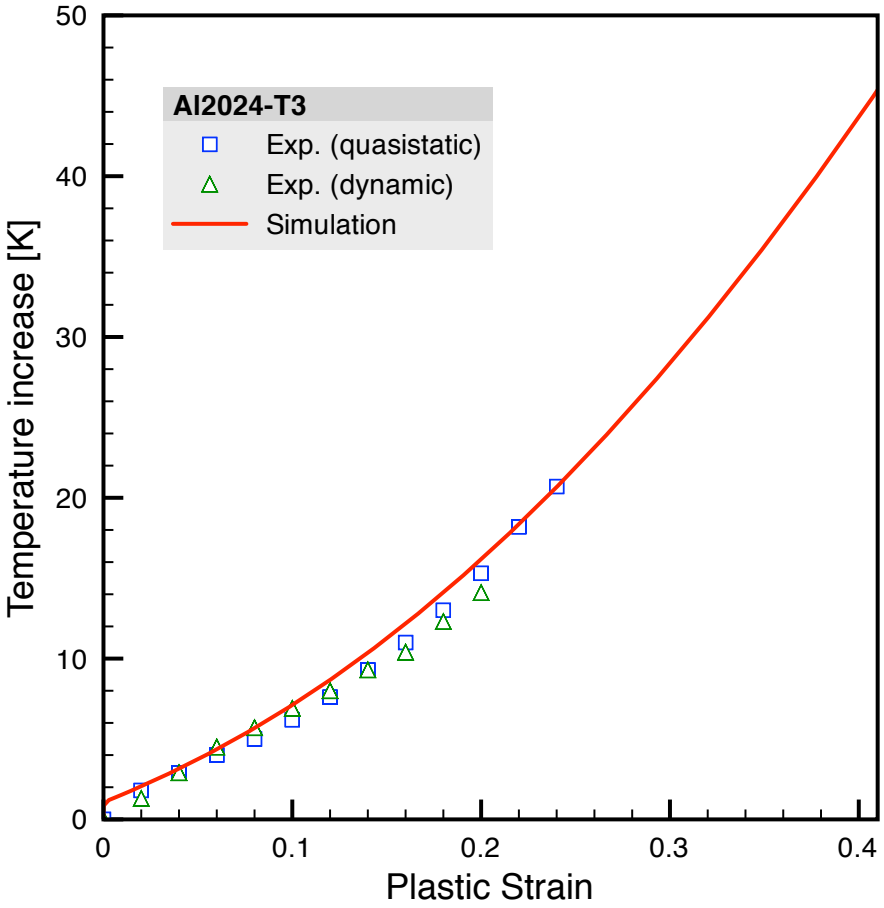

Figure 5.19: Adiabatic heating curve for rate-independent 2023-T3 aluminum alloy

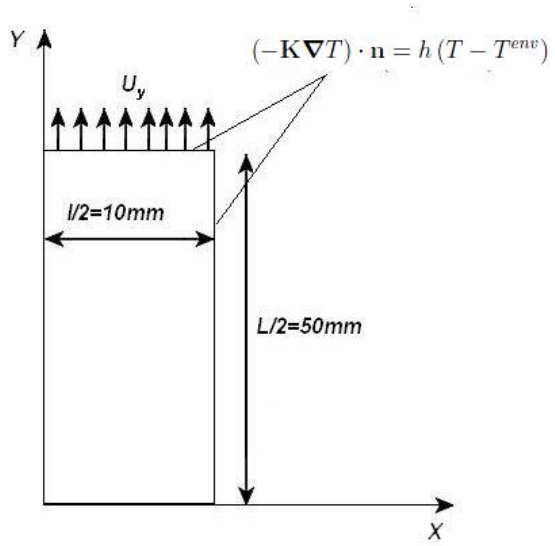

Figure 5.20: Necking of a rectangular bar, the center of the bar corresponds to the axes origin

Initial conditions The rectangular plate is supposed having a uniform temperature at $t = 0s$ of value $293K$, the initial condition are given by

$$\begin{cases} u(0) = 0\ m \\ \dot{u}(0) = 0\ m.s^{-1} \\ \theta(0) = 0K \\ \dot{\theta}(0) = 0K.s^{-1} \end{cases} \tag{5.21}$$

Mesh The choice of mesh is critical in numerical simulation designs. In addition to that it affects the computational cost, it affects also the precision of the obtained results. The mesh is applied, by symmetry, on the eighth of the plate. This is given by figure 5.21

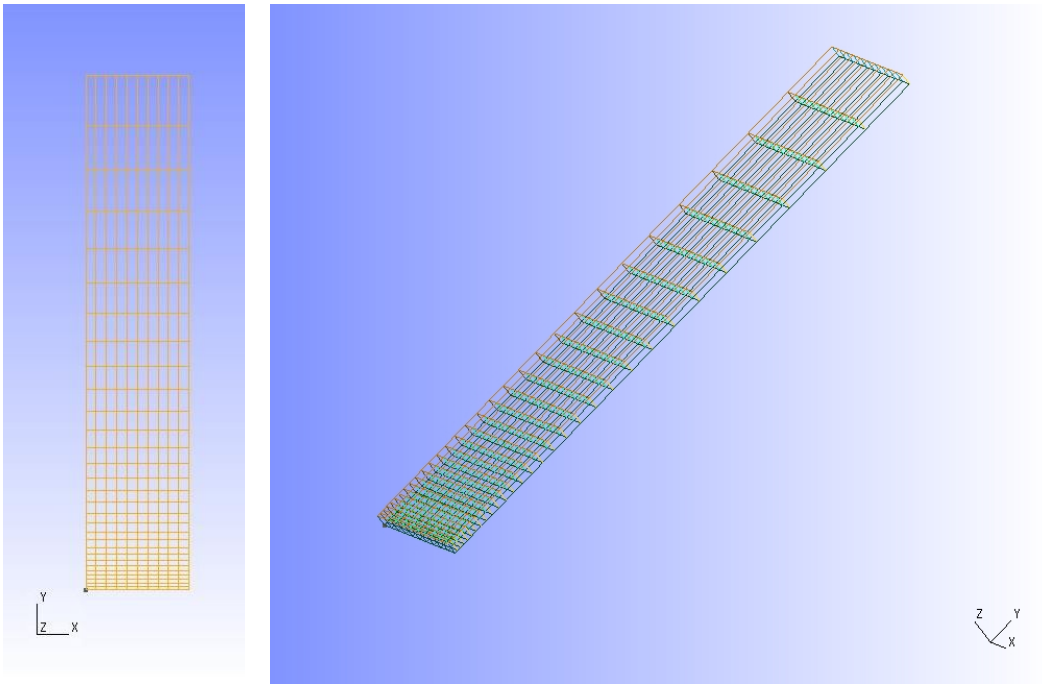

Figure 5.21: Mesh chosen for the simulation, necking of a rectangular bar

Adaptive time step The chosen time step follows the same rule as previous application, that is given by table 5.3, and algorithmic parameters have been chosen as follows:

1. $\Delta t_{max} = 1$ sec
2. $\Delta t_{min} = 10^{-6}$ sec
3. Maximum number of iterations $= 20$

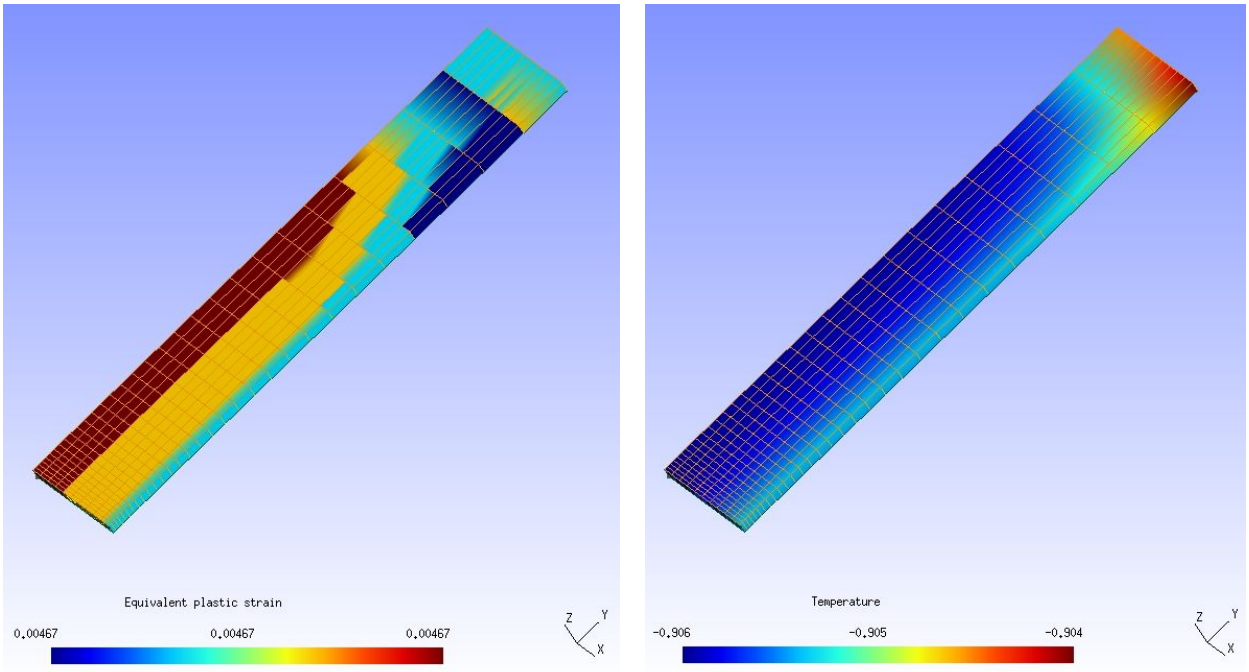

Figure 5.22: Appearance of an inhomogeneity of the temperature field caused by the convective boundary conditions (figure on the right), although the deformation is homogenous (figure on the left) for a simulation time close to $0.5s$

5.3.3 Results

Although the deformation, and thus the associated heating, is initially completely homogeneous, heat exchange with the environment quickly creates an inhomogeneity in the temperature field (see figure 5.22 at a time close to $0.5s$).

Note that the temperature variation in the rod is initially negative, because thermoelastic effects (thermal expansion) dominate at this stage.

The results given by figures 5.23 5.24 and 5.25 shows the displacement, equivalent plastic strain and the temperature field for a time $t = 40s$. We can see clearly that despite the absence of initial geometric defects, the deformation gradually localizes in the middle of the bar, leading to its necking.
The inhomogeneity in the temperature field (although it is initially low) leads to the softening of elastic and plastic mechanical properties, which in turn causes an inhomogeneity in the mechanical field (total and plastic deformation).

5.3.4 Algorithmic analysis

As done in previous applications, we will summarize and comment the efficiency of the algorithms that we have described so far.

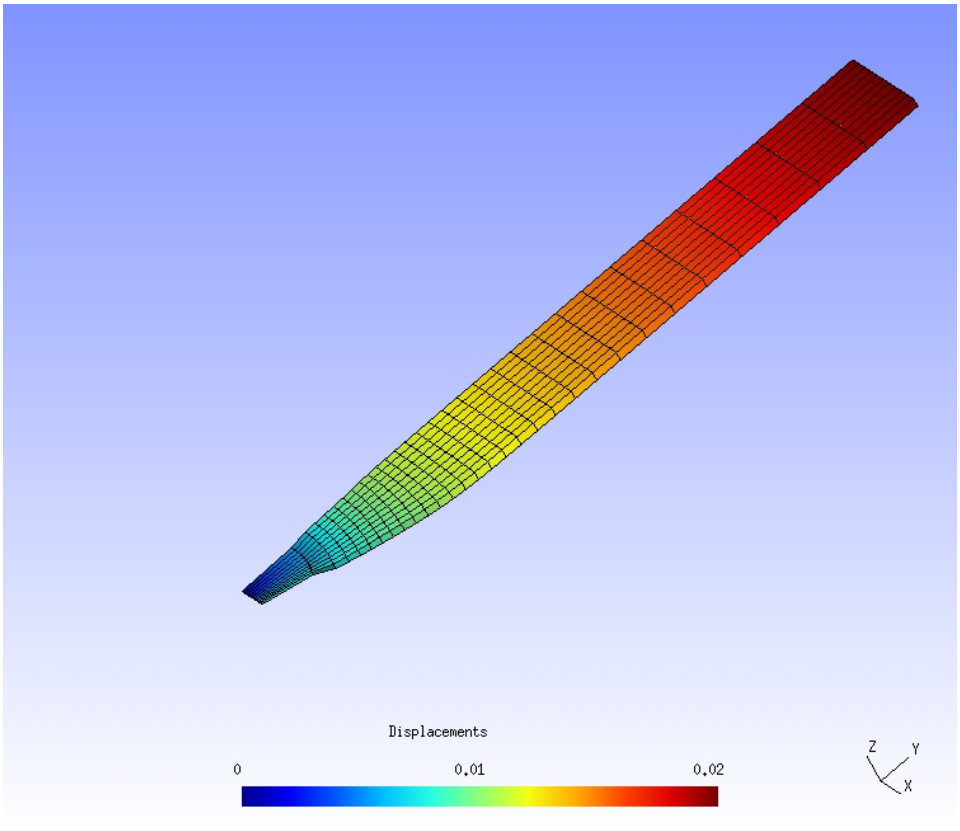

Figure 5.23: Displacement field (m) for $t = 40s$, see figure (5.24)

Table 5.15 summarizes the results of each algorithmic scheme, the simulation is done with a precision equal to 10^{-8} and is run for $15s$ of total simulation time.

Table 5.15: Comparison between the three algorithmic schemes, with a precision of 10^{-8} and a simulation time of 15 s

Algorithm	Total iteration number	Elapsed computational time
Newton	51	$2min\ 38s$
Alternate	58	$8m\ 45s$
Uzawa 1	90	–
Uzawa 2	112	$20m\ 47s$
Modified Uzawa 3	1161	$1h\ 49m\ 52s$
Uzawa 4	1052	–

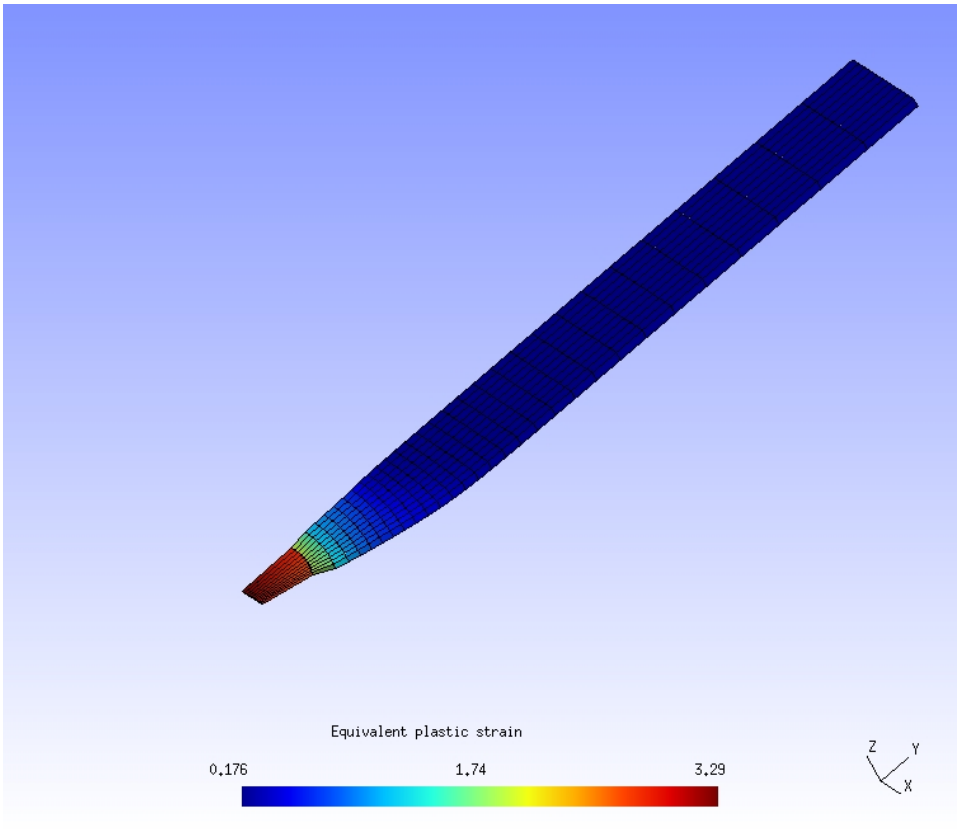

Figure 5.24: Equivalent plastic strain for $t = 40s$, localization of deformation that results from convective boundary conditions

Table 5.15 show an important result, Newton scheme seem to reduce the total iteration number and time cost, whereas Uzawa-like algorithms (that dominated Newton's in the thermo-visco-elastic application), seem to be much less efficient.
When running the simulation, the softening mechanism of mechanical properties, and thus total and plastic deformation seem to affect more and more the simulation cost for t beyond $15s$, where the algorithmic schemes execute more iterations to converge. For this we show the limitation of some algorithms, and the deterioration of others.

Table 5.16 shows the limitation of the alternated algorithm and Uzawa 2, while Newton scheme exhibit the best computational cost.

5.3.5 Conclusion

In this application we have applied the variational formulation to an example considering the traction of a rectangular rod, with an elasto-plastic behavior, leading to its necking due to the inhomogeneity of the temperature field.
Different algorithmic schemes have been applied, in particular Newton, Alternated and

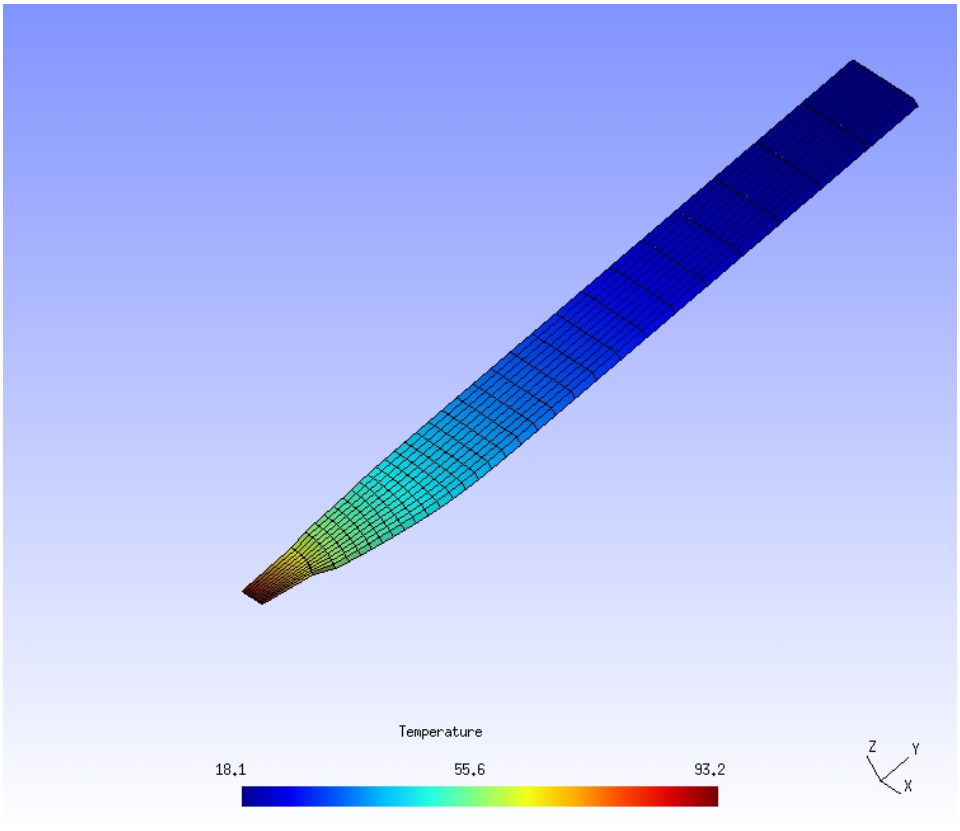

Figure 5.25: Temperature increase (K) for $t = 40s$, localization of temperature that results from convective boundary conditions

Table 5.16: Limitation of different algorithmic schemes, simulation is ran with a precision of 10^{-8} and a simulation time of $40s$

Algorithm	Total iteration number
Newton	2437
Alternate	Limitation at $t = 17s$
Uzawa 1	Limitation at $t = 19s$
Uzawa 2	Limitation at $t = 18.4s$
Modified Uzawa 3	7854
Uzawa 4	6742

Uzawa-like scheme (as described previously).
An important conclusion can be extracted through this application, is that Uzawa-scheme that used to exhibit the best performance between the three schemes in the

case of thermo-visco-elastic application, seems to loose its role in this case, and Newton scheme has acceded to the throne.
We can therefore deduce that there is no absolute scheme that exhibits best performance. Therefore according to the type of coupling, the use of Newton, Uzawa-like or the alternated scheme can behave differently.

Conclusion and Perspective

As we have discussed throughout this manuscript, thermo-mechanical coupling in materials is due to multiple effects such as thermo-visco-elasticity, visco-plasticity, viscous dissipation, dependence of mechanical characteristics on temperature (and so on...) Numerical simulations of these kind of coupling is challenging, especially when a strong coupling effect is present.

We have exposed throughout this work that algorithmic approaches found in the engineering literature of coupled problems fall within two alternative strategies, the monolithic or simultaneous solution scheme that consists of resolving simultaneously mechanical and thermal balance equation, and staggered schemes, in which the coupled system is partitioned therefore the mechanical and thermal problems are solved alternatively.

The main objective of this work was the validation, analysis and improvement of monolithic algorithmic schemes via an energy-consistent variational formulation of coupled thermo-mechanical problems. Note that the presented formulation does not include mechanical inertial effect, but transient thermal effects are taken into account. However, they appear dependent on the loading rate, the problem keeps the form of a quasi-stationary problem. The variational approach has many advantages (see chapter 4), especially that it leads to a symmetric numerical formulation, thus overcoming the disadvantages of classical monolithic strategies that often lead to non-symmetric formulations.

Since the variational formulation allows to write mechanical and thermal balance equation under the form of an optimization problem of a scalar energy-like functional, different optimization algorithmic schemes were used, the classical Newton-Raphson scheme, the alternated algorithm, and Uzawa-like algorithms.
We recall briefly that alternated scheme consists in minimizing with respect to displacement, at a constant temperature, then maximizing with respect to temperature at a constant displacement until convergence, while Uzawa-like scheme consists of limiting the maximization on the temperature to only one iteration (see chapter 4).

To show the validation of the energetic formulation, and compare the efficiency of different algorithms, various applications of coupled thermo-mechanical problems have been exposed in details, such as thermo-visco-elastic strong coupled problem from a simplified problem consisting of an infinitesimal control volume to a more general $2D$ and $3D$ cou-

pled thermo-elastic boundary-value problem, and then another application of a necking in a bar with an thermo-elasto-plastic coupling.
In all cases the effects of heat capacity, intrinsic dissipation and the heat exchange with the environment are included in the model.

The simplified case, showed that all three algorithms exhibit good performance, but Uzawa-like algorithms seem to reduce the global time cost then the two others.
After many test, we also showed that the solution of the scalar energy-like functional is a saddle point. Note that this results motivated us to use specific algorithms, such as Uzawa scheme.

The results of a more general $2D$ thermo-visco-elastic problem shows an evolution and propagation of a localized deformation zone that is accompanied by a localized temperature zone. A reference solution validated the obtained results.
Although Newton exhibits good performance in the beginning, it encounters convergence difficulties when coupling becomes stronger and localization develops, causing the limitation of the scheme. This limitation is caused by the non-convergence at the minimal time step allowed. The alternated scheme offers more interesting results since it has overcome the limitation for low precision, and allows better performance at higher ones. Uzawa scheme encounters some problems of convergence, on top of that the extraction of sub-matrices from the total matrix influences considerably the time cost. Therefore we decided to proceed in another manner by treating at first the thermal problem, and then the mechanical problem by limiting the minimization of the displacement field to one iteration. This approach seems to reduce more the global time cost and iteration numbers.

Eventually, the variational formulation is applied to the example of traction of a rectangular rod, with an elasto-plastic behavior, leading to its necking due to the inhomogeneity of the temperature field.
An interesting result is concluded, Uzawa-scheme that used to exhibit the best performance between the three schemes in the case of thermo-visco-elastic application, seems less efficient in this application, while Newton scheme exhibits good performance by overcoming the limitation of other schemes and performs with a better computational cost. This might due to the different types of coupling in each problem, recalling that we have considered a brutal transition for mechanical coefficients with respect to temperature in the visco-elastic model, whereas in the elasto-plastic application, mechanical properties are set constants and thermo-plastic properties (Yield stress dissipated) are modeled with a smoother transition.

Through those various applications, we have showed the capacity of the energy-consistent variational formulation to deal with coupled problems, in addition to its encouraging good performance. The aim of the application of different algorithmic schemes is to find the one that exhibits best performance, and what can be concluded (through these applications) that there is no unique absolute scheme that achieved this task. There-

fore according to the type of coupling, the use of Newton, Uzawa-like or the alternated scheme can behave differently.

Perspective It is still interesting to try to optimize the computation of Schur complement, since the extraction of sub-diagonal matrixes from the total matrix and the evaluation of the Schur complement deteriorates considerably the computational time. The extraction from a skyline matrix being not affordable, sparse storage may improve its evaluation, still need to test it.
We can use for example an optimized system, for example MUMPS (a MUltifrontal Massively Parallel sparse direct Solver), to evaluate the Schur complement. For this we just need to introduce $\mathbf{K}_{UU}$,$\mathbf{K}_{TT}$, $\mathbf{K}_{TU}$ and $\mathbf{K}_{UT}$ in sparse matrix storage (storage of non zero elements), and then MUMPS will evaluate the Schur complement in an optimized way.

Another solution lays on using iterative solver instead of direct solvers. We recall that our problem is to solve the following

$$[\mathbf{K}_c]\{\delta\mathbf{T}\} = \{-\mathbf{R}_T\} \tag{5.22}$$

where $[K_c]$ is given by

$$[\mathbf{K}_c] = [\mathbf{K}_{TT}] - [\mathbf{K}_{TU}][\mathbf{K}_{UU}]^{-1}[\mathbf{K}_{UT}] \tag{5.23}$$

If we choose the conjugate gradient method as an iterative method, the solution of 5.22 transforms into minimizing the following functional:

$$f(\delta\mathbf{T}) = \frac{1}{2}\{\delta\mathbf{T}\}^T[\mathbf{K}_c]\{\delta\mathbf{T}\} - \{\delta\mathbf{T}\}^T\{-\mathbf{R}_T\} \tag{5.24}$$

The resulting algorithm to solve 5.22 is detailed as follow :

We set

$$\begin{aligned} \mathbf{r}_0 &= \{-\mathbf{R}_T\} && (5.25)\\ \mathbf{p}_0 &= \mathbf{r}_0 && (5.26)\\ k &= 0 && (5.27) \end{aligned}$$

repeat

$$\begin{aligned} \alpha_k &= \frac{\mathbf{r}_k^T\mathbf{r}_k}{\mathbf{p}_k^T\mathbf{K}_c\mathbf{p}_k} && (5.28)\\ \{\delta\mathbf{T}\}_{k+1} &= \{\delta\mathbf{T}\}_k + \alpha_k\mathbf{p}_k && (5.29)\\ \mathbf{r}_{k+1} &= \mathbf{r}_k - \alpha_k[\mathbf{K}_c]\mathbf{p}_k && (5.30) \end{aligned}$$

if $\mathbf{r}_{k+1}$ is sufficiently small **then** exit loop **end if**

$$\begin{aligned} \beta_k &= \frac{\mathbf{r}_{k+1}^T \mathbf{r}_{k+1}}{\mathbf{r}_k^T \mathbf{r}_k} && (5.31) \\ \mathbf{p}_{k+1} &= \mathbf{r}_{k+1} + \beta_k \mathbf{p}_k && (5.32) \\ k &= k+1 && (5.33) \end{aligned}$$

end repeat

Note that α and β are scalar and $\mathbf{p}_k$ is a vector.
The computation of $[\mathbf{K}_c]\{\mathbf{p}_k\}$ in the algorithm will be treated as follow

$$[\mathbf{K}_c]\{\mathbf{p}_k\} = [\mathbf{K}_{TT}]\{\mathbf{p}_k\} - [\mathbf{K}_{TU}][\mathbf{K}_{UU}]^{-1}[\mathbf{K}_{UT}]\{\mathbf{p}_k\} \tag{5.34}$$

we set

$$[\mathbf{K}_{UT}]\{\mathbf{p}_k\} = \{\mathbf{V}\} \tag{5.35}$$

and

$$[\mathbf{K}_{UU}]^{-1}\{\mathbf{V}\} = \{\mathbf{W}\} \tag{5.36}$$

Is this case we obtain $\{W\}$ by solving

$$[\mathbf{K}_{UU}]\{\mathbf{W}\} = \{\mathbf{V}\} \tag{5.37}$$

therefore equation 5.34 becomes

$$[\mathbf{K}_c]\{\mathbf{p}_k\} = [\mathbf{K}_{TT}]\{\mathbf{p}_k\} - [\mathbf{K}_{TU}]\{\mathbf{W}\} \tag{5.38}$$

In this case equation 5.38 shows that the construction of the Schur complement is constructed by an alternative way (1 solve of equation 5.37, and 3 multiplication of $[Matrix] \times \{Vectors\}$, and eventually one addition).
Note that the use of this algorithm requires that the total matrix and therefore the Schur complement is a positive definite matrix.

In the chapter of application we have showed that the used of the Schur complement does no change dramatically the iteration numbers (if we compare Uzawa1 and Uzawa2, or Uzawa3 and 4 the performance of each algorithm is comparable), therefore it is interesting to try to use other methods for future work as staggered algorithms, since the base of this work lay on the use of monolithic solution that may lead to impossibly large system and do not take advantage of the time scale involved in the problem.
The use of the staggered strategies will overcome these drawbacks and hopefully, will lead to better computational costs. These strategies still need to be tested via variational approach and to be compared to monolithic solution.

Table 5.17: Isothermal staggered scheme

1	*Predict the temperature field*	$\mathbf{z}^{thermal}(t = t^{k+1}) = \mathbf{z}^{thermal}(t = t^k)$
2	*Solve for the mechanical field*	$\inf_{\varphi_{n+1}} \Phi_n^{**}(\boldsymbol{\varphi}_{n+1}, \overline{T}^p_{n+1})$
3	*Which provides*	$\mathbf{z}^{mechanical}(t = t^{k+1})$
4	*Correct the temperature field*	$\sup_{T_{n+1}} \Phi_n^{**}(\overline{\boldsymbol{\varphi}}_{n+1}, T_{n+1})$
5	*Which provides*	$\mathbf{z}^{thermal}(t = t^{k+1})$
6	*Compute velocity, acceleration and flux fields*	$\dot{\boldsymbol{\varphi}}, \ddot{\boldsymbol{\varphi}}$ *and* $\mathbf{H}$
7	*Move to next step*	$t = t + \Delta t$

Isothermal staggered scheme This scheme partitions the thermo-mechanical problem (without a fixed point) according to different coupled field (displacement and temperature), and the different optimization algorithms may be applied to each partition. In variational form we can write it as

$$\begin{cases} \inf_{\varphi_{n+1}} \Phi_n^{**}(\boldsymbol{\varphi}_{n+1}, \overline{T}^p_{n+1}) \\ \sup_{T_{n+1}} \Phi_n^{**}(\overline{\boldsymbol{\varphi}}_{n+1}, T_{n+1}) \end{cases}$$

In this case the phase 1 is solved by an optimization algorithm (say Newton-Raphson), followed by phase 2 where we may apply another optimization algorithm (and another discretization and time increment if we wish) then we move to the next time step without verifying the balance equations.
This scheme is summarized in table

Adiabatic staggered scheme This scheme partitions the problem into two:
The first phase is an adiabatic elasto-dynamic phase where the entropy is held constant, followed by a heat conduction phase at constant mechanical configuration. In variational

Table 5.18: Adiabatic staggered scheme

1	*Solve for the local adiabatic problem*	$\inf\limits_{\varphi_{n+1}} \sup\limits_{T^A_{n+1}} \Phi^{**}_n(\boldsymbol{\varphi}_{n+1}, T^A_{n+1})$ *where* $\chi(\boldsymbol{G}_{n+1})$ *is ignored*
2	*Which provides*	$\boldsymbol{\varphi}$ *and* T^A
3	*Correct the temperature field*	$\sup\limits_{T_{n+1}} \Phi^{**}_n(\overline{\boldsymbol{\varphi}}_{n+1}, T_{n+1})$
4	*Which provides*	$\mathbf{z}^{thermal}(t = t^{k+1})$
5	*Compute velocity, acceleration and flux fields*	$\dot{\boldsymbol{\varphi}}, \ddot{\boldsymbol{\varphi}}$ *and* $\mathbf{H}$
6	*Move to next step*	$t = t + \Delta t$

form, this is given by :

$$\begin{cases} \inf\limits_{\varphi_{n+1}} \sup\limits_{T^A_{n+1}} \Phi^{**}_n(\boldsymbol{\varphi}_{n+1}, T^A_{n+1}) \text{ where } \chi(\boldsymbol{G}_{n+1}) \text{ is ignored} \\ \sup\limits_{T_{n+1}} \Phi^{**}_n(\overline{\boldsymbol{\varphi}}_{n+1}, T_{n+1}) \end{cases}$$

Note that the phase 1 feature a local adiabatic problem where the temperature as this level is an internal variable. The phase 2 is like the isothermal staggered scheme where the optimization algorithm is applied on the temperature field at a constant mechanical configuration. The staggered scheme is summarized in table 5.18

Conclusion générale

Comme nous l'avons vu tout au long de ce manuscrit, les sources de couplage thermomécanique dans les matériaux viscoélastiques sont multiples : thermo-élasticité, dissipation visqueuse, évolution des caractéristiques mécaniques avec la température. La simulation numérique de ces couplages en calcul des structures présente encore un certain nombre de défis, spécialement lorsque les effets de couplage sont très marqués (couplage fort). De nombreuses approches algorithmiques ont été proposées dans la littérature pour ce type de problème. Ces méthodes vont des approches monolithiques, traitant simultanément l'équilibre mécanique et l'équilibre thermique, aux approches étagées, traitant alternativement chacun des sous-problèmes mécanique et thermique. La difficulté est d'obtenir un bon compromis entre les aspects de précision, stabilité numérique et coût de calcul.

Récemment, une approche variationnelle des problèmes couplés a été proposée par Yang *et al.* , qui permet d'écrire les équations d'équilibre mécanique et thermique sous la forme d'un problème d'optimisation d'une fonctionnelle scalaire. Cette approche variationnelle présente notamment les avantages de conduire à une formulation numérique à structure symétrique, et de permettre l'utilisation d'algorithmes d'optimisation.

L'objectif principal de ce travail était la validation, l'analyse et l'amélioration des schémas algorithmiques monolithique par une approche énergétique variationnelle pour le problème thermo-mécanique couplé. A Noter que la formulation présentée n'inclut pas les effets d'inertie mécanique, mais les effets thermiques transitoires sont pris en compte. Cependant, ils apparaissent sous la forme d'une dépendance à la vitesse de chargement, le problème à résoudre apparait comme un problème quasi-stationnaire et non-linéaire. A noter que l'équation d'équilibre thermique utilisée ici est basée sur un bilan d'entropie calculé sur l'incrément temporel en cours, alors que les approches classiques sont basées sur une équation d'équilibre des flux instantanés.

L'approche variationnelle présente de nombreux avantages (voir chapitre 4), surtout qu'elle conduit à une structure symétrique, évitant ainsi les inconvénients des stratégies monolithiques classiques qui conduisent souvent à des formulations non-symétriques. Comme la formulation variationnelle permet d'écrire les équations d'équilibres mécanique et thermique sous la forme d'un problème d'optimisation d'une fonctionnelle scalaire, différent algorithmes d'optimisation ont été utilisés tel que, le schéma de Newton-Raphson

classique, un schéma d'optimisation alternée, et des algorithmes de type Uzawa.
On rappelle que, la procédure de l'algorithme alterné consiste à effectuer successivement des minimisations (maximisations) par rapport au déplacement (température), tout en gardant la température (déplacement) constante, jusqu'à convergence. Tandis que les schémas de type Uzawa consistent à limiter la maximisation sur la température (ou la minimisation sur le déplacement) à une seule itération.

Pour montrer la validation de la formulation énergétique variationnelle, et comparer l'efficacité de différents schémas algorithmiques, différents problèmes de couplage thermo-mécaniques ont été exposé en détails, allant d'un problème simplifié consistant en un volume élémentaire de matière, à des problèmes plus généraux aux conditions aux limites (2D et 3D), avec des comportements thermo-visco-élastique ou élasto-plastique. Dans tous les cas, les effets de capacité thermique, de dissipation intrinsèque et d'échange de chaleur avec l'environnement sont inclus dans le modèle.

Le cas simplifié, a montré que les trois algorithmes offrent une bonne performance, mais les algorithmes de types Uzawa semblent réduire le plus le coût du temps global de calcul. De même, on obtient un second résultat intéressant que la fonctionnelle présente toujours un point de selle dans chaque cas envisagé.
Le problème thermo-visco-élastique aux conditions limites (2D et 3D) montre une évolution et propagation d'une zone de déformation localisée qui est accompagné par une zone de localisation de température . Les résultats sont comparés à une solution de référence, qui valide bien l'approche variationnelle.

Bien que le schéma de Newton offre une bonne performance au début, il rencontre des difficultés de convergence lorsque la température atteint la zone de transition (forte variation des modules élastique et visqueux) et la localisation se développe, causant la limitation du schéma. Cette limitation est due à la non-convergence du schéma au pas de temps minimal défini par défaut. Le schéma alterné offre des résultats plus intéressants surtout qu'il surmonte la limitation observée avec le schéma de Newton pour des faibles précisions, et permet un meilleur rendement pour des tolérances plus importante. Enfin, on applique le schéma de type Uzawa. Des difficultés ont été rencontrées à cause de l'extraction des sous-matrices de couplage de la matrice tangente, de plus l'évaluation du complément de Schur influence considérablement le temps de calcul global.
Un deuxième type d'algorithme de type Uzawa qui consiste à limiter la minimisation sur le champs de déplacement à une seule itération a également été étudié. Ce dernier schéma semble réduire le coût global du temps de calcul.

Finalement, l'approche variationnelle est appliqué au problème de déclenchement thermique de la striction d'un barreau rectangulaire, avec un comportement élasto-plastique. Les différents algorithmes ont été appliqués afin de tester leurs performances. L'agorithme de Newton semble offrir les meilleurs performance dans ce cas. Rappelons que pour ce problème, le type de couplage est différent du problème précédent où on a considéré une

transition brutale des coefficients mécaniques par rapport à la température, or pour ce problème de striction de la barre, les propriétées mécaniques évoluent progressivement par rapport à la température.

Grâce à ces différentes applications, nous avons montré la capacité de l'approche variationnelle énergétique de traiter les problèmes multiphysiques couplés, ainsi que sa bonne performance. L'application des différents schémas algorithmiques a pour but de comparer les performances que chacun peut offrir, et ce qui peut être conclu est qu'il n'existe pas de schéma absolu unique qui a des meilleurs performances indépendamment du type du problème. Ainsi, selon le type de couplage, l'utilisation d'un schéma ou un autre peut se comporter différemment.

Appendix A

Stability overview

We have already exposed in chapter 3 two types of time stepping method, the monolithic scheme that lead to unconditional stability if we use an implicit scheme, and the staggered algorithms that are designed to overcome the large system obtained by simultaneous schemes, but this is often at the sacrifice of unconditional stability.

In this paragraph we will expose a quick overview about stability analysis of different schemes as exhibited by Simo and Miehe [108] , for this we consider, for simplicity, a coupled non-linear thermo-elastic problem as defined in chapter 3, in which the results are generalizable to other coupled problems.
We recall that the thermo-elastic problem, neglecting inertial forces, can be written under the following form (see section 3.6.2)

$$\dot{\mathcal{X}}(t) = \mathbf{A}\mathcal{X}(t) \tag{A.1}$$

where

$$\mathcal{X}(t) = \left\{ \begin{array}{c} \mathbf{u}(t) \\ \mathbf{v}(t) \\ \theta(t) \end{array} \right\} \tag{A.2}$$

$$\mathbf{A}\mathcal{X}(t) = \left\{ \begin{array}{l} \mathbf{v} \\ \dfrac{1}{\rho_0}\boldsymbol{\nabla}\cdot\left(\overline{\overline{\overline{\mathbf{C}}}} : (\boldsymbol{\nabla}^s\mathbf{u} - \theta\boldsymbol{\alpha})\right) \\ \dfrac{1}{\tilde{c}}\boldsymbol{\nabla}\cdot\left[\tilde{\mathbf{K}}\cdot\boldsymbol{\nabla}\theta\right] - \dfrac{1}{\tilde{c}}\boldsymbol{\alpha} : \overline{\overline{\overline{\mathbf{C}}}} : \boldsymbol{\nabla}^s\mathbf{v} \end{array} \right\} \tag{A.3}$$

The linearized thermo-elastic problem is called stable if it inherits the contractivity property. In numerical analysis context, an algorithm inherits the contractivity property [108, 8, 14, 18] if

$$\frac{1}{2}\frac{d}{dt}\|\mathcal{X}(t)\|^2 = \frac{1}{2}\frac{d}{dt}\left(< \dot{\mathcal{X}}(t), \mathcal{X} >\right) =< \mathbf{A}\mathcal{X}, \mathcal{X} >\leq 0 \tag{A.4}$$

where

$$< \mathbf{A}\mathcal{X}, \mathcal{X} >= \int_{\Omega} \mathcal{X}\mathbf{A}.\mathcal{X} dV \tag{A.5}$$

Where $\mathcal{X}$ and $\mathbf{A}\mathcal{X}$ are given by equation A.2 and A.3 given in chapter 3 (section application to a thermo-elastic problem).

The norm is given by

$$\|\mathcal{X}(t)\|^2 =< \mathcal{X}, \mathcal{X} >= \int_{\Omega} \left(\boldsymbol{\nabla}^s \mathbf{u} : \mathbf{C} : \boldsymbol{\nabla}^s \mathbf{u} + \rho_0 \mathbf{v}.\mathbf{v} + \tilde{c}\theta^2 \right) dV \tag{A.6}$$

A.1 Monolithic scheme

What we have developed so far (see chapter 3 section application) monolithic or simultaneous solution.
To verify the contractivity property of the thermo-elastic problem, equation A.4 shall be satisfied

$$\begin{aligned} < \mathbf{A}\mathcal{X}, \mathcal{X} >= \int_{\Omega} \Bigg\{ & \boldsymbol{\nabla}^s \mathbf{v} : \overline{\overline{\overline{\mathbf{C}}}} : \boldsymbol{\nabla}^s \mathbf{u} + \rho_0 \frac{1}{\rho_0} \mathbf{div} \left[\overline{\overline{\overline{\mathbf{C}}}} : (\boldsymbol{\nabla}^s \mathbf{u} - \theta \boldsymbol{\alpha}) \right] .\mathbf{v} \\ & + \tilde{c} \frac{1}{\tilde{c}} \left[div \left(\mathbf{K}.\boldsymbol{\nabla}\theta \right) - \boldsymbol{\alpha} : \overline{\overline{\overline{\mathbf{C}}}} : \boldsymbol{\nabla}^s \mathbf{v} \right] \theta \Bigg\} dV \end{aligned} \tag{A.7}$$

Where

$$\int_{\Omega} \left\{ \boldsymbol{\nabla}^s \mathbf{v} : \overline{\overline{\overline{\mathbf{C}}}} : \boldsymbol{\nabla}^s \mathbf{u} - \boldsymbol{\alpha} : \overline{\overline{\overline{\mathbf{C}}}} : \boldsymbol{\nabla}^s \mathbf{v} \right\} dV = \int_{\Omega} \boldsymbol{\nabla}^s \mathbf{v} : \overline{\overline{\overline{\mathbf{C}}}} : \left(\boldsymbol{\nabla}^s \mathbf{u} - \theta \boldsymbol{\theta} \alpha \right) dV = 0 \tag{A.8}$$

and

$$\int_{\Omega} \mathbf{div} \left[\overline{\overline{\overline{\mathbf{C}}}} : (\boldsymbol{\nabla}^s \mathbf{u} - \theta \boldsymbol{\alpha}) \right] .\mathbf{v} dV = - \int_{\Omega} \boldsymbol{\nabla}^s \mathbf{v} : \overline{\overline{\overline{\mathbf{C}}}} : \left(\boldsymbol{\nabla}^s \mathbf{u} - \theta \boldsymbol{\theta} \alpha \right) dV + \int_{\delta\Omega} \left(\overline{\overline{\overline{\mathbf{C}}}} : (\boldsymbol{\nabla}^s \mathbf{u} - \theta \alpha) \right) .\mathbf{n} dA = 0 \tag{A.9}$$

Equations A.8 and are the result of divergence theorem, which correspond to the cancelation of thermal stresses and the structural elastic heating terms taking place in those equations. Therefore, equation A.10 becomes

$$< \mathbf{A}\mathcal{X}, \mathcal{X} >= \int_{\Omega} div \left(\mathbf{K}.\boldsymbol{\nabla}\theta \right) dV = - \int_{\Omega} \boldsymbol{\nabla}\theta \mathbf{K} \boldsymbol{\nabla}\theta dV + \int_{\delta\Omega} \theta \left(\mathbf{K}\boldsymbol{\nabla}\theta \right) \mathbf{n} dA \tag{A.10}$$

Where

$$\int_{\delta\Omega} \theta \left(\mathbf{K}\boldsymbol{\nabla}\theta \right) \mathbf{n} dA = 0 \qquad \text{Homogeneous boundary condition}$$

then

$$< \mathbf{A}\mathcal{X}, \mathcal{X} >= \int_{\Omega} div \left(\mathbf{K}.\boldsymbol{\nabla}\theta \right) dV = - \int_{\Omega} \boldsymbol{\nabla}\theta \mathbf{K} \boldsymbol{\nabla}\theta dV \leq 0 \tag{A.11}$$

Equation A.11 is the proof of contractivity of A, therefore the simultaneous solution scheme inherit the contractivity property, therefore it is unconditionally stable. Equation A.11 shows that energy lost is due to conductivity.

A.2 Isothermal split

The coupled problem is now split into two operators, the first one where the temperature is held constant, and the second purely thermal phase where the mechanical configuration (displacement) is held constant. This split is known as the isothermal staggered split that can be written as follow

$$\mathbf{A} = \mathbf{A}_1 + \mathbf{A}_2 \tag{A.12}$$

Where

$$\mathbf{A}_1\mathcal{X} = \left\{ \begin{array}{l} \mathbf{v} \\ \dfrac{1}{\rho_0}\mathbf{div}\left[\overline{\overline{\overline{\mathbf{C}}}} : (\boldsymbol{\nabla}^s\mathbf{u} - \theta\boldsymbol{\alpha})\right] \\ 0 \end{array} \right\} \qquad \text{Problem 1: mechanical phase at a fixed temperature} \tag{A.13}$$

$$\mathbf{A}_2\mathcal{X} = \left\{ \begin{array}{l} 0 \\ 0 \\ \dfrac{1}{\tilde{c}} div\left[\tilde{\mathbf{K}}.\boldsymbol{\nabla}\theta_{n+\alpha}\right] - \dfrac{1}{\tilde{c}}\boldsymbol{\alpha} : \overline{\overline{\overline{\mathbf{C}}}} : \boldsymbol{\nabla}^s\mathbf{v}_{(n+\alpha)\ or\ (n+1)} \end{array} \right\} \qquad \text{Problem 2: Heat conduction phase} \tag{A.14}$$

It has been shown [108] that the admissible isothermal split of the problem of evolution does not define sub-problems which inherit the contractivity property of the original problem ($\mathbf{A}_1$ cannot generate a quasi-contractive semigroup, thus breaking the contractive structure of the original problem), thus there is no guarantee of stability for the staggered isothermal phase.

A.3 Adiabatic split

Now the coupled thermo-elastic problem is split into another two operators, where the first is an adiabatic elasto-dynamic phase, which the entropy of the system is held constant, and the second one is a heat conduction phase at fixed configuration, this is written as

$$\mathbf{A}_1\mathcal{X} = \left\{ \begin{array}{l} \mathbf{v} \\ \dfrac{1}{\rho_0}\mathbf{div}\left[\overline{\overline{\overline{\mathbf{C}}}} : (\boldsymbol{\nabla}^s\mathbf{u} - \theta\boldsymbol{\alpha})\right] \\ -\dfrac{1}{c}\boldsymbol{\alpha} : \overline{\overline{\overline{\mathbf{C}}}} : \boldsymbol{\nabla}^s\mathbf{u} \end{array} \right\} \qquad \text{Problem 1: Elasto-dynamic phase} \tag{A.15}$$

$$\mathbf{A}_2\mathcal{X} = \left\{ \begin{array}{l} 0 \\ 0 \\ \frac{1}{\tilde{c}} div\left[\tilde{\mathbf{K}}.\boldsymbol{\nabla}\theta_{n+\alpha}\right] \end{array} \right\} \qquad \text{Problem 2: Heat conduction phase} \tag{A.16}$$

The inner product of the two operators is given by

$$\langle \mathbf{A}_1\mathcal{X}, \mathcal{X} \rangle = 0 \tag{A.17}$$

and

$$\langle \mathbf{A}_2\mathcal{X}, \mathcal{X} \rangle = -\int_\Omega \boldsymbol{\nabla}\theta.\overline{\overline{\tilde{\mathbf{K}}}}.\boldsymbol{\nabla}\theta dV \leq 0 \tag{A.18}$$

We can remark that the adiabatic mechanical phase preserves the total energy of the system ($\mathbf{A}_1$ is an operator with no dissipation), whereas the dissipation in the heat conduction phase is the same as in the coupled problem, therefore the adiabatic split preserves the contractivity property, rendering the scheme unconditionally stable.

A.3.1 Limitation of the adiabatic staggered scheme

Although the adiabatic scheme is cited as the ultimate solution of instability that may be encountered after the use of isothermal staggered scheme, adiabatic staggered scheme is limited for a random time discretization and presence of a strong coupling. In fact,this scheme has the features of unconditional instability when considering time discretization characterized by a constant time step [114].
Therefore, it cannot be always limited with such type of discretizaton, especially while implementing a general software for coupled thermo-mechanical problems.

Adam [114] has illustrated this phenomenon by considering a simple case consisting of a traction of an axisymmetric element with a thermo-elastic behaviour. Figure A.1 show the evolution of the temperature of the upper side.

Time discretization is caracterized by constant time step except between 4.9 and 5 *sec* where it is added an additional time at $t = 4.999$ *sec*.
Is is thus found in this moment with two consecutive time steps of very different sizes, an error of evaluation of the temperature field when using the adiabatic scheme.
Similarly, of a given fraction where $\frac{(\Delta t)_{n-1}}{(\Delta t)_n} \neq 1$, the evolution error of temperature is more important at the presence of strong coupling.
On the other hand this phenomenon does not appear when using a constant time step , as in the case illustrated by Armero and Simo [108]

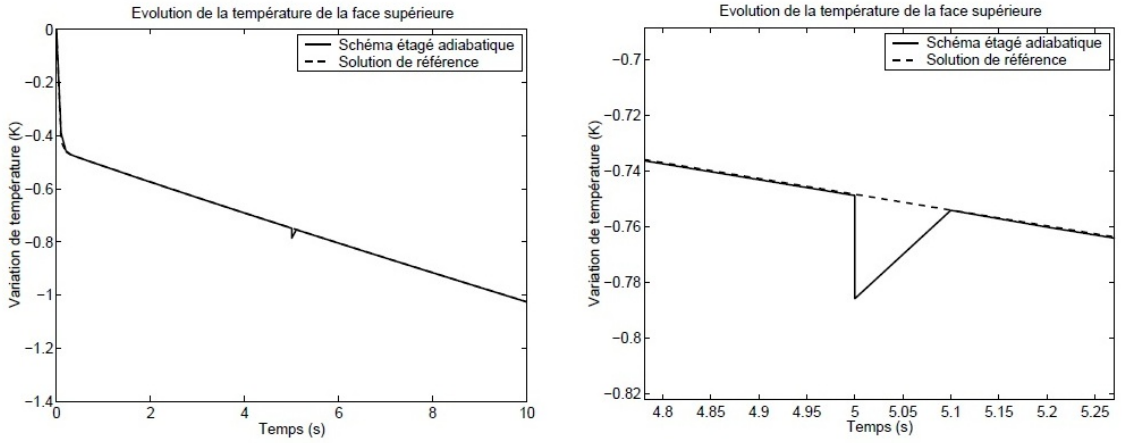

Figure A.1: Limitation of the adiabatic scheme at time $t = 4.999s$, while the evolution of the temperature [114]

Appendix B

Complementary results for the thermo-visco-elastic behaviour of a rectangular plate with a hole in 2D plane

In this annex we will show the complementary results of thermo-visco-elastic behaviour of a rectangular plate with a hole in 2D plane, as described in chapter 5 (section 5.1). In These complementary results, we show the results of Velocities and Heat Flux for time $10s$ and $30s$.

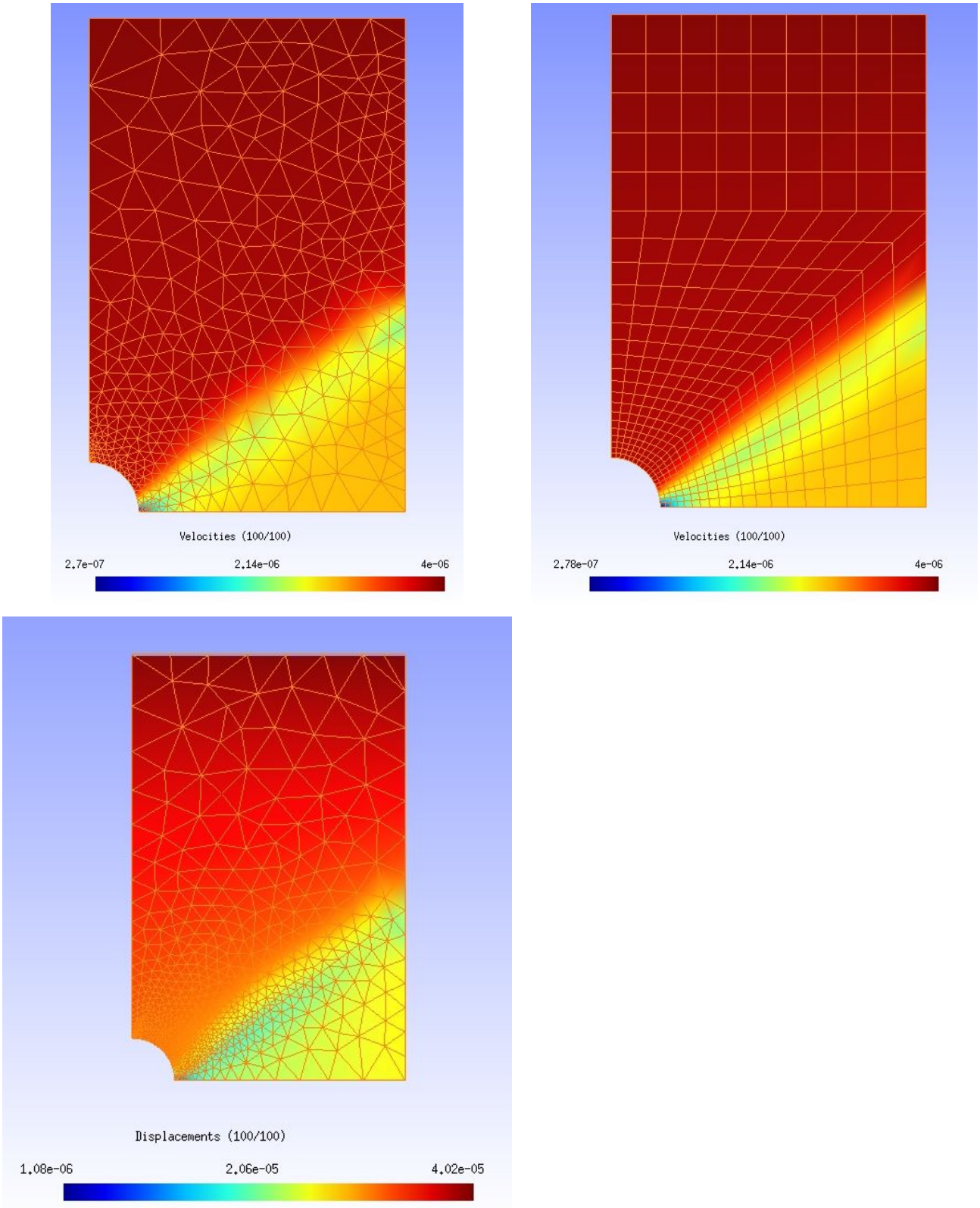

Figure B.1: Velocities ($m.s^{-1}$) at time $t = 10sec$, showing different meshes, on the top left "mesh 1", on the top right "mesh 2" and on the bottom "mesh 3"

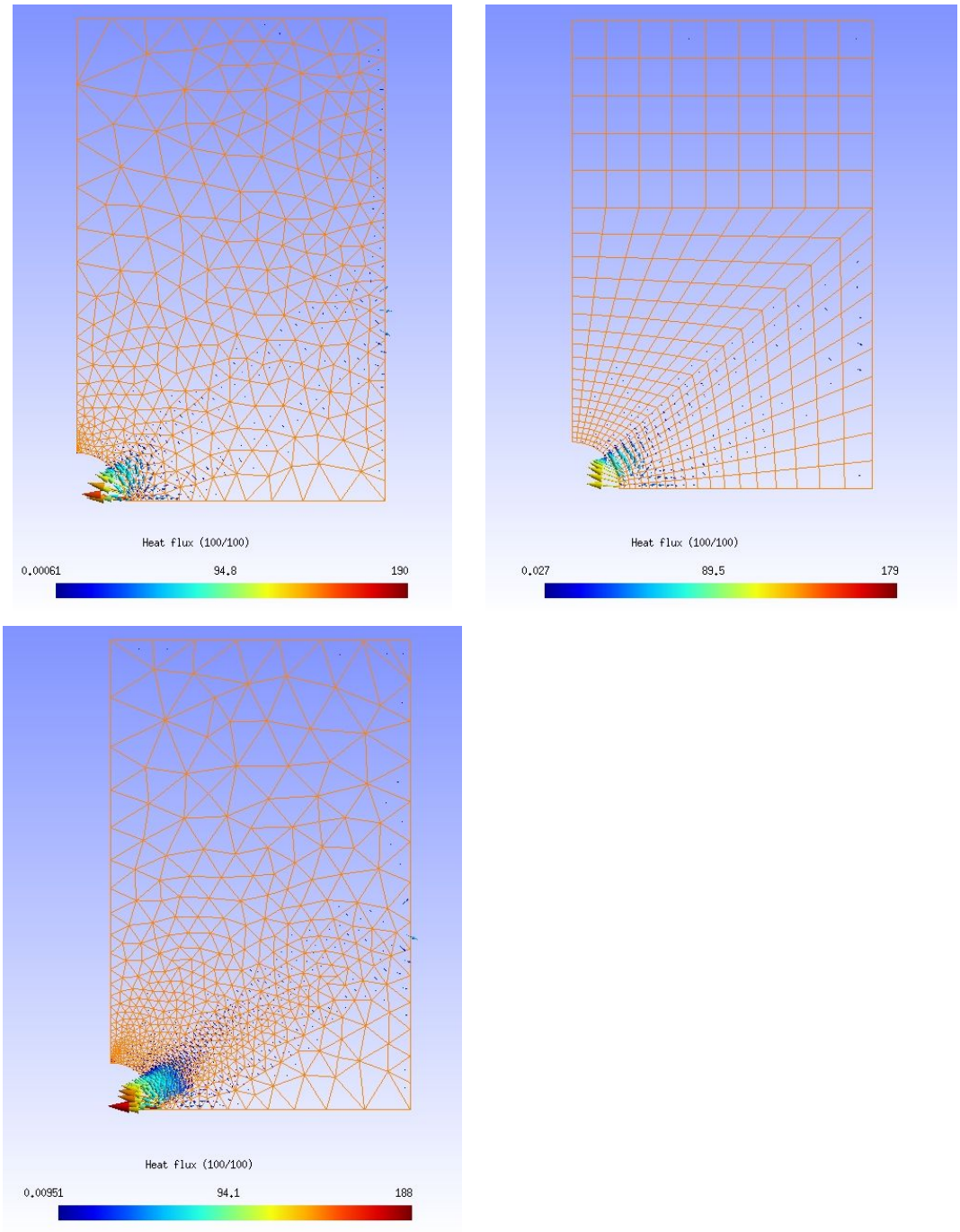

Figure B.2: Heat flux ($W.m^{-2}$) at time $t = 10sec$, showing different meshes, on the top left "mesh 1", on the top right "mesh 2" and on the bottom "mesh 3"

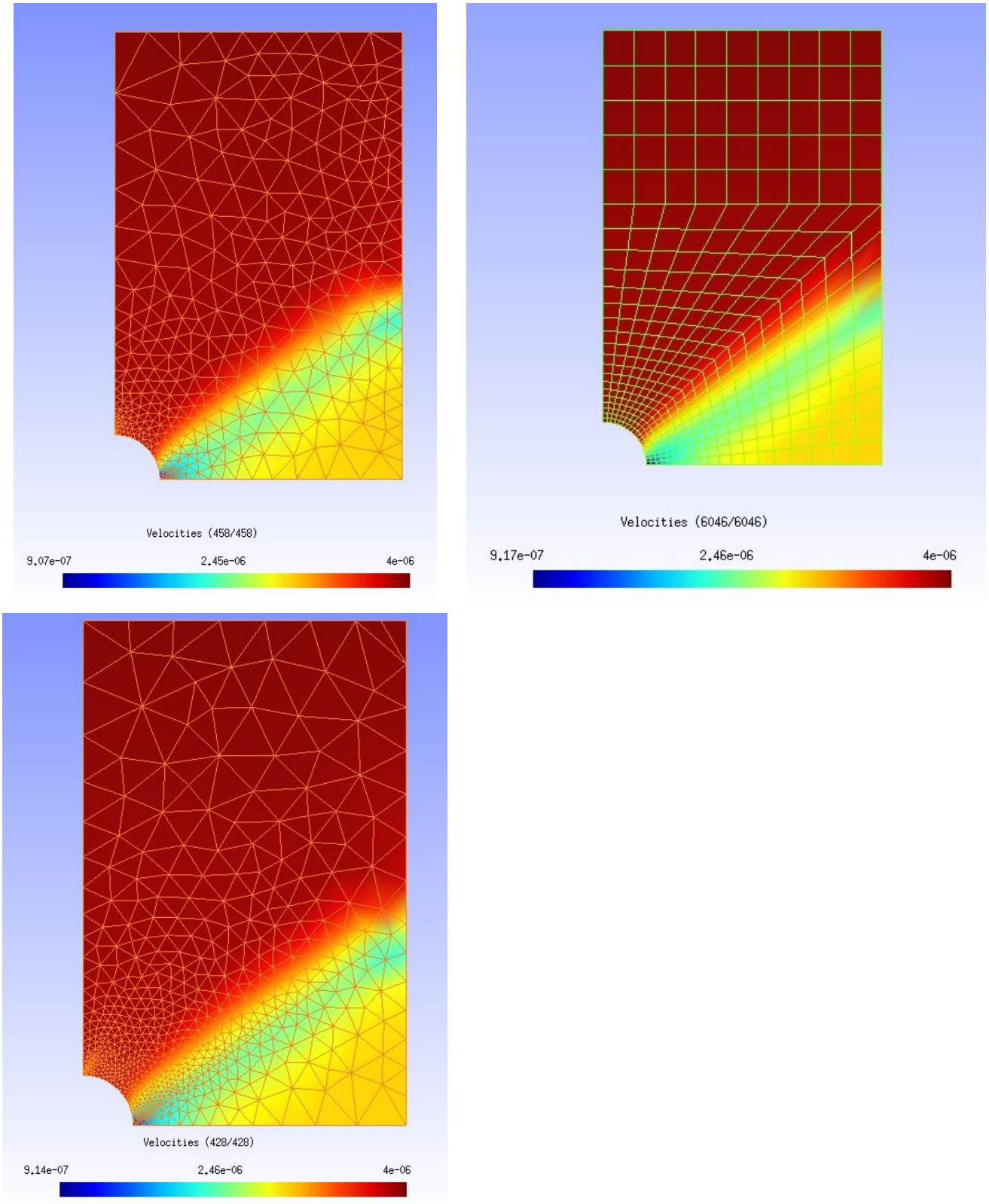

Figure B.3: Velocities ($m.s^{-1}$) at time $t = 30sec$, showing different meshes, on the top left "mesh 1", on the top right "mesh 2" and on the bottom "mesh 3"

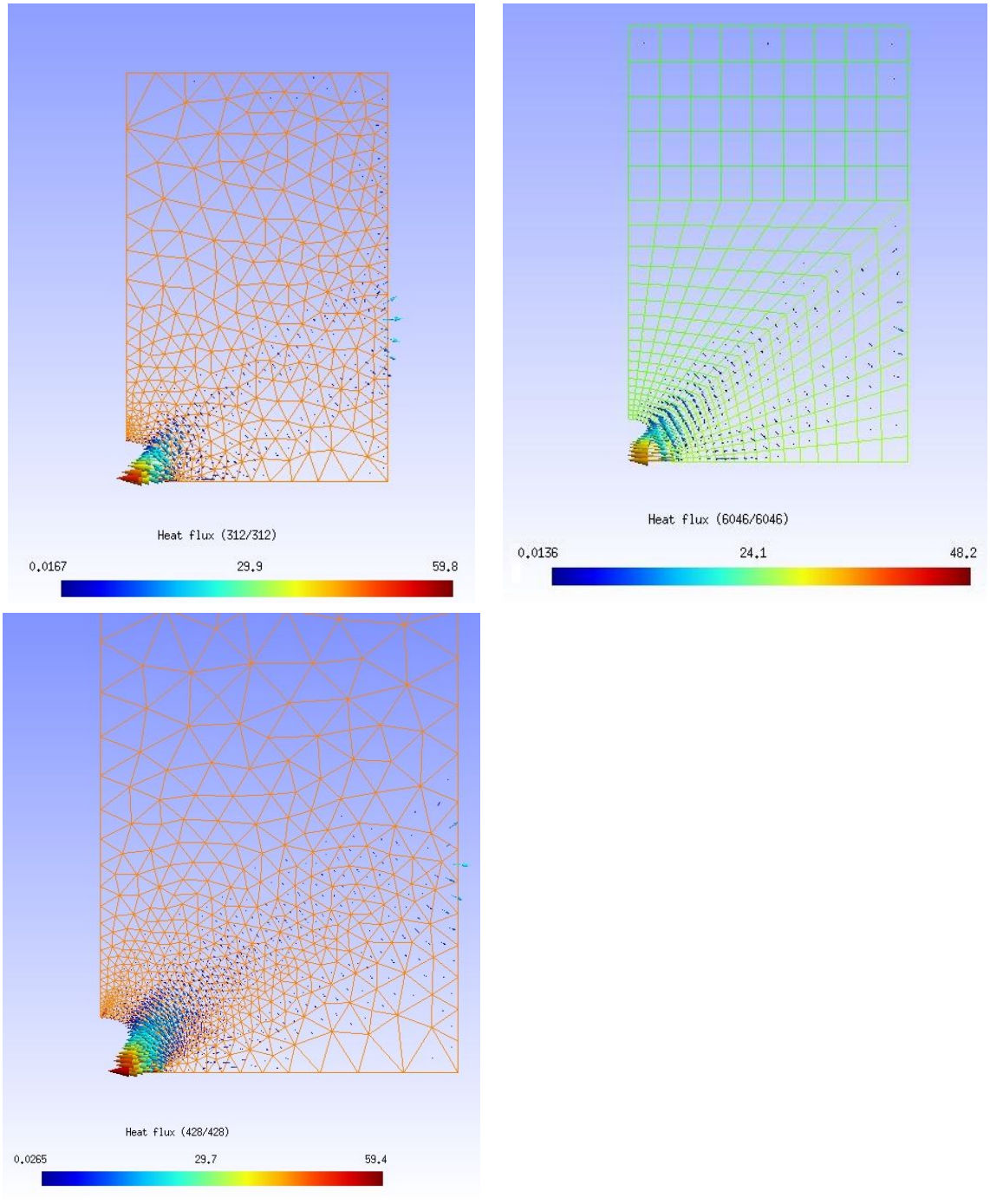

Figure B.4: Heat flux ($W.m^{-2}$) at time $t = 30sec$, showing different meshes, on the top left "mesh 1", on the top right "mesh 2" and on the bottom "mesh 3"

Bibliography

[1] E. Fancello J. Ponthot and L. Stainier. A variational formulation of constitutive models and updates in non-linear finite viscoelasticity. *Computational Methods in Applied Mechanics*, 65:1831–1864, 2006. 71

[2] Geankoplis, Christie John (2003) Transport processes and separation process principles : (includes unit operations) (4th ed. ed.). Upper Saddle River, NJ: Prentice Hall Professional Technical Reference. ISBN 0-13-101367-X 20

[3] J.D. Achenbach. *Wave Propagation in Elastic Solids*,5th printing, North Holland, Amesterdam 1987.

[4] J. Lemaitre and J.-L. Chaboche. *Mécanique des matériaux solides*. 1985. 34, 52

[5] J.H. Argyris and J. St. Doltsinis. On the natural formulation and analysis of large deformation coupled thermo-mechanical problems', *Computer Methods in Applied Mechanics and Engineering*, 25, 195-253, 1981. 51

[6] M. Ortiz, L. Stainier, 1999. The variational formulation of viscoplastic constitutive updates. *Comput. Methods Appl. Mech. Eng.* 171 (3-4), 419-444. 69

[7] K.C.Park; C.A. Felippa and J.A.DeRuntz. Stabilization of staggered solution procedures for fluid-structure interaction analysis. *Computational Methods for Fluid-Structure Interaction Problems*, 26:94–124, 1977. 51

[8] J. M. Ball and G. Knowles. 'Lyapunov functions for thermomechanics with spatially varying boundary temperatures', *Arch. Rational Mech. Anal.*, 92, 193-204, 1986. 134

[9] K.C. Park and C.A. Felippa. Computational methods in transient analysis. In T. Belytschko and T.J.R Hughes, editors, *Partitioned analysis of coupled problems*, North-Holland, Amesterdam, 1983. 42, 51

[10] P. A. C. Raats « Steady Gravitational Convection Induced by a Line Source of Salt in a Soil », in Soil Science Society of America Journal, no 33, 1969, p. 483-487 22

[11] D.E. Carlson 'Linear Thermoelasticity', in S. Fluegge (ed.), *Handbuch der Physik*, Bd. VI/2a, Springer-Verlag, Berlin, 172, pp. 297-346.

[12] Z. Tonkovic, J. Soric, and W. Kratzig. 'On nonisothermal elastoplastic analysis of shell components employing realistic hardening responses.' *International Journal of Solids and Structures*, 38:5019-5039, 2001. 34

[13] I. Klotz, R. Rosenberg, Thermodynamics - Basic Concepts and Methods, 7th ed., Wiley (2008) 24

[14] C.M. Dafermos, 'Contraction semigroups and trend to equilibrium in continuum mechanics', *Springer Lecture Notes in Mathematics* 503, 1976, pp. 295-306. 134

[15] A. Rosakis J. Hodowany, G. Ravichandran and P. Rosakis. Partition of plastic work into heat and stored energy in metals. *Experimental Mechanics*, 40(2):113–123, 2000. 102

[16] I. St. Doltsinis, 'Aspects of modelling and computation in the analysis of metal forming', *Eng. Computat.*, 7, 2-20, 1990.

[17] P. Duhem, *Traité d'Energetique ou de Thermodynamique Générale*, Gauthier Villars, Paris, 1911.

[18] J. L. Ericksen, 'Thermoelastic stability', Proc. 5th National Cong. on Applied Mechanics, 1966, pp. 187-193. 134

[19] K. C. Park Partitioned transient analysis procedures for coupled-field problems: accuracy analysis, *J. Appl. Mech.,* 47, 370-376, 1980. 6

[20] M. A. Biot, 1956. Thermoelasticity and irreversible thermodynamics. *J. Stat. Phys.* 27, 250-253. 69

[21] K. C. Park and C. A. Felippa, Partitioned transient analysis procedures for coupled-field problems: accuracy analysis, *J. Appl. Mech.,* 47, 919-926, 1980. 6

[22] M. E. Gurtin, 'Thermodynamics and stability', Arch. Rational Mech. Anal, 59, 53-96, 1975.

[23] W. Han, S. Jensen, B.D. Reddy, 1997. Numerical approximations of problems in plasticity: error analysis and solution algorithms. *Numer. Linear Algebra Appl.* 4, 191-204. 69

[24] K. C. Park and C. A Felippa, 'Partitioned analysis of coupled problems', in T. Belytschko and T.J.R Hughes (eds.) *Computational Methods in Transient Analysis*, North Holland, Amsterdam, 1983. 6, 51

[25] H. Parkus. *Thermoelasticity*, 2nd edn, Springer -Verlag, Wien, 1976.

[26] Han, W., Reddy, B.D., Schroeder, G.C., 1997. Qualitative and numerical analysis of quasi-static problems in elastoplasticity. *SIAM J. Numer. Anal.* 34, 143-177. 69

[27] J.J. Aklomis and W.J. Mackwright. *Introduction to polymer visco-elasticity.* Wiley interscience, second edition edition, 1983. 81

[28] B. Halphen and Q. Nguyen. Sur les matériaux standard généralisés. *Journal de mécanique*, 14:39–63, 1975. 31, 70

[29] J. C. Simo 'Algorithms for static and dynamic mutiplicative plasticity that preserve the classical return mapping schemes of the infinitesimal theory', *Computational Methods in Applied Mechanics and Engineering, 1991* 101

[30] J. C. Simo and C. Miehe. Associative coupled thermoplasticity at finite strains: Formulation, numerical analysis and implementation' *Computational Methods in Applied Mechanics and Engineering* 49, 101

[31] O. C. Zienkiewicz, D. K. Paul and A. H. Chan, Unconditionally stable staggered solution procedure for soil-pore fluid interaction problems *Computational Methods in Applied Mechanics and Engineering*, 26, 1039-1055, 1988. 6, 42, 51

[32] J.T. Oden and W.H. Armstrong, 'Analysis of Nonlinear Dynamic Coupled Thermoviscoelasticity Problems by the Finite Element Method', *Computers and Structures*, Vol. 1, pp. 603-621, 1971. 6, 42

[33] W. K. liu and H. G. Chang, 'A Note on Numerical Analysis of Dynamic Coupled Thermoelasticity' *Computational Methods in Applied Mechanics and Engineering*, Vol. 50, 1033-1041, 1983.

[34] V. I. Danilovskaya, On a Dynamical Prolem of Thermoelasticity, *Prikladnaya Matematika i Mechanika*, Vol. 13,No 3, pp. 341-344, 1952.

[35] G. I. Taylor and H. Quinney. ' The latent heat remaining in a metal after cold work.' *Proc. of the Royal Society*, A163:157-181, 1937. London. 34

[36] J. C. Simo. 'Nonlinear stability of the time discrete variational problem in nonlinear heat conduction and elastoplasticity', *Computational Methods in Applied Mechanics and Engineering* 88, 111-131, 1991.

[37] Y. Dubois-Pelerin, 'Linear Thermomechanical Coupling by the Staggered Method', IREM Internal report, Ecole Polytechnique Federale de Lausanne, 1989. 6

[38] M. Zhou, G. Rachivadran, and A. J. Rosakis. Dynamically propagating shear bands in impact-loaded prenotched plates - II : numerical simulations. *Journal of Mechanics and Physics of Solids*, 44:1007-1032, 1996. 34

[39] K. C. Park, C. A. Felippa and J. A DeRuntz "Stabilization of Staggered Solution Procedures for Fluid-Structure Interaction Analysis", *Computational Methods for Fluid-Structure Interaction Problems*, ed. by Delytshcko and Geers, ASME Applied Mechanics Symposia Series, AMD, 26, 94-124, 1977 42, 51

[40] M.Kleiber P. Wriggers, C. Miehe and J.C. Simo. Computer methods in applied mechanics and engineering (complas 2). In E. Hinton Owen and E. Oñate, editors, *On the coupled thermo-mechanical treatment of necking problems via FEM*, pages 527–542, Barecelona, Spain, 1983. Pineridge Press. 100

[41] K.C.Park and C.A.Felippa. Computational methods in transient analysis. In T. Belytschko and T.J.R Hughes, editors, *Partitioned analysis of coupled problems*, North-Holland, Amesterdam, 1983. 42, 49

[42] K. C. Park, "Partitioned Transient Analysis Procedure for coupled-Field Problems: Stability Analysis" *J. Appl. Mech.*, Vol. 47, No. 2, pp.370-376, 1980 6, 42

[43] R. E. Nickell and J.L. Sackman, "The Extended Ritz Method Applied to Transient Coupled Thermoelastic Boundary-Value Problems", *Rep. No. 67-3, Structures and Materials Research,* University of California at Berkeley, 1967. Linear Coupled Thermoelasticity, J. Appl. Mech., Vol. 35, PP. 255-266, 1968 6

[44] N.Charalambakis, 2011. Shear Stability and Strain, Strain-rate and Temperature Dependent 'Cold' Work. International Journal of Engineering Science 39 (17), 1899-1911. 39, 100

[45] J. Fourier Théorie analytique de la chaleur, Paris, 1822 21

[46] S. R. Chen and G. T. Gray, 1996. Constitutive behavior of tantalum and tantalum-tungsten alloys. Metallurgical and Materials Transactions A 27 (10), 2994-3006. 100

[47] Y. Bamberger Mécanique de l'ingénieur, Tome II, Ed. Hermann, Paris, 1981 17

[48] B. Halphen and Q. S. Nguyen *Sur les matériaux standards généralisés,* Journal de Mécanique, Vol. 14, pp. 39-63, 1975 17

[49] J. L. Nowinsky Theory of thermoelasticity, Noordhoff International, Alphen aan den Rijn, 1978.

[50] J.C. Simo and C. Miehe. Associative coupled thermoplasticity at finite strains : Formulation, numerical analysis and implementation. *Computer Methods in Applied Mechanics and Engineering*, 98:41–104, 1992. 34, 100

[51] J. J. Aklomis and W. J. Machwright *Introduction to polymer viscoelasticity,* 2^{nd} editions, Wiley interscience, 1983.

[52] A. Monlinari and R. J. Clifton *Analytical characterization of shear localization in thermoviscoplastic materials,* Journal of Applied Mechanics, 54, 806-812, 1987.

[53] D. Assaker. *Analyse thermomécanique non-linéaire par éléments finis des traitements thermiques des métaux.* PhD. thesis, Université de Liège, 1989-90. 101

[54] M. Biot. In proceedings of the third us national congress of applied mechanics. In ASME, editor, *Linear thermodynamics and the mechanics of solids*, pages 1–18, 1958.

[55] G. A. Maugin. *The thermomechanics of nonlinear irreversible behaviors,* volume 27 of Series *on Nonlinear Science*. World Scientific leon o. chua edition, 1999. 71

[56] J. Mandel *Cours de mécanique des milieux continus,* Gauthier-Villard, Paris, 1966. 27

[57] B. Booley and J. Weiner. *Theory of thermal stresses*. Wiley, 1960. 17

[58] O.T Bruhms, H. Xiao and A. Meyers. A self-consistent eulerian rate type model for finite deformation elasto-plasticity with isotropic damage. *International Journal of Solids and Structures,* 38: 657-683, 2001. 31

[59] A. Chrysochoos. Bilan énergétique en élastoplasticité grandes déformations. *Journal de mécanique théorique et appliqué,* 4(5) :589-614, 1985. 101

[60] A. Chrysochoos and R. Peyroux. Analyse expérimentale et modélisation numérique des couplages thermomécanique dans les matériaux solides. *Revue générale de thermomécanique,* 37: 852-606, 1998. 101

[61] M. Ortiz and L. Stainier. The variational formulation of viscoplastic constitutive update. *Computational Methods in Applied Mechanics*, 171:419–444, 1999. 6

[62] J. Vassoler E. Fancello and L. Stainier. A variational constitutive update algorithm for a set of isotropic hyperelastic-viscoplastic material models. *Computational Methods in Applied Mechanics*, 197:4132–4148, 2008. 71, 101

[63] M. G. Cooper, B. B. Mikic and M. M. Yovanovich. Thermal contact conductance. *International Journal of Heat and Mass Transfer,* 12: 279-300, 1969. 71

21

[64] M. A. Biot, 1958. Linear thermodynamics and the mechanics of solids. In: Proceedings of the Third US National Congress of Applied Mechanics. ASME, pp. 1-18. 69

[65] G. Batra, 1989. On a principle of virtual work for thermo-elastic bodies. *J. Elasticity* 21, 131-146. 69

[66] G. Dhatt and G. Touzot. *Une présentation de la méthode des éléments finis.* Collection Université de Compiègne, Maloine s.a. edition, 1984.

[67] P. Germain and P. Muller *Introduction à la mécanique des milieux continus,* Ed. Dunond, Paris, 1985 17

[68] M. Hogge. Modélisation des transferts de chaleur et de matière. Notes de cours - LTAS - Université de Liège. 55

[69] Unconditionally stable algorithms for nonlinear heat conduction. *Computer Methods in Applied Mechanics and Engineering,* 10: 135-139, 1977.

[70] M. Ortiz, E. A. Repetto and L. Stainier. A theory of subgrain dislocation structrues in ductile single crystals. *Journal of the Mechanics and Physics of Solids,* 48: 2077-2114, 2000.

[71] P. Perzyna. Thermodynamics Theory of plasticity. In Chia-Shun Yih, editor, *Advances in Applied Mechanics*, volume 11, pages 313-355. Academic Press, 1971. 101

[72] A. Molinari, M. Ortiz, 1987. Global viscoelastic behavior of heterogeneous thermoelastic materials. *Int. J. Solids Struct.* 23(9), 1285-1300 69

[73] L. Stainier Notes relatives au cours donné à Montpellier, 2006. 49, 70, 101

[74] J.C. Simo and C. Miehe. Associative coupled thermoplasticity at finite strains : Formulation, numerical analysis and implementation. *Computer Methods in Applied Mechanics and Engineering*, 46:201–215, 1992. 49

[75] J. H.Lienhard (2008) A Heat Transfer Textbook (3rd ed.). Cambridge, Massachusetts: Phlogiston Press. ISBN 978-0-9713835-3-1. 20

[76] J. R.Welty, C. E. Wicks and R. E. Wilson (1976) Fundamentals of momentum, heat, and mass transfer (2 ed.). New York: Wiley 21

[77] P. Radovitzky and M. Ortiz. Error estimation and adaptive meshing in strongly nonlinear dynamic problems. *Computer Methods in Applied Mechanics and Engineering,* 172: 203-240, 1999.

[78] M. Ortiz and E. A. Repetto. Nonconvex energy minimization and dislocation structures in ductile single crystals. *Journal of the Mechanics and Physics of Solids,* 47:397-462, 1999.

[79] L. Stainier. 19ème congrès français de mécanique. In *Une approche variationnelle des couplages thermo-mécaniques en calcul des structures*, Marseille, France, Août 2009. Institut de Recherche en Génie Civil et Mécanique (GeM UMR 6183 CNRS), Ecole Centrale de Nantes. 48, 49, 70

[80] Y. Dubois-Pelerin. Linear thermomechanical coupling by the staggered method. *IREM Internal Report*, 1989. 42, 49

[81] Çengel, Yunus A. (2003) Heat Transfer: a practical approach. McGraw-Hill series in mechanical engineering (2nd ed.). 23

[82] G. T. Camacho and M. Ortiz. Adaptive Langrangian modeling of ballistic penetration of metallic targets. *Computer Methods in Applied Mechanics and Engineering*, 60:813-821, 1997. 34

[83] A. Chrysochoos, H. Pham and O. Maisonneuve *Experimental and theoretical analysis of thermomechanical coupling*, extended paper related to SMIRT conference, 1996. 17

[84] A. Ibrahimbegovic and L. Chorfi. Covariant principal axis formulation of associated coupled thermoplasticity at finite strains and its numerical implementation. *International Journal of Solids and Structures*, 39:499–528, 2002. 100

[85] M. Ortiz and L. Stainier. The variational formulation of viscoplastic constitutive updates. *Computer Methods in Applied Mechanics and Engineering,* 171: 419-444, 1999. 71

[86] E. Fancello, J. P. Ponthot and L. Stainier. A variational formulation of constitutive models and updates in non-linear finite viscolasticity. *International Journal for Numerical Methods in Engineering,* 2006. 71

[87] W. K. Belvin and K. C. Park Structural tailoring and feedback control synthesis: an interdisciplinary approach, *J. guidance, control & dynamics,* 13, 424-429, 1990. 6

[88] G. Herrmann, 1963. On variational principles in thermoelasticity and heat conduction. *Q. Appl. Math.* 22, 151-155. 69

[89] C. Farhat and R. X. Roux Implicit parallel processing in structural mechanics, *Computat. Mech. Advances,* 2, 1-124, 1994. 6

[90] D. Van Nostrand McCulloch, Richard, S. (1876) Treatise on the Mechanical Theory of Heat and its Applications to the Steam-Engine, etc.. 24

[91] C. Farhat;Y. Dubois-Pelerin; K. C. Park. An unconditionally stable staggered algorithm for transient finite element analysis of coupled thermoelastic problems. NASA Contractor Report 189066, University of Colorado, Boulder Colorado, Ecole Polytechnique Federale de Lausanne, November 1991. 51

[92] D.K. Paul O.C. Zienkiewicz and A. H. Chan. Unconditionally stable staggered solution procedure for soil-pore fluid interaction problems. *International Journal For Numerical Methods In Engineering*, 88:111–131, 1991. 51

[93] A. Chrysochoos and J.C. Dupré. Proceedings of the eurotherm seminar nb. 27. In Euro Thermique, editor, *An infra-red set-up for continuum thermomechanics, Quantitative Infra-Red Thermography*, pages 129–134, 1992. 88

[94] F. A. Felippa Refined finite element analysis of linear and nonlinear two-dimensional structures, *PhD Dissertation*, Department of Civil Engineering, University of California at Berkeley, Berkeley, CA, 1966 6

[95] F. A. Felippa and K. C. Park. Compuational aspects of time integration procedures in structural dynamics, Part I: Implementation, *J. Appl. Mech.,* 45, 595-602, 1979. 6

[96] Faghri, A., Zhang, Y., and Howell, J. R., 2010 Advanced Heat and Mass Transfer, Global Digital Press, Columbia, MO. 21

[97] C. A. Felippa and K. C. Park Staggered transient analysis procedures for coupled transient analysis procedures for coupled dynamic systems: formulation, *Comp. Meths. Appl. Mech. Engrg.,* 24, 61-112, 1980. 6

[98] J. Besson, G. Cailletaud, J-L. Chaboche, and S. Forest. *Mécanique non linéaire des matériaux.* Hermes Science Publications, 2001. 17

[99] F. Meissonnier. *Couplages Thermomécaniques et Homogéneisation.* PhD thesis, Université Montpellier 2, Décembre 1996. 25, 81, 88, 89, 93

[100] C. A. Felippa, K. C. Park and C. Farhat. Partitioned analysis of coupled mechanical systems, Invited Plenary Lecture, 4th World Congress in Computational Mechanics, Buenos Aires, Angentina, July 1998, expanded verion in Comp. Meths. Appl. Mech. Engrg., 190, 3247-3270, 2001. 6

[101] C. A. Felippa and K. C. Park Staggered transient analysis procedures for coupled mechanical systems: formulation. *Computer Methods in Applied Mechanics and Engineering* 1980;24:61-111. 13

[102] C. A. Felippa and T. L. Geers Partitioned analysis for coupled mechanical system. *Engineering Computation* 1988; 5:123-133 13

[103] K. C. Park and C. A. Felippa, Partitioned analysis of coupled systems, chapter 4 *in computational Methods for Transient Analysis*, T. Belytschko and T. J. R Hughes, eds., North-Holland, Amsterdam-New York, 157-219, 1983. 6

[104] K. C. Park and C. A. Felippa, Recent advances in partitioned analysis procedures, in: Chapter 11 of *Numerical Methods in Coupled Problems*, ed. by R. Lewis, P. Bettess and E. Hinton, Wiley, Chichester, 327-352, 1984. 6

[105] Meyers and Chawla. *Mechanical Behaviors of Materials*, volume 580. Prentice Hall, Inc, 1999. 36

[106] R.W Lewis and B.A Schrefler. *The finite Element Method in the Deformation and Cosolidation of Porus Media.* Wiley, New York, 1987. Reference 30, Chapter 8. 42

[107] M. Ben-Amoz, 1965. On a variational theorem in coupled thermoelasticity. *J. Appl. Mech.* 32, 943-945. 69

[108] F. Armero and J.C. Simo. A new unconditionally stable fractional step method for non-linear coupled thermomechanical problems. *International Journal for Numerical Methods in Engineering*, 35,737-766, 1992. 6, 42, 50, 69, 134, 136, 137

[109] C. A. Felippa, K. C. Park and C. Farhat Partitioned analysis of coupled mechanical systems *Computer Methods in Applied Mechanics and Engineering* 13: 3247-3270, 2001. 11

[110] J.H. Argyris and J. Doltsinis. On the natural formulation and analysis of large deformation coupled thermomechanical problems. *Computer Methods in Applied Mechanics and Engineering*, (53):297–329, 2002. 42, 49

[111] K. C. Park. Partitioned transient analysis procedures for coupled-field problems: Stability analysis. *Journal of Applied Mechanics*, 47(2):370–376, 1980. 42

[112] D.Dureisseix D.Néron. A computational strategy for thermo-poroelastic structures with a time-space interface coupling. *International Journal for Numerical Methods in Engineering*, (75):1053–1084, 2008. 6, 42

[113] J.P. Ponthot. *Traitement unifié de la mécanique des milieux continus solides en grandes transformation par la méthode des éléments finis.* PhD thesis, Université de Liège, Liège, Belgique, 1995. 49

[114] L. Adam *Modélisation du comportement thermo-élasto-viscoplastique des métaux soumis à des grandes déformations , Application au formage superplastique.* PhD thesis, Université de Liège, 2003. 30, 49, 51, 52, 100, 137, 138

[115] Q. Yang; L. Stainier; and M. Ortiz. A varitional formulation of the coupled thermo-mechanical boundary value problem for general dissipative solids. *Journal of the Mechanics and Physics of Solids*, 54:401–424, 2006. 7, 70, 77

[116] J.T. Oden, J.N. Reddy, 1976. Variational Methods in Theoretical Mechanics. Springer, Berlin. 69

[117] P. Wriggers, C. Miehe, M. Kleiber and J. C. Simo. On the coupled thermo-mechanical treatment of necking problems via FEM. in D.R.J. Owen, E. Hinton, and E. Oñate, editors, *International Conference on Computational Plasticity*(COMPLAS 2), pages 527-542, Barcelona, Spain, 1989. Pineridge Press. 34